PONTIFICIA UNIVERSIDAD CATÓLICA DEL ECUADOR

FACULTAD DE CIENCIAS EXACTAS Y NATURALES

ESCUELA DE CIENCIAS BIOLÓGICAS

Systematics of the *Pristimantis chloronotus* species group (Anura, Craugastoridae) with insights into their historic biogeography

Disertación previa a la obtención del título Licenciada en Ciencias Biológicas

MARÍA JOSÉ NAVARRETE MÉNDEZ

QUITO, 2017

Certifico que la disertación de Licenciatura en Ciencias Biológicas de la Srta. María José Navarrete ha sido concluida de conformidad con las normas establecidas; por lo tanto, puede ser presentada para la calificación correspondiente

Santiago R. Ron, Ph. D

Director de la disertación

Quito, 7 de febrero de 2017

A mis abuelos: *Elías* y *Carmita*,
Benjamín y *María Ester*

INDEX

LIST OF FIGURES ……..……...……..VII

LIST OF TABLES ……..…….VIII

LIST OF SUPPLEMENTARY MATERIAL ……...……IX

MANUSCRITO PARA LA PUBLICACIÓN ……...X

Abstract ...……..……..12

1. Introduction ...……..……13

2. Materials and methods ...…….……...16

2.1. *Taxon sampling* ……..16

2.2. *DNA extraction, amplification, and sequencing* ……17

2.3. *Phylogenetic reconstruction* ……...18

2.4. *Protocol for species delimitation* ……...20

2.4.1. *Morphological Analyses* ……..23

2.4.2. *Environmental Species delimitation* ……25

2.4.3. *Divergence Times and Ancestral Altitude Reconstruction* ……..25

3. Results ……..……..……26

3.1. *Phylogenetics and species delimitation* ……26

3.2. *Morphology* ……27

3.3. *Geographic distribution and environmental envelop* ……29

3.4. *Integrative taxonomy* ……..30

3.5. *Systematic accounts* ……...31

3.5.1. *Content* ……32

3.5.2. *Distribution* ……32

3.5.3. *Remarks* ……..……..……32

3.6. *Divergence time and ancestral altitude reconstruction* …….33

4. Discussion …….33

4.1. *Species limits and phylogeny* …….33

4.2. *Divergence times and altitudinal reconstruction: origin of P. chloronotus* species group ……..……..37

4.3. *Implications for conservation* ……... 40

Acknowledgments ……..……..…42

Literature cited ……..……..43

Figures ……..……...63

Tables ……..……77

Supplementary material ……95

Appendix ……..…….106

LIST OF FIGURES

Figure 1. Phylogeny of *Pristimantis chlotonotus* species group ……..64

Figure 2. Axes I and II from Principal Components Analysis based on 10 morphometric variables of 15 of the 20 clades of the *Pristimantis chloronotus* species group. **A.** PCA for females. **B.** PCA for males ……67

Figure 3. Dorsolateral view of live individuals of the *Pristimantis chloronotus* species group …….69

Figure 4. Ventral view of live individuals of the *Pristimantis chloronotus* species group ……70

Figure 5. Map showing sampling localities for DNA sequences of *Pristiminatis chloronotus* species group and used for phylogenetic, environmental and chronobiogeographic analyses ……..72

Figure 6. Axes I and II from Principal Components Analysis based on 19 bioclimatic variables taken from distribution localities of the *Pristimantis chloronotus* species group …….75

Figure 7. Phylogenetic tree of *Pristimantis chloronotus* species group, with divergence time estimates in millions of years and ancestral altitude reconstruction …….76

LIST OF TABLES

Table 1. Pairwise uncorrected genetic distances among clades of the *Pristimantis chloronotus* species group …….78

Table 2. Summary of morphometric measurements for adult females of the *Pristimantis chloronotus* species group. ……..……..80

Table 3. Summary of morphometric measurements for adult males of the *Pristimantis chloronotus* species group …….82

Table 4. Qualitative morphological characters for species of the *Pristimantis chloronotus* species group ……...…….84

Table 5. Qualitative morphological characters: definition of skin structures for species of the *Pristimantis chloronotus* species group ……...….85

Table 6. Qualitative morphological characters: coloration patterns of species of the *Pristimantis chloronotus* species group ……88

Table 7. Sympatric species of the *Pristimantis chloronotus* species group.……..……92

Table 8. Node ages in millions of years and altitudinal reconstruction in meters of representative lineages of *Pristimantis chloronotus* species group ……..93

Table 9. Genetic studies of cryptic diversity in *Pristimantis* frogs …….....…94

LIST OF SUPPLEMENTARY MATERIAL

Figure S1. Putative species delimitation of members of the *Pristimantis chloronotus* species group, recognized by the bPTP analysis …….....96

Figure S2. Bayesian chronogram with 95% highest posterior density (HPD) for *Pristimantis chloronotus* species group ……...……..98

Table S1. List of primers used in the present study for amplification and sequencing of two mitochondrial genes (16s and ND1) and one nuclear gene (RAG1) ……..100

Table S2. PCR protocols: thermal conditions and cycles for each gene (Mitochondrial: 16S, ND1; Nuclear: RAG1) ……....100

Table S3. Principal component analysis on environmental data for *Pristimantis chloronotus* species group ……...101

Table S4. Principal component analysis of morphometric data for *Pristimantis chloronotus* species group ……...103

Table S5. Results of the discriminant function analysis of females specimens based on eight morphometric variables ……..104

Table S6. Results of the discriminant function analysis of males specimens based on eight morphometric variables ……..105

MANUSCRITO PARA LA PUBLICACIÓN

Revista

Molecular Phylogenetics and Evolution

Título

Systematics of the *Pristimantis chloronotus* species group (Anura, Craugastoridae) with insights in their historic biogeography

Autores

María José Navarrete[*] y Santiago Ron

Correo electrónico

[*] majonavarrete4@gmail.com

Dirección

Museo de Zoología, Escuela de Biología, Pontificia Universidad Católica del Ecuador, Avenida 12 de Octubre y Roca, Apartado 17-01-2184, Quito, Ecuador

El presente trabajo se presenta en el formato de la Revista *Molecular Phylogenetics and Evolution* a partir de la siguiente página.

Systematics of the *Pristimantis chloronotus* species group (Anura, Craugastoridae) with insights into their historic biogeography

María José Navarrete, Santiago R. Ron

Museo de Zoología, Escuela de Biología, Pontificia Universidad Católica del Ecuador, Avenida 12 de Octubre y Roca, Apartado 17-01-2184, Quito, Ecuador

Keywords: Taxonomy, Andes, phylogenetics, cryptic species, Neotropics, biogeography, conservation

Abstract

With 490 species, *Pristimantis* is the most speciose genus of vertebrates reaching its highest diversity along the slopes of the northern Andes. The processes that originated this spectacular diversity have been studied at the family level (i.e., a bottom up approach) with the caveat that taxon sampling has been sparse. Analyses based on extensive species sampling focused on small clades (i.e., top down sampling) are still missing. Herein we assess the phylogeny and taxonomic status of a clade of 20 species of *Pristimantis* from the eastern Andean slopes. Our analyses rely on three independent lines of evidence: external morphology, environmental data, and genetics. We obtained a phylogeny based on mitochondrial and nuclear genes (*16S, ND1* and *RAG1*). To estimate the timing of the origin of contemporary species, we inferred a time-calibrated phylogeny with reconstruction of altitudinal ancestral areas. Based on our phylogeny we propose the recognition of the *P. chloronotus* species group. This clade, which is strongly supported, is composed by 15 formally described species (*P. ardyae*, *P. chloronotus*, *P. colonensis*, *P. eriphus*, *P. hernandezi*, P. *huicundo*, *P. incanus*, *P. inusitatus*, *P. llanganati*, *P. lividus*, *P. ortizi*, *P. roni*, *P. supernatis*, *P. thymelensis*, and *P. yanezi*), 4 confirmed candidate species,

and 1 unconfirmed candidate species. Morphometric and environmental analyses show little differentiation among species in spite of considerable genetic divergence (uncorrected *p*-distances among species 3%−15% for *16S*). Our analyses estimated the origin of the *P. chloronotus* species group in the Oligocene, when the elevation of the northern Andes was no more than half its modern altitude. The major events of diversification within the *P. chloronotus* species group coincide temporally with the major sequential bouts of Andean orogenesis in the Miocene-Pleistocene transition. Furthermore, the current allopatric distribution of sister lineages of the *P. chloronotus* species group suggest that the spatio-temporal diversification in this clade is causally linked to Andean uplift and palaeo-climate change through vicariance. Our results give insights in the evolutionary processes that generate diversity in the Tropical Andes, one of Earth's biodiversity hotspots.

1. Introduction

The Tropical Andes are widely recognized as a global biodiversity hotspot due to high regional species richness and endemism (Myers et al., 2000; Jenkins et al., 2013). The uplift of the Andes Cordillera has played an important role in the diversification of various groups of organisms such as plants (e.g., Hughes and Eastwood, 2006; Luebert et al., 2011; Sanín et al., 2016), birds (e.g., Cadena et al., 2007; Brumfield and Edwards, 2007; Chaves and Smith, 2011; Quintero et al., 2013), reptiles (e.g., Duellman, 1979), and mammals (e.g., Patton and Smith, 1992). It has been suggested that the diversification in montane Andean systems resulted from geographic isolation (Lynch and Duellman, 1997; Cadena et al., 2007) and the genesis of novel and contrasting environments (Graham et al., 2004; Hughes and Eastwood, 2006; Brumfield and Edwards, 2007; Smith et al., 2007). Nevertheless, the

inventory of the Tropical Andes biodiversity is still incomplete (e.g., Muchhala et al., 2005; Ramírez, 2005; Peralta et al., 2005; Ortega-Andrade et al., 2015) and the speciation mechanisms underlying these exceptional richness patterns are poorly understood.

Historical and environmental characteristics of the Andean region have influenced the origin and maintenance of multiple levels of diversity (e.g., species richness, functional diversity, endemism) (Vellend and Geber, 2001; Elmer et al., 2007; Swenson et al., 2012). Hypotheses of historical factors such as Andean orogeny and the resulting climatic gradients in combination with spatial patterns of standing genetic variation (Bermingham and Moritz, 1998; Muñoz-Ortíz et al., 2015) and geographic range data (Graham et al., 2004) would allow us to assess the evolutionary processes that have shaped the diversity and distributions of contemporary organisms (Bermingham & Moritz, 1998). Furthermore, some studies have integrated the use of phylogenies with environmental data to infer patterns of diversification (Graham et al., 2004) and test alternative hypotheses about mechanisms of speciation (i.e., allopatric, parapatric and sympatric speciation) in the tropical Andes (Moritz et al., 2000; Graham et al., 2004; Ribas et al., 2007; Chaves et al., 2011; Mendoza et al., 2015; Muñoz-Ortíz et al., 2015). The orogenesis and climate fluctuations of the northern Andes (Jørgensen and León-Yánez, 1999; Sklenář and Jørgensen, 1999) have influenced the diversification of species with limited vagility such as frogs (Lynch and Duellman, 1997). In the northern Andes, the most diverse group of frogs is the direct developing genus *Pristimantis*. They reach peak species-richness in the Andean slopes of Colombia, Ecuador, and northern Peru (Frost, 2016). Currently, 490 species of *Pristimantis* are recognized representing ~7% of amphibians worldwide (Frost, 2016). Moreover, recent systematic reviews based on genetic evidence have shown that species

richness is significantly underestimated (e.g., Elmer et al., 2007; Ortega-Andrade et al., 2015; Rivera-Correa and Daza, 2016; Navarrete et al., 2016, Székely et al., 2016). Undescribed morphologically cryptic species often equal or exceed the number of described species (e.g., Elmer et al., 2007; Ortega-Andrade et al., 2015) and the discovery of morphologically distinct new species is common even in well-sampled regions (e.g., Valencia et al., 2013). Hence the urgent need of species-level thorough systematic studies based on a combination of genetic data and other independent sets of characters.

The mechanisms that originated this striking diversity within *Pristimantis* have been studied at the family or genus levels (Heinicke et al., 2007; Pinto-Sánchez et al., 2012; Mendoza et al., 2015). This sampling design is called “bottom up” (Wiens et al., 2005) and seeks to resolve only the higher-levels of taxonomic relationships, even if relying on an incomplete set of species. In some cases “bottom up” sampling obscures the inference of phylogenetic relationships, patterns of diversity, or speciation mechanisms due to poor sampling or misidentified specimens (e.g., Heinicke et al., 2007; Hedges et al., 2008; Mendoza et al., 2015). The alternative is a “top-down” sampling design, which is based on extensive species-level sampling, and is focused on small clades. This is advantageous at resolving species-level relationships and ensuring the basic data to evaluate even complex patterns of distribution and diversity.

In this study we apply a “top-down” systematic review of an Andean clade of *Pristimantis* that inhabits cloud forests of the eastern slopes of Colombia and Ecuador to explore the mechanisms that generated their diversity. Species of this clade are characterized by having green color and tuberculate skin. We use mitochondrial and nuclear DNA sequence data to estimate the phylogenetic relationships of this phenotypically distinct group of species. Our

aims are to (1) test whether our focal species belong to a single clade and clarify their phylogenetic relationships; (2) to assess the genetic distance thresholds used to delimit species boundaries within our group of study and (3) identify the most likely speciation mechanisms of our sampled species in order to improve the understanding of the extraordinary diversification of Andean *Pristimantis*.

2. Materials and methods

2.1. Taxon sampling

Individuals were sampled based on two diagnostic shared morphological features related to coloration and tuberculation, such as greenish or mossy dorsum coloration and conical tubercles on upper eyelids, heels and tarsus. We also included samples that have shown to belong to the same internal group of these greenish frogs in a larger *Pristimantis* phylogeny (Ron, not published).

For the molecular phylogenetic analyses we sampled 139 individuals of *Pristimantis* representing 28 species formally described deposited at the Museo de Zoología of the Pontificia Universidad Católica del Ecuador (QCAZ) and Museo Ecuatoriano de Ciencias Naturales (MECN). We also included 19 sequences, representing at least 12 species of *Pristimantis* from GenBank. A summary of localities, coordinates, GenBank accession numbers, and museum ID for vouchers is given in Appendix A.

All of our data analyses follow the taxonomic classification of *Pristimantis* proposed by Pyron and Wiens (2011). Previous studies suggest that *Pristimantis* is closely related to the clades containing *Oreobates* and *Craugastor* (Hedges et al., 2008; Heinicke et al., 2009; Pyron and Wiens, 2011; Padial et al., 2014). We therefore rooted our phylogeny using as

outgroups sequences of *Oreobates quixensis*, *Craugastor longirostris*, and *Hypodactylus* sp. We included sequences of *Pristimantis altamazonicus*, *P. appendiculatus*, *P. buckleyi*, *P. crenunguis*, *P. colomai*, *P. galdi*, *P. incomptus*, *P. katoptroides*, *P. laticlavius*, *P. librarius*, *P. ockendeni*, *P. orcesi*, *P. pyrrhomerus*, *P. quaquaversus*, *P. rubicundus*, *P. verecundus*, and *P. w-nigrum* to assess the position of our sampled clade within *Pristimantis*. Specimens in the ingroup include *Pristimantis ardyae* Reyes-Puig et al., 2013, *P. chloronotus* (Lynch, 1969), *P. colonensis* (Mueses-Cisneros, 2007), *P. eriphus* (Lynch and Duellman, 1980), *P. hernandezi* (Lynch and Ruiz-Carranza, 1983), *P. huicundo* (Guayasamin, Almeida-Reinoso and Nogales-Sornosa, 2004), *P. incanus* (Lynch and Duellman, 1980), *P. inusitatus* (Lynch and Duellman, 1980), *P. llanganati* Navarrete, Ron and Venegas, 2016, *P. lividus* (Lynch and Duellman, 1980), *P. ortizi* (Guayasamin, Almeida-Reinoso and Nogales-Sornosa, 2004), *P. roni* Yánez-Muñoz, Bejarano-Muñoz, Brito M., and Batallas 2014, *P. supernatis* (Lynch, 1979), *P. thymelensis* (Lynch, 1972), and *P. yanezi* Navarrete, Ron and Venegas, 2016.

2.2 DNA extraction, amplification, and sequencing

DNA extraction and amplification were carried out at the Laboratory of Molecular Biology of Museo de Zoología of the Pontificia Universidad Católica del Ecuador (QCAZ). Genomic DNA was extracted from liver or thigh muscle tissues preserved in 95% ethanol using Fujita's guanidine thiocyanate protocol (Esselstyn et al. 2008). We used Polymerase Chain Reaction (PCR) to amplify one fragment of 16S rRNA (16S), NADH dehydrogenase subunit 1 (ND1) and adjacent tRNAs ($tRNA^{Leu}$, $tRNA^{Ile}$ and $tRNA^{Gln}$). We also amplified the nuclear gene for recombination-activating 1 (RAG1). In some cases we only amplified the first DNA fragment of 16S (Appendix A). PCR primers are listed in Supplementary

material Table S1. PCR reactions were carried out under standard protocols with 25 µl reaction using 0.25 µl Qiagen Taq DNA polymerase, 2.5 µl Buffer 10X with 1.5 µl of $MgCl_2$ at 50 mM, 0.5 µl dNTPs at 10 mM, 0.5 µl each of forward and reverse primers at 10 mM, 1 µl of extracted DNA and 18.25 µl H_2O. Thermal cycling conditions are listed in Supplementary material Table S2. We cleaned our PCR amplicons with AP-itExoSAP-it (Affymetrix, Cleveland, OH) to remove unincorporated primers and dNTPs. These products were isolated via electrophoresis on 1% agarose gels. All fragments were sequenced in both directions by Macrogen Inc. (Seoul, Republic of Korea).

Forward and reverse sequences were assembled and manually edited in GeneiousPro 5.4.6 (Biomatters Ltd.). Leading and trailing ends were trimmed manually to remove low quality bases. The resulting sequences were subjected to nucleotide BLAST search using the NCBI database (http://blast.ncbi.nlm.nih.gov/Blast.cgi) for corroborating the identity of the sequences. Multiple sequence alignments were performed in Geneious using the MAFFT 6.0 (Katoh and Standley, 2013) plugin under default parameters. A posterior manual correction of the alignment was made using Mesquite v2.75 (Maddison and Maddison, 2011).

2.3 Phylogenetic reconstruction

We carried out separated analyses for each gene data set (first fragment of 16S, ND1 and RAG-1) under maximum likelihood (ML) in Garli v2.0 (Zwickl, 2006) searching for significant incongruences in phylogenetic relations (Wiens, 1998), and to visualize species that constitute monophyletic units in both trees. The search for incongruences is an important step to evidence hybridization or introgression among individuals (Barley et al.,

2013), as well as errors in laboratory work. Two replicates per region were carried out, each one starting from a stepwise tree and using GTR + I + G as substitution model. Other search parameters were set to default values. We compared by eye the topology of the resulting trees.

Phylogenetic analyses were performed using a combined matrix of 16S + ND1 + flanking tRNA genes + RAG1 sequences. Coding and non-coding regions and each of the three codon positions evolve under different rates. Hence, we partitioned the matrix by gene and codon position to select the substitution models that better fit each partition and the optimal partition scheme. Selection was carried out in the software PartitionFinder v1.1.1 (Lanfear et al., 2012) under the greedy algorithm using the Bayesian Information Criterion (BIC) to choose among alternative models and partitions. We defined nine *a priori* partitions: one partition for each codon position in protein coding loci (ND1 and RAG1, total = 6) plus one for each non-coding loci (16S, $tRNA^{leu}$ and $tRNA^{ile}$, total = 3).

We analyzed the data under Maximum Likelihood (ML) and Bayesian approaches. The maximum likelihood tree was estimated using Garli v2.0 (Zwickl, 2006). The search consisted of 40 independent runs: 20 under stepwise-addition starting tree (streefname = stepwise) and 20 with a random starting tree (streefname = random). Analyses were terminated until all searches resulted in similar likelihood values at 20000 generations (genthreshfortopoterm = 20000), indicating an efficient search. We chose the phylogeny with the highest likelihood. To estimate support values for the nodes, we performed non-parametric bootstrapping with 200 pseudoreplicates. Each search was performed with random starting trees (streefname = random), 5000000 generations as maximum for each run (stopgen = 5000000), and other parameters were used with default settings. The

consensus tree was estimated in Mesquite v2.75 (Maddison and Maddison, 2011) under a majority rule consensus set at 50%. Bootstrap values ≥70% were considered to indicate strong support following Hillis and Bull (1993).

Bayesian phylogenetic inference using Markov chain Monte Carlo (MCMC) sampling was performed in MrBayes v.3.1.2. (Ronquist et al., 2012). We conducted 4 parallel and independent runs, each for 3×10^7 generations, sampling every 1000 generations. Each run used one cold and three heated Markov chains (with default heating values). The prior of the rate matrix was a uniform dirichlet and we assumed equal probabilities for all topologies. The first 50% of generations were discarded as burn-in. Each run was considered finished when after 3×10^7 generations the average standard deviation of split frequencies was < 0.05 and effective sample size (ESS) was > 200 for all parameters. Values for ESS were obtained in Tracer v1.5 (Rambaut and Drummond 2007). Clades with posterior probabilities > 0.95 were considered strongly supported.

2.4 Protocol for species delimitation

The species concept used in this study corresponds to a general lineage concept (i.e., unified species concept), with species viewed as separately evolving metapopulation lineages (Simpson, 1961; Wiley, 1978; de Queiroz, 1998; de Queiroz, 2005; de Queiroz, 2007). Many studies largely follow this framework to delineate species boundaries and establish protocols to improve estimates of organismal diversity (e.g., Vieites et al., 2009; Padial et al., 2010; Ortega-Andrade et al., 2015).

To assess species limits, we applied an integrative taxonomy framework (*sensu* Dayrat, 2005; Vieites et al., 2009). Integrative taxonomy attempts to delineate species based on

congruence among multiple sets of independent characters (e.g., genetic markers, ecological niche, morphology, reproductive compatibility, etc.; Dayrat, 2005). Congruence between independent character sets among a set of individuals is evidence that they represent a species because it is unlikely that such a pattern can arise by chance alone (Padial et al., 2010). Although the integrative taxonomy has been widely debated (e.g., Valdecasas et al., 2008; Cook et al., 2010), its use and acceptance have increased in the last years (e.g., Vieites et al., 2009; Glaw et al., 2010; Caminer and Ron, 2014; Ortega-Andrade et al., 2015).

Species limits were assessed using genetic, morphologic, and environmental characters following the protocol of candidate species proposed by Vieites et al. (2009). We classified *Pristimantis* lineages into 3 categories: (1) Confirmed candidate species (CCS), (2) Unconfirmed candidate species (UCS), and (3) Deep conspecific lineages. Candidate species (CCS and UCS) were lineages separated from others by uncorrected *p* genetic distances above 3% for the gene 16S (Fouquet et al., 2007). A candidate species was considered CCS when genetic variation was concordant with variation in morphological characters with diagnostic significance for *Pristimantis* (e.g., skin texture, size) or environmental characters (e.g., humidity, temperature, elevation). A candidate species was considered UCS when suitable morphological and environmental characters were unavailable. Deep conspecific lineages were characterized by having uncorrected *p* genetic distances >3% but genetic variation discordant with variation in morphological or environmental characters.

Uncorrected *p* genetic distances were obtained using software MEGA 6 (Tamura et al., 2013) using 500 bootstrap pseudoreplicates to estimate distance variance. We excluded

from genetic distance calculations samples QCAZ 19064 (*P.* sp. CCS1), QCAZ 25428 (*P. ockendeni*), QCAZ 25676 (*P. quaquaversus*), QCAZ 25852 (*P. librarius*), QCAZ 45733 (*P.* sp. CCS3), QCAZ 45775 (*P.* sp.), QCAZ 5956 (*P. ardyae*), QCAZ 49670 (*P. ortizi*), QCAZ 51923 (*P. incomptus*), QCAZ 52498 (*P. ardyae*), QCAZ 59034 (*P. incanus*), MT281 (*P. hernandezi*), and DQ195458 (*P. hernandezi*) because their 16S fragment was too short (less than 500 bp) and not comparable in length to other samples.

We also inferred species boundaries with a Poison tree processes model for species delimitation (PTP; Zhang et al., 2013). This model infers putative species boundaries on a phylogenetic tree by considering its topology and branch lengths and assuming that the number of substitutions between species is higher than within species. The performance of the PTP model for *de novo* species delimitation has been tested by Zhan et al. (2013) showing better results than the General Mixed Yule Coalescent (GMYC) as well as OUT-picking methods. The main advantage of PTP is that it models speciation rate in terms of the number of substitutions instead of time, so it neither requires an ultrametric input tree (as required for GMYC) nor a sequence similarity threshold input (as required for OUT-picking method). Therefore, PTP replaces computationally expensive and error-prone practices for an operational criteria of gene coalescence (Zhang et al., 2013; Cottontail et al., 2014). We carried out the analyses in the bPTP web server (http://species.h-its.org/ptp/).

As input we used a Bayesian tree based on the 16S dataset, estimated with MrBayes v.3.1.2 (Ronquist et al., 2012). The Bayesian analysis for the PTP was performed under the following parameters: 100000 MCMC generations, thinning value of 100, burn-in of 0.1 and the tree was selected using the methods described above in the 2.3 section. Prior to the

PTP analysis the out-groups were removed. We visually reviewed the given trace and confirmed the convergence of the MCMC chain as recommended (Zhang et al., 2013).

2.4.1 Morphological Analyses

The format, terminology, and definition of diagnostic characters followed Lynch and Duellman (1997), Duellman and Lehr (2009), and Arroyo et al. (2005). The qualitative characters were mainly patterns of coloration, condition of tubercles (i.e., presence/absence, position, and shape), condition of diagnostic skin structures (i.e., presence/absence of paravertebral folds, dorsolateral folds, discoidal folds, and supratympanic fold), texture of skin (i.e., dorsal, ventral, and flanks), shape of head in lateral and dorsal view, and condition of toes and fingers (i.e., lateral fringes, comparative lengths). These character states of qualitative variables were treated as discrete. Fingers and toes were numbered preaxially to postaxially from I to IV and I to V, respectively. Comparative lengths of Toes III and V were determined when both were adpressed against Toe IV; lengths of Fingers I and II were compared when adpressed against each other. All of those observations, except the condition of toes and fingers, were also based on photographs of 34 live specimens (Appendix A) and preserved individuals included in the phylogenetic analyses.

For morphometric analyses we measured 88 alcohol-preserved adult specimens from the herpetological collections at Museo de Zoología of the Pontificia Universidad Católica del Ecuador (QCAZ) and Museo Ecuatoriano de Ciencias Naturales (MECN,). A list of measured specimens is given in Appendix A. Sex and reproductive condition were determined by inspection of secondary sexual traits of male frogs (i.e., vocal slits, extended vocal sac, nuptial pads) and by direct gonadal examination. Measurements were taken with

digital calipers (to nearest 0.01 mm) as appropriate, while fine-scale measurements (i.e. tympanum-eye distance) were made using a microscope eyepiece. The measurements used in the analyses were: SVL (snout–vent length), HL (head length, obliquely from angle of jaw to tip of snout), HW (head width, at level of angle of jaw), ED (eye diameter, distance between the anterior and posterior borders of the visible eye), IOD (interorbital distance, distance between the medial edge of the orbits), EW (upper eyelid width, length of the visible eye along the outer edge of eyelid), IND (internarial distance, distance between the inner edges of nares), E–N (eye–nostril distance, distance between the anterior corner of orbit and the posterior margin of nares), TY (tympanum diameter, horizontal distance between the borders of the tympanic annulus), E–Y (tympanum–eye distance, straight distance between posterior corner of the orbit and anterior margin of tympanum).

We conducted two types of multivariate statistical analyses using the morphometric measurements to assess differentiation among species. Principal Component Analyses (PCA) were used to reduce morphometric variables. Linear discriminant functional analysis (DFA) was conducted subsequently to determine if individuals could be assigned (based on morphometric data) to the correct species groups identified previously by molecular data. Specimens with missing measurements were not included in the DFA analysis. To avoid the effect of sexual dimorphism, the analyses were performed separately for males (n = 55) and females (n = 33). To evaluate variation in shape independent of size, PCA was applied to the residuals of linear regressions between the nine measured variables and SVL. Only components with eigenvalues > 1 were retained. The DFA was applied to the measured variables without size correction. All morphological measurements were log- transformed

to reduce heteroscedasticity and to improve normality. Statistical analyses were performed in software JMP 8.0.1 (SAS Institute Inc., 2009).

2.4.2 Environmental Species delimitation

The species analyzed herein are distributed in the Amazonian Andean slopes and Páramo of the south of Colombia and in central and northern Ecuador. We extracted climatic data only for localities of individuals with genetic sequences (Appendix A) from WorldClim bioclimatic layers with a spatial resolution of about 30" (Hijmans et al., 2005). Values were extracted with ArcGis v10.1 using the function "Extract Multi Values to Points". Bioclimatic variables are listed in Supplementary material Table S3. Principal Component Analyses (PCA) were performed with all bioclimatic variables to quantify niche differences between our sampled species (Broennimann et al., 2012).

2.4.3 Divergence Times and Ancestral Altitude Reconstruction

In order to investigate the altitudinal origins of our sampled clade and its subsequent history of dispersal along the altitudinal gradient, we reconstructed ancestral altitudes for all the species using Bayesian inference in software BEAST 1.8.0 (Drummond et al., 2012). The analysis infers simultaneously the phylogeny, divergence times, and ancestral altitudes.

Estimates of divergence times were based on node ages estimated by Pyron (2014). Pyron (2014) analysis contained 3309 species of amphibians and was calibrated using the fossil record. In our analysis, we set 7 calibration points: (1) 70. 47 Million years ago (Ma), for the divergence between the genus *Craugastor* from the clade *Oreobates* + *Hypodactylus*, + *Pristimantis*, (2) 68.70 Ma for the divergence between *Hypodactylus* and *Oreobates* +

Pristimantis, (3) 67.21 Ma for the divergence between *Oreobates* and *Pristimantis*, (4) the split between *P. eriphus* and the clade *P. chloronotus* + *P. supernatis* with an age of 24.67 Ma, (5) the most recent common ancestor (MRCA) of *P. chloronotus* and *P. supernatis*: 13.40 Ma (7) and the divergence between *P. verecundus* and *P. pyrrhomerus* at 23.64 Ma. Details regarding the primary calibrations are found in Pyron (2014).

The topology was inferred under substitution models estimated by PartitionFinder. A Yule speciation prior was used for branching rates. Molecular dates were estimated using a relaxed Bayesian clock (Drummond et al., 2012). The analyses were conducted with uncorrelated substitution rates among branches and the rate for each branch was drawn from a lognormal distribution (Drummond et al., 2006).

We reconstructed ancestral altitudes as a continuous character (see Appendix A) using the Bayesian stochastic search variable selection (BSSVS; Lemey et al., 2009). Parameters were estimated using five independent runs of 60 million generations each, sampled every 10000 generations. Convergence and effective sample sizes were checked in the software Tracer v1.5 (Rambaut and Drummond 2007). Results were compared for convergence using a burn-in of 10%. Finally, summary trees and posterior probabilities were obtained with TreeAnnotator v1.8.0 (Rambaut and Drummond, 2016). These analyses were carried through the CIPRES portal (Miller et al., 2010).

3. Results

3.1 Phylogenetics and species delimitation

All of the relationships recovered in the single gene and combined genes analyses were similar and did not show incongruences with high support (here we present the tree

obtained from the combined data; Fig. 1). The resulting full dataset of 3 genes and 2 intervening tRNAs contained 3146 bp (1304 bp of 16S, 87 bp of $tRNA^{leu}$, 958 bp of ND1, 70 bp of $tRNA^{ile}$, and 652 bp of RAG-1).

PartitionFinder selected a scheme of five partitions and models: (i) *16S*, *ND1* 1^{st} codon position, $tRNA^{ile}$, $tRNA^{gln}$, $tRNA^{leu}$ [GTR + I + G]; (ii) *ND1*, 2^{nd} position [HKY + I + G]; (iii) *ND1*, 3^{rd} position [GTR + I + G]; (iv) *RAG1*, 1^{st} position, *RAG1*, 2^{nd} position [HKY + I + G]; (v) *RAG1*, 3^{rd} position [K80 + G]. The ML analysis (best topology log likelihood = –32889.4; Fig. 1) yielded a tree that was topologically consistent with the Bayesian consensus tree, except for intraspecific branches and the relationship between *P. ortizi* and *P. supernatis*. There is strong support for the monophyly of our study group (BB = 94, PP = 1) and relationships among species with the exception of the clade *P. lividus* and *P. eriphus*. Within the ingroup, the earliest divergence occurs between the northern-most species, *Pristimantis hernandezi*, and the remaining species, which are separated in two widely sympatric clades (Fig. 1).

Uncorrected *p*-distances between species are detailed in Table 1 (a, b). The genetic distances between the samples of the ingroup ranged from 0% to 14.9% for 16S. We identified twenty species, based on genetic distances (threshold of 3%), which were also strongly supported clades in the phylogenetic analyses (Fig. 1).

3.2 Morphology

A total of 88 adult specimens were examined for morphometric analyses. After $\log_{10}$ transformation, almost all the variables fitted a normal distribution, for females ($W > 0.9363$; $P > 0.0532$; $n = 33$) and for males ($W > 0.9633$; $P > 0.091$; $n = 55$; except for E-N

measurements $W = 0.9491$; $P = 0.021$). Morphometric measurements of all the males and females, and results of the normality tests are summarized in Table 2 and Table 3.

Our morphological analyses focused on 14 out of 20 clades from Figure 1: *P. inusitatus, P. ardyae, P.* sp. CCS1, *P. llanganati, P. ortizi, P. colonensis, P. huicundo, P. thymelensis, P. incanus, P.* sp. CCS3, *P. roni, P.* sp. CCS4, *P. yanezi, P. lividus, P. eriphus*. For the remaining clades (*P. hernandezi*, *P.* sp. UCS1, *P. chloronotus, P. supernatis*) there were no available samples. Extensive characterization of morphological variation within clades was not possible because of the sparse taxon sampling for some groups. Six specimens of *P. thymelensis* (three females: QCAZ 40010, QCAZ 40012, QCAZ 52276, and three males: QCAZ 40011, QCAZ 40020, QCAZ 40021) lack external tympanum and, hence, TY and E–Y measurements are missing.

Loadings, eigenvalues, and percentage of variance explained by the Principal Components Analysis (PCA) are provided in Supplementary material Table S4. The PCA did not show differences among clades both among males and females (Fig. 2). Two components with eigenvalues > 1.0 were extracted from the PCA for females (Supplementary material Table S4). The two components accounted for 58% of the total variation. The highest loadings of the PCA for females were length and width of head, and eye–nostril distance for PC1, interorbital distance, internarial distance, and tympanic diameter for PC2. Principal component analysis for males found three components with eigenvalues > 1.0 (Supplementary material Table S4). The tree components accounted for 70% of the total variation. The highest loadings were head width, eye–nostril distance, and tympanum-eye distance for PC1, interorbital distance and internarial distance for PC2. PC3 loaded strongly on tympanum diameter and tympanum–eye distance (negatively).

The discriminant function analyses (DFA) of the morphometric data can successfully separate our sampled species, once sex is taken into account. Percentages of correct classification of the DFA were high in females (97%), correctly assigning 29 out of 30 specimens (Supplementary material Table S5). In males the percentage of correct classification was lower (75%), with 39 out of 52 specimens correctly assigned to their group (Supplementary material Table S6).

Qualitative characters, particularly color patterns and skin tuberculation, allowed differentiation between the sampled clades (Fig. 3 and Fig. 4), except for *P.* sp. CCS3 and *P.* sp. CCS4 that share similarities correlated with patterns of coloration at dorsum, flanks, venter, and iris between them and also with *P. eriphus*. A detailed description of these characters is presented in the following sections. A detailed summary of the qualitative traits of the species is presented in Tables 4, 5, and 6.

3.3 Geographic distribution and environmental envelope

We analyzed 28 localities for all the sampled species of the ingroup. The number of localities per clade was: 2 in *Pristimantis hernandezi*, 2 in *P. ardyae*, 1 in *P. chloronotus*, 3 in *P. colonensis*, 7 in *P. eriphus*, 2 in *P. huicundo*, 1 in *P. incanus*, 2 in *P. inusitatus*, 3 in *P. lividus*, 4 in *P. llanganati*, 1 in *P. ortizi*, 3 in *P. roni*, 1 in *P. supernatis*, 7 in *P. thymelensis*, 2 in *P. yanezi*, 2 in *P.* sp. CCS1, 1 in *P.* sp. CCS2, 1 in *P.* sp. CCS3, 2 in *P.* sp. CCS4, and 1 in *P.* sp. UCS1 (See Appendix A). All localities are in Andean montane forests and paramo of the Amazon slopes from southern Colombia to central and northern Ecuador. The only exception is *P. thymelensis*, which occurs in paramo of the eastern and western cordilleras. Seven localities shelter sympatric species (Table 7; Fig. 5).

The PCA for environmental variables shows few differences between our species except for *P. thymelensis* and *P. ortizi*, which inhabit colder areas than the other species (Fig. 6). Environmental variables, loadings, eigenvalues and percentage of explained variance are presented in Supplementary material Table S3. Three components with eigenvalues > 1.0 were extracted. Loadings for PC1 were high for temperature and precipitation variables, explaining 73.49% of the total variance. PC2 had a high positive loading on isothermality and a high negative loading on temperature seasonality, explaining 11% of the total variance. PC3 explained 7.3% of the total variance and loaded highly on mean diurnal temperature range, temperature seasonality, temperature annual range, and precipitation seasonality.

3.4 Integrative taxonomy

The PTP model for species delimitation identified a total of 28 putative species (20 species are the same than those recovered in our phylogenetic analyses; section 3.1), eight more than those presented in Fig. 1. Two putative species were recognized within what is known as *P. colonensis*. This split of a single clade into two putative species also occurs in other clades such as: *P. eriphus*, *P. huicundo*, *P. inusitatus*, *P. lividus*, *P. llanganati P. roni*, and *P.* sp. CCS1. (Supplementary material Fig. S1.). The branch lengths in the phylogeny, the genetic distances and the results from the PTP model suggest the presence of five undescribed species, two of them with only one available voucher (QCAZ 45851, QCAZ 46218; Fig. 1; Supplementary material Fig. S1.).

We define our undescribed lineages according to the categories of candidate species proposed by Vieites et al. (2009). Based on combined genetic and morphological evidence,

we are able to recognize fifteen clades, four confirmed candidate species and one unconfirmed candidate species. We assigned the UCS to QCAZ 45851 because although it is genetically divergent and a well-supported clade, we lack morphological data to test its status. The study of intra and interspecific morphological variation is the core of the description of new species (Dayrat, 2005). We do not describe any of the potential new species because we could not characterize adequately the variation within the CCS due to some unavailable vouchers. Undescribed CS represents a 35% increase in species richness, from 15 to 20 in our sampled clade.

3.5 Systematic accounts

We propose the creation of a new species group based primarily on our molecular phylogeny and inferred species limits to make the *Pristimantis* genus more manageable. We name the species group based on the earliest described species contained in the clade (*P. chloronotus*, following the International Code of Zoological Nomenclature, 1999). The species in this group have the characteristic morphology of most *Pristimantis* including T-shaped terminal phalanges, toes without membranes, and Toe V longer than Toe III. Frogs in the *P. chloronotus* group are characterized by a spiny appearance (i.e. presence of conical tubercles on dorsum, eyelids, heels and outer edge of tarsus), secondarily lost in *P. huicundo*, and (1) head about as wide as body; (2) tympanic annulus and tympanic membrane evident, tympanum sometimes concealed beneath the skin in *P. thymelensis*; (3) cranial crests absent, lateral margins of frontoparietals upturned in *P. thymelensis* and *P. roni*; (4) terminal discs on the digits expanded, secondarily lost in *P. thymelensis*; (5) Finger I shorter than Finger II; (6) Toe V longer than Toe III, usually reaches the distal margin of the distal subarticular tubercle on Toe IV; (7) lateral fringes present or absent on

digits; (8) subarticular tubercles well defined; (9) dorsolateral folds absent; (10) skin on venter areolate; (11) SVL range 14.78–30.21 mm in males, and 22.39–37.77 mm in females; (12) in life, dorsum greenish yellow to green, or greenish-brown, dorsum yellow to brown in *P. ardyae*, *P. colonensis*, *P. lividus*, *P. thymelensis*, and *P. yanezi*. Flanks, groins, posterior surfaces of thighs, and concealed surfaces of shanks bearing conspicuous coloration (e.g. red with glossy white points in *P. incanus*, bright yellow in *P. inusitatus* and *P. eriphus*, white or tan with black or dark brown diagonal stripes in *P. eriphus* and *P. llanganati* (Fig. 3, Fig. 4, Table 4, 5, 6).

3.5.1 Content

Fifteen formally described species: *Pristimantis ardyae*, *P. colonensis*, *P. chloronotus*, *P. eriphus*, *P. hernandezi*, *P. huicundo*, *P. incanus*, *P. inusitatus*, *P. llanganati*, *P. lividus*, *P. ortizi*, *P. roni*, *P. supernatis*, *P. thymelensis*, and *P. yanezi* (Fig. 1; Fig. 3; Fig. 4).

3.5.2 Distribution

Montane forests in the Amazonian slopes of the Andes of Ecuador and Colombia, from 1269 to 4640 m (Fig. 5). *Pristimantis thymelensis* and *P. ortizi* occurs in paramo, and only *P. thymelensis* also inhabits the western Andean Cordillera.

3.5.3 Remarks

The *P. chloronotus* species group is strongly supported (BB = 94, PP = 1) in our molecular phylogeny (Fig. 1). Our results agree with previous studies (e.g., Hedges et al., 2008; Pyron et al., 2011; Padial et al., 2014) with *P. eriphus*, *P. chloronotus*, and *P. supernatis* nested in

the same clade, but differ in the placement of *P. thymelensis* (Pyron et al., 2011; Padial et al., 2014) due to errors in the identification of genetic samples in the GenBank.

3.6 Divergence times and ancestral altitude reconstruction

The resulting tree inferred by BEAST (Fig. 7) is consistent with our phylogeny presented in section 3.1 (Fig. 1) (ML analysis), except for discrepancies occurring at nodes with low support in the reconstruction performed by BEAST. The differences between both trees are the position of three taxa: *P. ortizi* (PP = 0.3), *P. supernatis* (PP = 0.65) and *P. chloronotus* (PP = 0.32). Results of the chronobiogeographical analysis are summarized in Fig. 7 and Table 8. According to this analysis the *Pristimantis chloronotus* species group diverged from other congeners in the Oligocene 30.3 Ma (million years ago) (high posterior density interval [HPD] = 26.23–34.92) and began radiating 26 Ma, in the late Oligocene (HPD = 24.43–28.82).

The *Pristimantis chloronotus* species group originated at mid-altitudes (~2075 m), in montane forests. Elevation range and habitat type is highly conserved as shown by 17 out of 20 actual species inhabiting mid-elevations in montane forests. Our results show a single Miocene colonization of low temperature environments by the most recent common ancestor of *P. ortizi*, *P. huicundo*, and *P. thymelensis* in 8.9844 Ma (Fig. 7). Node ages of other taxa are presented in Table 8.

4. Discussion

4.1 Species limits and phylogeny

Our results show a high content of undescribed diversity within a well-sampled clade belonging to the largest genus of vertebrates in the world. The underestimation of species

richness within the *Pristimantis chloronotus* group results from the lack of taxonomic studies, and insufficient field sampling (e.g., Navarrete et al., 2016). We found seven new species (including two described by Navarrete et al., 2016) in a group of 15 described species. This large increase, 46% in species number, is consistent with recent molecular-based taxonomic reviews of *Pristimantis*, which have shown similar or higher content of undescribed species (e.g., 300% Elmer and Cannatella, 2008; 300% Ortega-Andrade et al., 2015; 200% Arteaga et al., 2016; Table 9).

The bPTP model for species delimitation overestimated the number of recognized species to 28. This issue can be attributed to the unbalanced dataset (large disparity in numbers of individuals among species). In general, this method has already found some failures when there is poor taxon sampling or when there is an uneven sampling per species (Zhang et al., 2013; Blanco-Bercial et al., 2014). The overestimation of putative species has been reported for other taxa as well (e.g., crustaceans, Blanco-Bercial et al., 2014; insects, Lin et al., 2015).

The genetic distances between species of the *P. chloronotus* species group range from 3.0% to 14.9% (Table 1) and fall within a broad range of values reported for other Neotropical frogs (e.g., Fouquet et al., 2014; Caminer and Ron, 2014) and also for other *Pristimantis* (e.g., Elmer and Cannatella, 2008; Guayasamin et al., 2015; Hutter and Guayasmin, 2015). A revision of recent gene-based taxonomic reviews within *Pristimantis* (Table 9) shows that intra-group genetic distances vary widely among groups. The small genetic distances used to delimit species in Amazonian *Pristimantis* (Ortega-Andrade et al., 2015; 1.6 for 16S) indicates that low levels of genetic diversity (under the 3% threshold, Fouquet et al., 2004) could also be an indicative of candidate species. Setting genetic distances thresholds

to define species boundaries is problematic because the level of genetic differentiation between nascent sister species depends on speciation mode. On the lower end, species that originate via hybridization or adaptive-radiation are likely to show low genetic distances (e.g., Lamichhaney et al., 2015) In contrast, species that diverge predominantly via genetic drift in allopatry should require longer time to develop reproductive incompatibility resulting in larger genetic distances (Coyne and Orr 2004). Moreover, interspecific genetic distances are gene and taxon dependent and gene trees may be inconsistent with species trees (Vences and Wake 2007). The different scenarios of speciation make impractical choosing a threshold for genetic distances to define species limits. Genetic distances, however, can be used as a reference to identify taxonomic units that could represent species. In combination with other datasets (e.g., morphology, environmental niche) genetic information is opening a new era of species discovery in the tropics (Ortega-Andrade et al., 2015). Therefore, the high-uncorrected *p* values underpin a likely scenario for allopatric diversification in the *P. chloronotus* species group.

The still inadequate taxonomy of *Pristimantis* is perhaps the result of its high diversity and high intraspecific morphological plasticity (Hedges et al., 2008; Guayasamin et al., 2015). Although previous phylogenies of *Pristimantis* (Hedges et al., 2008; Pyron and Wiens, 2011; Pinto-Sánchez et al., 2012; Padial et al., 2014; Guayasamin et al., 2015; Mendoza et al., 2015; Pyron et al., 2011; Padial et al., 2014) only included three species of our group (i.e., *P. eriphus*, *P. chloronotus* and *P. supernatis*) they were consistent with our phylogeny in showing a strongly supported clade. The only incongruences pertain the placement of "*P. thymelensis*" and "*P. inusitatus*" as result of misidentified sequences in GenBank. The most inclusive phylogenies of *Pristimantis* (Hedges et al., 2008; Pyron et al., 2011; Pinto-

Sánchez et al., 2012; Padial et al., 2014, Mendoza et al., 2015) showed that most of the traditional species groups, which were proposed using morphological evidence, were not monophyletic. Species of the *Pristimantis chloronotus* group were formerly placed in paraphyletic species groups due to incorrect interpretation of the highly variable and homoplastic morphology of the genus (e.g., relative lengths of Toes III and V, tubercles, coloration, and cranial crests). For example, the erroneous placement of *P. thymelensis* in numerous and non-related clades (*P. orcesi* species group, Guayasamin, 2004; *P. myersi* species group, Padial et al., 2014).

Integrative taxonomy seeks for congruence among data sets as the main criterion to delimit species boundaries (Cardoso et al., 2009). On our study the most informative dataset to delimit species were the genetic and qualitative morphological sets. In contrast, neither the morphometric nor the environmental sets performed well at differentiating species (Fig. 2; Fig. 6). The DFA yielded correct classifications ranging from 76% to 96%. Nevertheless, the probability of including individuals in a particular group with DFA depends on the relative abundance of that group (Wollerman and Wiley, 2002). So our data was probably not the best linear unbiased estimator of correct grouping given the uneven sampling of individuals per species.

We were able to find qualitative morphological characters diagnostic of the *Pristimantis chloronotus* group. Although no synapomorphy has been yet identified for the *P. chloronotus* species group, the presence of abundant and prominent tubercles and the mossy or greenish coloration (spiny appearance) are two of the most taxonomic useful characteristics shared by almost all the species of the *P. chloronotus* group, except for a secondary loss in *P. thymelensis*. Furthermore, many unrelated species share with the *P.*

chloronotus species group similar morphology that resembles "spiny" appearance. Some phylogenies have shown that these complexes of frogs are not closely related to members of the *P. chloronotus* species group, including *P. galdi* (Hedges et al., 2008; Pyron and Wiens, 2011; Pinto-Sánchez et al., 2012), *P. mutabilis* (Guayasamin et al., 2015), and *P. katoptroides* (Ron, unpublished; sequences of *P. katoptroides* used as outgroup in our phylogenetic analyses). We suggest that the presence of "spiny" appearance in these unrelated groups of frogs is the result of convergent evolution associated with environmental camouflage rather than sexual selection or dimorphism (e.g., *P. mutabilis*, Guayasamin et al., 2015). The qualitative variables are useful to differentiate among species of our group, even when juveniles are included. Similar results have been reported for other *Pristimantis* species groups (e.g., Arroyo et al., 2005; Ortega-Andrade et al., 2015).

4.2 Divergence times and altitudinal reconstruction: origin of *Pristimantis chloronotus* species group

All species of the *Pristimantis chloronotus* species group occur in the eastern versant of the Andes in southern Colombia and central and northern of Ecuador, except for *P. thymelensis* that occurs also in paramo of the western Andean cordillera in Carchi province. Seventeen out of twenty species inhabit montane cloud forest, two upper montane forests and paramo, and one paramo exclusively. Our estimates show that the most recent common ancestor (MRCA) of the *P. chloronotus* species group occurred at mid-altitudes (Fig. 7). Our results also suggest that the species occurring in paramo (*P. ortizi*, *P. huicundo* and *P. thymelensis*) originated from a single event of colonization at 8.98 Ma.

There is disagreement between our age estimate of paramo colonization and the trajectory of Andean orogenesis. Results suggest that the MRCA of *P. ortizi*, *P. huicundo*, and *P. thymelensis* reached an altitude of an average 3000 m during the late Miocene (8.98 Ma), which is inconsistent with the maximum elevation available at that time. Because of the recent uplift of the northern Andes, the upland environments where *P. thymelensis*, *P. ortizi*, and *P. huicundo* are found have been available for colonization only since the late Pliocene or Pleistocene, 2–4 Ma (Burnham and Graham, 1999; Gregory-Wodzicki, 2000).

The planet dramatically cooled in the Eocene- Pleistocene transition (Sage et al., 2012). Moreover, since the Miocene there was an intense global cooling trend that radically changed the environment of South America and could explain the progression from lowland to upland biotas (Gregory-Wodzicki, 2000). These climate changes shifted vegetation formations to lower elevations. Cloud forest and paramo were lower in altitude and less isolated between each other than they are today (Lynch and Duellman, 1997). Therefore, it is possible that the ancestor of *P. ortizi*, *P. huicundo*, and *P. thymelensis* (species of the *P. chloronotus* species group living in high altitudes) was exposed to cold climate conditions, even at mid-altitudes (elevations below 3000 m) and adapted to inhabit in low temperature environments as suggested for other amphibians (Navas, 2006).

The most recent common ancestor of the major clade of the *P. chloronotus* species group occurred during the late Oligocene, node age at 30.3 Ma. This timing is compatible with estimates of the origin of *Pristimantis* at 37 Ma (Heinicke et al., 2007) or 67.2 Ma (Pyron, 2004). It has been suggested that *Pristimantis* began an explosive diversification at 24 Ma (Heinicke et al., 2007), which is consistent with the split of the *P. chloronotus* species group into two major subclades by 26 Ma and the subsequent rapid radiation of the group

during the Oligocene-Pleistocene transition. These cladogenic events were probably linked with the Andean uplift and also associated to climatic changes that result in cycles of habitat isolation, genetic isolation, and speciation (Lynch and Duellman, 1997), similar to patterns shown for other taxa such as plants, birds, and insects (Antonelli et al., 2010; Turchetto-Zolet et al., 2013; Quintero et al., 2013; Sanín et al., 2016; Nattier et al., 2016).

We propose that the diversification of the *P. chloronotus* species group was strongly tied to Andean orogeny. Therefore, both geographic isolation and complex environmental gradients have played important roles in the genesis of new species. The current distributional ranges of our studied specimens (Fig. 5) and their position in the phylogenetic tree (Fig. 1) suggests that the *P. chloronotus* species group diversified by allopatric speciation, with subsequent range shifts into sympatry (Fig. 5; Table 7). We propose vicariance as the most common scenario for diversification within the *P. chloronotus* species group. This can be inferred from current distribution patterns, for example the current distribution of the clade containing *P. inusitatus*, *P. ardyae*, *P. llanganati*, *P.* sp. CCS1, and *P.* sp. UCS1 are allopatric with their sister clade containing *P. chloronotus*, *P. ortizi*, *P. supernatis*, *P. colonensis*, *P. huicundo*, *P.* sp. CCS2, and *P. thymelensis* (Fig. 1; Fig. 5), with a small area of sympatry in the surroundings of Napo province. The same case for *P. inusitatus* and their sister species *P. ardyae*, *P. llanaganti*, *P.* sp. CCS1, and *P.* sp. UCS1 (Fig. 1; Fig. 5). Also, *P. roni* and their sister taxa *P. incanus*, *P.* sp. CCS3, and *P.* sp. CCS4 inhabits in allopatry. As shown in our environmental analysis there is no significant differences between the bioclimatic conditions within the *P. chloronotus* species group (Fig. 6). If allopatric sister species are consistently inhabiting identical or nearly identical environmental space, then there is no major effect of ecology in

the diversification of the group (in relation to the bioclimatic variables examined), suggesting alternatives such as incidental divergence in isolation, produced most likely by vicariance events (Graham et al., 2004). In the other hand, there are seven cases of sister species living in sympatry (reported section 3.3): For example, *P. ardyae* overlaps with the range of its sister group, *P. llanganati*, *P.* sp. CCS1, and *P.* sp. UCS1. Speciation in those cases could have occurred by niche partitioning or differential selection. Allopatric speciation with subsequent secondary contact it is also a possibility. Allopatry regulated by geographical barriers is the most common (or at least the most reported) speciation mode (e.g., Coyne and Orr 2004; Ribas et al., 2007; McCormack et al., 2010); but also there is strong evidence for parapatric speciation along ecological gradients as an important mechanism of diversification of Andean amphibians (Lynch and Duellman, 1997).

4.3 Implications for conservation

Montane systems are important reservoirs of diversity and endemism in tropical regions (Smith et al., 2007; Hutter et al., 2013)). This is especially true for *Pristimantis* that reaches its peak of diversity in the Andes of Colombia, Ecuador, and Peru (Lynch and Duellman, 1997; Duellman and Lehr, 2009). It is widely known that several taxonomic groups reach their highest species richness at intermediate elevations with narrow distributional ranges (e.g., McCain 2005; Oomen and Shanker, 2005) that are increasingly threatened due to anthropogenic disturbances in the environment (Cuesta et al., 2012), which is also true for *Pristimantis* (Young et al., 2004). The discovery of hidden species richness (cryptic and non-cryptic) has profound implications for evolutionary, biogeography, and conservation studies (Bickford et al., 2007; Devictor et al., 2010; Glaw et al., 2010). Our results show that the diversity within *Pristimantis* is still underestimated and highlight the importance of

incorporating dense sampling, robust phylogenetic methods, and integrative analysis to improve our knowledge on species richness.

The complex topography and the high levels of local endemism (Ricketts et al., 2005) make Andean systems especially sensitive to anthropogenic disturbances (e.g., agriculture, cattle rising, logging, mining) (Cincotta et al., 2000; Herzog et al., 2011) and climate change (Bush et al., 2004; Raxworthy et al., 2008; Cuesta et al., 2012). Geographic range is an important criterion to assess the conservation status of species (Agapow et al., 2004) as the probability of extinction is higher for those species inhabiting small areas (Thomas et al., 2004). Our study shows that all species of the *Pristimantis chloronotus* group have small distributional ranges (Fig. 5) and live in montane forests, only two of them reached the paramo (Fig. 7).

The present study offers a more reliable measure of the species richness of the hyperdiverse *Pristimantis* genus, discovering at least five new candidate species (Fig. 1). Results show high genetic distances (3% to 14.9%; Table 1) among species of the *P. chloronotus* group, these values are similar to those reported for other *Pristimantis* that inhabits montane regions and could be a consequence of allopatric speciation reported for the *P. chloronotus* group in this study. We also present novel insights into the historical biogeography of the *Pristimantis* genus under a new sampling strategy: “top-down” sampling which shows a better resolution of the phylogenetic relationships and therefore offers a more reliable approach to understand patterns of diversification and distribution, speciation mechanisms, and historical origins of the biodiversity. Results show vicariance as the most likely scenario of diversification of the *P. chloronotus* species group, with subsequent shifts into parapatric or sympatric distributions (Fig. 5). Furthermore, our results are a new argument

for the protection of montane regions in order to maintain the processes that promote speciation and diversity.

Acknowledgments

This study was supported by grants from the Secretaría Nacional de Educación Superior, Ciencia, Tecnología e Innovación del Ecuador SENESCYT, Arca de Noé Initiative, and Dirección General Académica de la Pontificia Universidad Católica del Ecuador. The Ministerio de Ambiente del Ecuador provided research and collection permits. We thank Gabriela Castillo and Andrea Manzano for laboratory work, as well as Esther Cole, Martín Bustamante, Fernando Nogales, Elicio Tapia, Verónica Sáenz, Lourdes Echeverría, Pablo J. Venegas, Diego Almeida-Reinoso, and Edwin Nuñez, who helped obtaining samples in the field. Diego Paucar, FernandoAyala-Varela, and Yerka Sagredo for assisting access to the specimen and tissue collection. Special thanks to Mariane Targino for kindly providing a tissue of *P. hernandezi* from Colombia. John Jairo Mueses-Cisneros, Pablo J. Venegas, and Mario Yánez-Muñoz provided specimen and locality data. Nadia Páez, Simón Lobos, and Andrés Merino-Viteri gave valuable advice and help during the research. We thank Omar Torres-Carvajal, Andrés Merino-Viteri, and Rafael E. Cárdenas, for comments on the manuscript.

Literature Cited

AmphibiaWeb. Information on amphibian biology and conservation. [web application]. 2017. AmphibiaWeb, Berkeley, California. Available at http://amphibiaweb.org/. (Accessed: 3 Jan 2017).

Agapow, P.M., Binida-Emonds, O.R.P., Crandall, K.A., Gittleman, J.L., Mace, G.M., Marshall, J.C., Purvis, A., 2004. The Impact of Species Concept on Biodiversity Studies. Quart. Rev. Biol. 79, 161–179.

Antonelli, A., Quijada-Mascareñas, A., Crawford, A.J., Bates, J.M., Velazco, P.M., Wüster, W., 2010. Molecular studies and phylogeography of Amazonian tetrapods and their relation to geological and climatic models, in: Hoorn, C., Wesselingh, F. P. (Eds.), Amazonia: Landscape and Species Evolution: A Look into the Past, Wiley-Blackwell, West Sussex, UK, pp. 386-404.

Arroyo, S.B., Sánchez, P.M., Ramírez-Pinilla, M.P., Suárez, H.A., Miranda-Esquivel, D.R., 2005. Morphometric analysis to differentiate taxonomically seven species of *Eleutherodactylus* (Amphibia: Anura: Leptodactylidae) from an Andean cloud forest of Colombia. Zootaxa 1018, 1–14.

Arteaga, A., Pyron, R.A., Peñafiel, N., Romero-Barreto, P., Culebras, J., Bustamante, L., ... Guayasamin, J.M., 2016. Comparative Phylogeography Reveals Cryptic Diversity and

Repeated Patterns of Cladogenesis for Amphibians and Reptiles in Northwestern Ecuador. PloS one 11, e0151746.

Barley, A.J., White, J., Diesmos, A.C., Brown, R.M., 2013. The challenge of species delimitation at the extremes: diversification without morphological change in Philippine sun skinks. Evolution 67, 3556–3572. doi : 10.1111/evo.12219

Bickford, D., Lohman, D.J., Sodhi, N.S., Meier, P.K.L.Ng, R., Winker, K., Ingram, K.K., Das, I., 2007. Cryptic species as a window on diversity and conservation. Trends Ecol. Evol. 22, 148–155.

Blanco-Bercial L, Cornils A, Copley N, Bucklin A., 2014. DNA barcoding ofmarine copepods: assessment of analytical approaches to species identification. PLoS Curr. Tree Life 6: ecurrents.tol.cdf8b74881f87e3b01d56b43.

Broennimann, O., Fitzpatrick, M.C., Pearman, P.B., Petitpierre, B., Pellissier, L., Yoccoz, N.G., ..., Graham, C.H., 2012. Measuring ecological niche overlap from occurrence and spatial environmental data. Global Ecology and Biogeography 21, 481–497.

Brumfield, R.T., Edwards, S.V., 2007. Evolution into and out of the Andes: a Bayesian analysis of historical diversification in *Thamnophilus* antshrikes. Evolution 61, 346–367.

Burnham, R.J., Graham, A., 1999. The history of Neotropical vegetation: New developments and status. Ann. Missouri Bot. Gard. 86, 546–589.

Bush, M.B., Miles, S.R., Urrego, D.H., 2004. 48,000 Years of Climate and Forest Change in a Biodiversity Hot Spot. Science 303, 827–829. doi: 10.1126/science.1090795

Cadena, C.D., Klicka, J., Ricklefs, R.E., 2007. Evolutionary differentiation in the Neotropical montane region: molecular phylogenetics and phylogeography of Buarremon brush-finches (Aves, Emberizidae). Mol. Phylogenet. Evol. 44, 993-1016. doi:10.1016/j.ympev.2006.12.012

Caminer, M.A., Ron, S.R., 2014. Systematics of treefrogs of the *Hypsiboas calcaratus* and *Hypsiboas fasciatus* species complex (Anura, Hylidae) with the description of four new species. ZooKeys 370, 1–68. doi: 10.3897/zookeys.370.6291

Cardoso, A., Serrano, A., Vogler, A.P., 2009. Morphological and molecular variation in tiger beetles of the *Cicindela hybrida* complex: is an 'integrative taxonomy' possible? Mol. Ecol. 18, 648–664.

Chaves, J.A., Smith, T.B., 2011. Evolutionary patterns of diversification in the Andean hummingbird genus Adelomyia. Mol. Phylogenet. Evol. 60, 207–218. doi:10.1016/j.ympev.2011.04.007

Cincotta, R.P., Wisnewski, J., Engelman, R., 2000. Human population in the biodiversity hotspots. Nature 404, 990–992. doi:10.1038/35010105

Cook, L.G., Edwards, R.D., Crisp, M.D., Hardy, N.B., 2010. Need morphology always be required for new species descriptions?. Invertebrate systematics 24, 322–326. doi: 10.1071/IS10011

Cottontail, V. M., Kalko, E. K., Cottontail, I., Wellinghausen, N., Tschapka, M., Perkins, S. L., Pinto, C. M., 2014. High local diversity of *Trypanosoma* in a common bat species,

and implications for the biogeography and taxonomy of the *T. cruzi* clade. *PLoS One* 9, e108603.

Coyne, J.A., Orr, H.A., 2004. Speciation. Sinauer Associates, Sunderland, MA. 545 pp.

Cuesta, F., Muriel, P., Beck, S., Meneses, R.I., Halloy, S., Salgado, S., Ortiz, E., Becerra, M.T., 2012. Biodiversidad y Cambio Climático en los Andes Tropicales- Conformación de una red de investigación para monitorear sus impactos y delinear acciones de adaptación. Red Gloria-Andes, Lima- Quito. pp 1–180.

Dayrat, B., 2005. Towards integrative taxonomy. Biol. J. Linn. Soc-Lond. 85, 407–415. doi: 10.1111/j.1095-8312.2005.00503.x

de Queiroz, K., 1998. The general lineage concept of species, species criteria, and the process of speciation: a conceptual unification and terminological recommendations. In: Howard DJ, Berlocher SH, editors. Endless forms: species and speciation. Oxford: Oxford University Press; 57–75.

de Queiroz, K., 2005. Ernst Mayr and the modern concept of species. Proc. Natl. Acad. Sci. U.S.A. 102, 6600–6607.

de Queiroz, K., 2007. Species concepts and species delimitation. Syst. Biol. 56, 879–886.

Devictor, V., Clavel, J., Julliard, R., Lavergne, S., Mouillot, D., Thuiller, W., Venail, P., Villéger, S., Mouquet, N., 2010. Defining and measuring ecological specialization. J. Appl. Ecol. 47, 15–25.

Drummond, A.J., Ho, S.Y.W., Phillips, M.J., Rambaut, A., 2006. Relaxed phylogenetics and dating with confidence. PLOS Biol. 4, 699–710.

Drummond, A.J., Suchard, M.A., Xie, D., Rambaut. A., 2012. Bayesian Phylogenetics with BEAUti and the BEAST 1.7. Molecular Biology and Evolution 29, 1969–1973.

Duellman, W. E., 1979. The herpetofauna of the Andes: patterns of distribution, origin, differentiation and present communities. In: The South American Herpetofauna: Its Origin, Evolution, and Dispersal (W. E. Duellman, ed.) pp. 371–459. Monograph of the Museum of Natural History, the University of Kansas, Kansas, USA.

Duellman, W.E., Lehr, E., 2009. Terrestrial-breeding frogs (Strabomantidae) in Peru. Natur and Tier – Verlag GmbH, Münster.

Elmer K.R., Cannatella D.C., 2008. Three new species of leaflitter frogs from the upper Amazon forests: cryptic diversity within *Pristimantis* "*ockendeni*" (Anura: Strabomantidae) in Ecuador. Zootaxa 1784: 11–38.

Elmer, K.R., Dávila, J.A., Lougheed, S.C., 2007. Cryptic diversity and deep divergence in an upper Amazonian frog, *Eleutherodactylus ockendeni*. BMC Evol. Biol. 7, 247. doi:10.1186/1471-2148-7-247.

Esselstyn, J.A., García, H.J.D., Saulog, M.G., Heaney, L.R., 2008. A new species of *Desmalopex* (Pteropodidae) from the Philippines, with a phylogenetic analysis of the Pteropodini. J.Mammal. 89: 815–825.

Fouquet, A., Gilles, A., Vences, M., Marty, C., Blanc, M., Gemmell, N. J., 2007. Underestimation of species richness in Neotropical frogs revealed by mtDNA analyses. PLoS Biol. 2, e1109.

Frost, D.R. 2016. Amphibian Species of the World: an Online Reference. Version 5.4. Available at: http:// research.amnh.org/herpetology/amphibia/index.php.

Gibbons, A., 1998. Calibrating the mitochondrial clock. Science 279, 28–29.

Glaw, F., Koehler, J., De la Riva, I., Vieites, D.R., Vences, M., 2010. Integrative taxonomy of Malagasy treefrogs: combination of molecular genetics, bioacoustics and comparative morphology reveals twelve additional species of Boophis. Zootaxa 2383, 1–82.

Graham, C.H., Ron, S.R., Santos, J.C., Schneider, C.J., Moritz, C., 2004. Integrating phylogenetics and environmental niche models to explore speciation mechanisms in dendrobatid frogs. Evolution 58, 1781–1793. doi: 10.1111/j.0014-3820.2004.tb00461.x

Gregory-Wodzicki, K.M., 2000. Uplift history of the Central and Northern Andes: a review. Geol. Soc. Am. Bull. 112, 1091–1105. doi: 10.1130/0016-7606(2000)112<1091:UHOTCA>2.0.CO;2

Guayasamin, J.M., 2004. The *Eleutherodactylus orcesi* species group (Anura: Leptodactylidae): comparative osteology and comments on its monophyly. Herpetological Monographs 18, 142–147.

Guayasamin, J.M., Almeida-Reinoso, D.P., Nogales-Sornosa, F., 2004. Two new species of frogs (Leptodactylidae: *Eleutherodactylus*) from the high Andes of northern Ecuador. Herpetological Monographs 18, 127–141.

Guayasamin, J.M., Krynak, T., Krynak, K., Culebras, J., Hutter, C.R., 2015. Phenotypic plasticity raises questions for taxonomically important traits: a remarkable new Andean rainfrog (*Pristimantis*) with the ability to change skin texture. Zool. J.Linn. Soc-Lond. 173, 913–928. doi: 10.1111/zoj.12222.

Hedges, S.B., Duellman, W.E., Heinicke, M.P., 2008. New World direct-developing frogs (Anura: Terrarana): molecular phylogeny, classification, biogeography, and conservation. Zootaxa 1737, 1–182.

Heinicke, M.P., Duellman, W.E., Hedges, S.B., 2007. Major Caribbean and Central American frog faunas originated by ancient oceanic dispersal. Proc. Natl. Acad. Sci. 104, 10092–10097. doi: 10.1073/pnas.0611051104

Heinicke, M., Duellman, W., Trueb, L., Means, D., MacCulloch, R., Hedges, S., 2009. A new frog family (Anura: Terrarana) from South America and an expanded direct-developing clade revealed by molecular phylogeny. Zootaxa 2211, 1–35.

Herpetological Animal Care and Use Committee. 2004. Guidelines for use of live amphibians and reptiles in field and laboratory research: Miami: American Society of Ichthyologists and Herpetologists.

Herzog, S.K., Martínez, R., Jørgensen, P.M., Tiessen, H., 2011. Climate change and biodiversity in the tropical Andes. Inter-American institute for global change research

(IAI) and Scientific committee on problems of the environment (SCOPE), Sao José dos Campos, Brazil, pp. 1–348.

Hijmans, R.J., Cameron, S.E., Parra, J.L., Jones, P.G., Jarvis, A., 2005. Very high resolution interpolated climate surfaces for global land areas. Int. J. Climatol. 25, 1965–1978.

Hillis, D.M., Bull, J.J., 1993. An empirical test of bootstrapping as a method for assessing confidence in phylogenetic analysis. Syst. Biol. 42, 182–192.

Hoorn, C., Wesselingh, F.P., Ter Steege, H., Bermudez, M.A., Mora, A., Sevink, J., ... Jaramillo, C., 2010. Amazonia through time: Andean uplift, climate change, landscape evolution, and biodiversity. Science 330, 927–931. doi: 10.1126/science.1194585

Hughes, C., Eastwood, R., 2006. Island radiation on a continental scale: exceptional rates of plant diversification after uplift of the Andes. Proc. Natl. Acad. Sci. U. S. A. 103, 10334–10339. doi:10.1073/pnas.0601928103

Hutter, C.R., Guayasamin, J.M., Wiens, J.J., 2013. Explaining Andean megadiversity: the evolutionary and ecological causes of glassfrog elevational richness patterns. Ecol. Lett. 16, 1135–1144.

Hutter, C.R., Guayasamin, J.M., 2015. Cryptic diversity concealed in the Andean cloud forests: two new species of rainfrogs (*Pristimantis*) uncovered by molecular and bioacoustic data. Neot. Biod 1, 36–59.

International Commission of Zoological Nomenclature. 1999. International code of zoological nomenclature, 4th ed. London: International Trust for Zoological Nomenclature.

IUCN 2016. The IUCN Red List of Threatened Species. Version 2016-2. <http://www.iucnredlist.org>. Downloaded on 26 August 2016.

Jenkins, C.N., Pimm, S.L., Joppa, L.N., 2013. Global patterns of terrestrial vertebrate diversity and conservation. Proc. Natl. Acad. Sci. U. S. A. 110, E2602–E2610. doi: 10.1073/pnas.1302251110

Jørgensen, P., León- Yánez, S., 1999. Catalogue of the Vascular Plants of Ecuador. Missouri Botanical Garden. St. Louis.

Katoh, K., Standley,D.M ., 2013. MAFFT multiple sequence alignment software version 7: improvements in performance and usability. Mol. Biol. Evol. 30, 772–780.

Lamichhaney, S., Berglund, J., Almén, M.S., Maqbool, K., Grabherr, M., Martinez-Barrio, A., ... Grant, B.R., 2015. Evolution of Darwin's finches and their beaks revealed by genome sequencing. Nature 518, 371–375. doi: 10.1038/nature14181

Lanfear, R., Calcott, B., Ho, S.Y.W.,Guindon, S., 2012. PartitionFinder: combined selection of partitioning schemes and substitution models for phylogenetic analyses. Mol. Biol. and Evol. 29, 1695–1701. http://dx.doi.org/10.1093/molbev/mss020

Lemey, P., Rambaut, A., Drummond, A.J., Suchard, M.A., 2009. Bayesian phylogeography finds its roots. PLoS Comput. Biol. 5, e1000520.

Lin, X., Stur, E., Ekrem, T., 2015. Exploring genetic divergence in a species-rich insect genus using 2790 DNA Barcodes. PloS one 10, e0138993.

Luebert, F., Hilger, H.H., Weigend, M., 2011. Diversification in the Andes: age and origins of South American *Heliotropium* lineages (Heliotropiaceae, Boraginales). Mol. Phylogenet. Evol. 61, 90–102.

Lynch, J.D., 1969. Identity of two Andean *Eleutherodactylus* with the description of a new species (Amphibia: Leptodactylidae). J.Herpetol. 3, 135–143.

Lynch, J.D., 1970. A new eleutherodactyline frog from Amazonian Ecuador. Proc. Biol. Soc. Wash. 83, 221–226.

Lynch, J.D., 1972. Two new species of frogs (*Eleutherodactylus*: Leptodactylidae) from the páramos of northern Ecuador. Herpetologica 28, 141–147.

Lynch, J.D., 1976. The species groups of the South American frogs of the genus *Eleutherodactylus* (Leptodactylidae). Occ. Pap. Mus. Nat. Hist. Univ. Kansas 61, 1–24.

Lynch, J.D., 1979. The identity of *Eleutherodactylus vertebralis* (Boulenger) with the description of a new species from Colombia and Ecuador (Amphibia: Leptodactylidae). J. Herpetol. 13, 411–418.

Lynch, J.D., 1981. Leptodactylid frogs of the genus *Eleutherodactylus* in the Andes of northern Ecuador and adjacent Colombia. Misc. Pub. Univ. Kansas 72, 1–46.

Lynch, J.D., Duellman, W.E., 1980. The *Eleutherodactylus* of the Amazonian slopes of the ecuadorian Andes (Anura: Leptodactylidae). Misc. Pub. Univ. Kansas 69, 1–86.

Lynch, J.D., Duellman, W.E., 1997. Frogs of the genus Eleutherodactylus in western Ecuador: systematics, ecology, and biogeography. Univ. Kansas Nat. Hist. Mus. Spec. Pub. 23, 1–236.

Lynch, J.D., Ruiz-Carranza, P.M., 1983. New frogs of the genus *Eleutherodactylus* from the Andes of Southern Colombia. T. Kansas Acad. Sci. 1903, 99–112.

Maddison, W.P., Maddison, D.R., 2011. Mesquite: A modular system for evolutionary analysis, version 2.75. Software accessible at http://mesquiteproject.org.

McCain, C.R., 2005. Elevational gradients in diversity of small mammals. Ecology 86, 366–372. doi:10.1890/03-3147

McCormack, J.E., Zellmer, A.J., Knowles, L.L., 2010. Does niche divergence accompany allopatric divergence in Aphelocoma jays as predicted under ecological speciation?: insights from tests with niche models. Evolution 64, 1231–1244.

Mendoza, A.M., Ospina, O.E., Cárdenas-Henao, H., García-R, J.C., 2015. A likelihood inference of historical biogeography in the world's most diverse terrestrial vertebrate genus: Diversification of direct-developing frogs (Craugastoridae: *Pristimantis*) across the Neotropics. Mol. Phylogen. Evol. 85, 50–58.

Miller, M., Holder, M., Vos, R., Midford, P., Liebowitz, T., Chan, L., Hoover, P., Warnow, T., 2010. The CIPRES Portals. CIPRES, <http://www.phylo. org/sub_sections/portal> (accessed 02.07.16).

Moritz, C., Patton, J.L., Schneider, C.J., Smith, T.B., 2000. Diversification of rainforest faunas: an integrated molecular approach. Annu. Rev. Ecol. Syst. 31, 533–563.

Muchhala, N., Patricio, M.V., Luis, A.V., 2005. A new species of Anoura (Chiroptera: Phyllostomidae) from the Ecuadorian Andes. J. Mammal. 86, 457–461.

Mueses-Cisneros, J.J., 2007. Two new species of the genus *Eleuterodactylus* (Anura: Brachycephalidae) from Valle de Sibundoy, Putumayo, Colombia. Zootaxa 1498, 35–43.

Muñoz-Ortiz, A., Velásquez-Álvarez, Á.A., Guarnizo, C.E., Crawford, A.J., 2015. Of peaks and valleys: testing the roles of orogeny and habitat heterogeneity in driving allopatry in mid-elevation frogs (Aromobatidae: Rheobates) of the northern Andes. J. Biogeogr. 42, 193–205.

Myers, N., Mittermeier, R.A., Mittermeier, C.G., da Fonseca, G.A.B., Kent, J., 2000. Biodiversity hotspots for conservation priorities. Nature 403, 853–858.

Nattier, R., Capdevielle-Dulac, C., Cassildé, C., Couloux, A., Cruaud, C., Lachaume, G., et al., 2016. Phylogeny and diversification of the cloud forest *Morpho sulkowskyi* group (Lepidoptera, Nymphalidae) in the evolving Andes. Zool. Scr. 1–14.

Navarrete, M., Ron, S.R., Venegas, P.J., 2016. Two new species of frogs of the genus *Pristimantis* (Anura: Craugastoridae) from Llanganates National Park in Ecuador with comments on the regional diversity of Ecuadorian *Pristimantis*. Zookeys 593, 139-162. doi: 10.3897/zookeys.593.8063

Navas, C., 2006, Patterns of distribution of anurans in high Andean tropical elevations: Insights from integrating biogeography and evolutionary physiology. Integrative and comparative biology 46, 82–91.

Oomen, M.A., Shanker., K., 2005. Elevational species richness patterns emerge from multiple local mechanisms in Himalayan woody plants. Ecology 86, 3039–3047. doi: 10.1890/04-1837

Ortega-Andrade, H.M., Rojas-Soto, O.R., Valencia, J.H., de los Monteros, A.E., Morrone, J.J., Ron, S.R., Cannatella, D.C., 2015. Insights from Integrative Systematics Reveal Cryptic Diversity in *Pristimantis* Frogs (Anura: Craugastoridae) from the Upper Amazon Basin. PloS Biol. 10, e0143392. doi: 10.1371/journal.pone.0143392

Padial, J.M., De la Riva, I., 2009. Integrative taxonomy reveals cryptic Amazonian species of *Pristimantis* (Anura: Strabomantidae). Zool. J. Linn. Soc-Lond. 155, 97–122.

Padial, J.M., Miralles, A., De la Riva, I., Vences, M., 2010. Review: The integrative future of taxonomy. Front Zool. 7, 1–14.

Padial, J.M., Grant, T., Frost, D.R., 2014. Molecular systematics of terraranas (Anura: Brachycephaloidea) with an assessment of the effects of alignment and optimality criteria. Zootaxa 3825, 1–132.

Páez-Moscoso, D.J., Guayasamin, J.M., 2012. Species limits in the Andean toad genus *Osornophryne* (Bufonidae). Mol. Phyl. and Evol. 65,805–822. doi: 10.1016/j.ympev.2012.08.001

Patton, J.L., Smith, M.F., 1992. mtDNA phylogeny of Andean mice: a test of diversification across ecological gradients. Evolution 46, 174–83.

Peralta, I.E., Knapp, S., Spooner, D.M., 2005. New species of wild tomatoes (Solanum section Lycopersicon: Solanaceae) from Northern Peru. Syst. Bot. 30, 424–434.

Pinto-Sánchez, N.R., Ibáñez, R., Madriñán, S., Sanjur, O.I., Bermingham, E., Crawford, A.J., 2012. The great American biotic interchange in frogs: multiple and early colonization of Central America by the South American genus *Pristimantis* (Anura: Craugastoridae). Mol. Phylogen. Evol. 62, 954–972.

Pyron, R.A., Wiens, J.J., 2011. A large-scale phylogeny of Amphibia including over 2800 species, and a revised classification of extant frogs, salamanders, and caecilians. Mol. Phylogen. Evol. 61, 543–583. doi: 10.1016/j.ympev.2011.06.012

Pyron, R. A., 2014. Biogeographic analysis reveals ancient continental vicariance and recent oceanic dispersal in amphibians. Systematic Biology 63, 779–797.

Quintero, E., Ribas, C.C., Cracraft, J., 2013. The Andean *Hapalopsittaca* parrots (Psittacidae, Aves): an example of montane-tropical lowland vicariance. Zool. Scr. 42, 28-43. doi:10.1111/j.1463-6409.2012.00567.x

Rambaut, A., Drummond, A.J., 2007. Tracer. Version 1.4. Available from: http:// beast.bio.ed.ac.uk/Tracer/.

Rambaut, A., Drummond, A.J., 2016. TreeAnnotator Version 1.8.3. http://beast.bio. ed.ac.uk.

Ramírez, S., 2005. *Euglossa paisa*, a new species of orchid bee from the Colombian Andes (Hymenoptera: Apidae). *Zootaxa 1065*, 51–60.

Raxworthy, C.J., Pearson, R.G., Rabibiso, N., Rakotondrazafy, A.M., Ramanamanjato, J., Raselimanana, A.P., Wu, S., Nussbaum, R.A. Stone, D.A., 2008. Extinction vulnerability of tropical montane endemism from warming and upslope displacement: a preliminary appraisal for the highest massif in Madagascar. Global Change Biology 14, 1703–1720.

Reyes-Puig, M.M., Reyes-Puig, J.P., Yánez-Muñoz, M.H., 2013. Ranas terrestres del género *Pristimantis* (Anura: Craugastoridae) de la Reserva Ecológica Río Zúñag, Tungurahua, Ecuador: Lista anotada y descripción de una especie nueva. Avances en Ciencias e Ingeniería 5, B5–13.

Ribas, C.C., Moyle, R.G., Miyaki, C.Y., Cracraft, J., 2007. The assembly of montane biotas: linking Andean tectonics and climatic oscillations to independent regimes of diversification in *Pionus* parrots. P. Roy. Soc. B-Biol. Sci 274, 2399–2408.

Ricketts, T.H., Dinerstein, E., Boucher, T., Brooks, T.M., Butchart, S.H., Hoffmann, M., Lamoreux, J.F., Morrison, J., Parr, M., Pilgrim, J.D., Rodrigues, A.S., Sechrest, W., Wallace, G.E., Berlin, K., Bielby, J., Burgess, N.D., Church, D.R., Cox, N., Knox, D., Loucks, C., Luck, G.W., Master, L.L., Moore, R., Naidoo, R., Ridgely, R., Schatz, G.E., Shire, G., Strand, H., Wettengel, W., Wikramanayake, E., 2005. Pinpointing and preventing imminent extinctions. Proc. Natl. Acad. Sci. U. S. A. 102, 18497–18501. doi:10.1073/pnas.0509060102

Rivera-Correa, M., Lamadrid-Feris, F., Crawford, A.J., 2016. A new small golden frog of the genus *Pristimantis* (Anura: Craugastoridae) from an Andean cloud forest of Colombia. Zootaxa 4066, 421–437. doi: 10.1163/15685381-00003037

Rivera-Correa, M., Daza, J.M., 2016. Molecular phylogenetics of the *Pristimantis lacrimosus* species group (Anura: Craugastoridae) with the description of a new species from Colombia. Acta Herpetol. 11, 31–45.

Ron, S.R., Guayasamin, J.M., Yánez-Muñoz, M.H., Merino-Viteri, A., Ortiz, D.A., Nicolalde, D.A., 2016. AmphibiaWebEcuador. Version 2016.0. http://zoologia.puce.edu.ec/Vertebrados/anfibios/AnfibiosEcuador [accessed 01-02-2016]

Ronquist, F., Teslenko, M., van der Mark, P., Ayres, D.L., Darling, A., Höhna, S., ... Huelsenbeck, J. P., 2012. MrBayes 3.2: efficient Bayesian phylogenetic inference and model choice across a large model space. Syst. Biol. 61, 539–542.

Sage, R.F., Sage, T.L., Kocacinar, F., 2012. Photorespiration and the Evolution of C4 Photosynthesis. Annu. Rev. Plant Biol. 63, 19–47.

Sanín, M.J., Kissling, W.D., Bacon, C.D., Borchsenius, F., Galeano, G., Svenning, J.C., OLivera, J., Ramírez, R., Trénel, P., Pintaud, J.C., 2016. The Neogene rise of the tropical Andes facilitated diversification of wax palms (Ceroxylon: Arecaceae) through geographical colonization and climatic niche separation. Bot. J. Linn. Soc. 182, 303–317.

SAS Institute Inc. 2009. Statitistical discovery software, JMP® 8, Cary, North Carolina, USA.

Simpson, G.G., 1961. Principles of animal taxonomy. New York, NY: Columbia University Press.

Sklenář, P., Jørgensen, P., 1999. Distribution patterns of páramos plants in Ecuador. J. Biogeogr. 26, 681–691.

Smith, S.A., De Oca, A.N.M., Reeder, T.W., Wiens, J.J., 2007. A phylogenetic perspective on elevational species richness patterns in Middle American treefrogs: why so few species in lowland tropical rainforests?. Evolution 61, 1188–1207. doi: 10.1111/j.1558-5646.2007.00085.x

Swenson, N.G., Enquist, B.J., Pither, J., Kerkhoff, A.J., Boyle, B., Weiser, M.D., et al., 2012. The biogeography and filtering of woody plant functional diversity in North and South America. Global Ecol. Biogeogr. 21, 798–808. doi:10.1111/j.1466-8238.2011.00727.x

Székely, P., Cogălniceanu, D., Székely, D., Páez, N., Ron, S.R., 2016. A new species of *Pristimantis* from southern Ecuador (Anura, Craugastoridae). ZooKeys 606, 77.

Tamura, K., Stecher, G., Peterson, D., Filipski, A., Kumar, S., 2013. MEGA6: molecular evolutionary genetics analysis version 6.0. Mol. Bio. Evol. 30, 2725–2729.

Thomas, C.D., Cameron, A., Green, R.E., Bakkenes, M., Beaumont, L.J., Collingham, Y.C., Erasmus, B.F.N., Ferreira de Siqueira, M., Grainger, A., Hannah, L., Hughes, L.,

Huntley, B., van Jaarsveld, A.S., Midgley, G.F., Miles, L., Ortega-Huerta, M.A., Peterson, A.T., Phillips, O.L., Williams, S.E., 2004. Extinction risk from climate change. Nature 427, 145–148.

Turchetto-Zolet, A.C., Pinheiro, F., Salgueiro, F., Palma-Silva, C., 2013. Phylogeographical patterns shed light on evolutionary process in South America. Mol. Ecol 22, 1193–1213.

Valdecasas, A.G., Williams, D., Wheeler, Q.D., 2008. 'Integrative taxonomy'then and now: a response to Dayrat (2005). Biol. J. Linn. Soc-Lond. 93, 211–216. doi: 10.1111/j.1095-8312.2007.00919.x

Valencia, J., Bejarano-Muñoz, E.P., Yánez-Muñoz, M.H., 2013. Una nueva especie de rana *Pristimantis* verde (Anura: Craugastoridae) de los bosques andinos del Distrito Metropolitano de Quito, Ecuador. Herpetotropicos 9, 25–35.

Vellend, M., Geber, M. A., 2005. Connections between species diversity and genetic diversity. Ecol. Lett. 8, 767–781. doi: 10.1111/j.1461-0248.2005.00775.x

Vences, M., Wake, D.B., 2007. Speciation, species boundaries and phylogeography of amphibians. Amphibian biology 7, 2613–2671.

Vieites, D.R., Wollenberg, K.C., Andreone, F., Köhler, J., Glaw, F., Vences, M., 2009. Vast underestimation of Madagascar's biodiversity evidenced by an integrative amphibian inventory. Proc. Natl. Acad. Sci. U. S. A. 106, 8267–8272. doi: 10.1073/pnas.0810821106

Wang, I. J., Crawford, A.J., Bermingham, E., 2008. Phylogeography of the Pygmy Rain Frog (*Pristimantis ridens*) across the lowland wet forests of isthmian Central America. Mol. Phylogen. Evol. 47, 992–1004.

Wiens, J.J., 1998. Combining data sets with different phylogenetic histories. Syst. Biol. 47, 568–581.

Wiens, J.J., Fetzner, J.W., Parkinson, C.L., Reeder, T.W., 2005. Hylid frog phylogeny and sampling strategies for speciose clades. Syst. Biol. 54, 778–807.

Wiley, E.O., 1978. The evolutionary species concept reconsidered. Syst. Zool. 27:17–26.

Wollerman, L., Wiley, H.R., 2002. Possibilities for error during communication by neotropical frogs in a complex acoustic environment. Behav. Ecol. Sociobiol. 52, 465–473. doi: 10.1007/s00265-002-0534-7

Yánez-Muñoz, M.H., Bejarano-Muñoz, P., Brito, J., Batallas, D., 2014. Terrestrial frogs of the Southeastern Andes of Ecuador II: A new species of spiny green *Pristimantis* of montane forests of Sangay National Park (Anura: Craugastoridae). Avances en Cienicas e Ingenierías 53, 1689–1699.

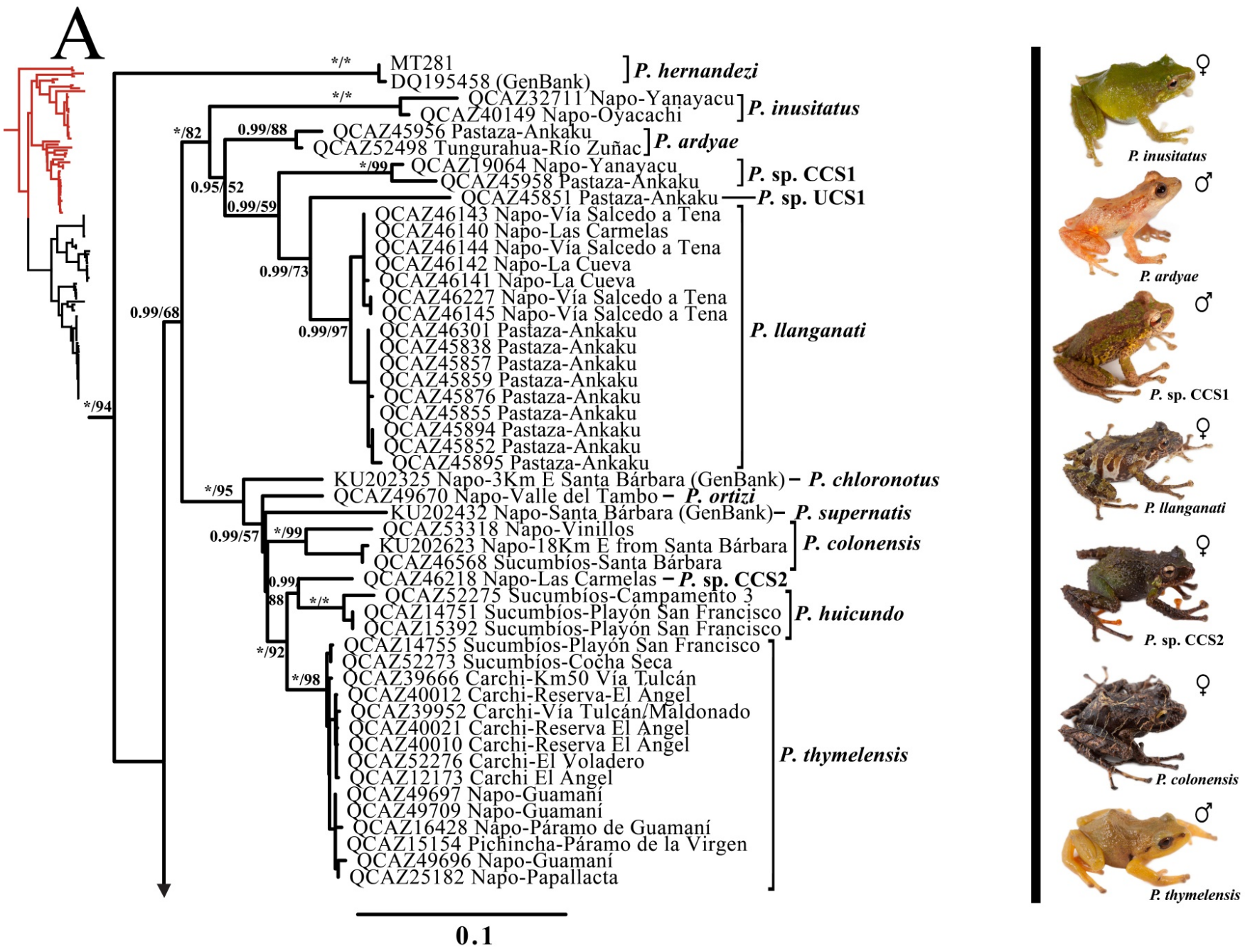
Young, B.E., Stuart, S. N., Chanson, J. S., Cox, N. A., Boucher, T. M., 2004. Disappearing Jewels: The Status of NewWorld Amphibians. NatureServe, Arlington, Virginia.

Zhang, J., Kapli, P., Pavlidis, P., Stamatakis, A., 2013. A general species delimitation method with applications to phylogenetic placements. Bioinformatics 29, 2869–2876.

Zwickl, D,. 2006. Genetic algorithm approaches for the phylogenetic analysis of large biological sequence datasets under the maximum likelihood criterion. Ph.D. thesis: The University of Texas at Austin.

Figures

Figure 1. Phylogeny of *Pristimantis chloronotus* species group. Maximum-likelihood tree obtained from analyses of DNA sequences from 114 specimens. We sequenced two mitochondrial genes (16S, ND1), and one nuclear gene (RAG1). Numbers above slashes correspond to Bayesian posterior probabilities (PP); asterisks represent PP = 1.0. Numbers below branches are ML bootstrap support (BB) values; asterisks represent BB = 100. PP and BB values < 0.50 or 50, respectively are not shown. Voucher numbers and localities of specimens are indicated for each terminal. Available photographs for each clade are shown in the right side.


A
/
MT281
DQ195458 (GenBank)
P. hernandezi
/
QCAZ32711 Napo-Yanayacu
QCAZ40149 Napo-Oyacachi
P. inusitatus
*/82
0.99/88
QCAZ45956 Pastaza-Ankaku
QCAZ52498 Tungurahua-Río Zuñac
P. ardyae
*/99
QCAZ19064 Napo-Yanayacu
QCAZ45958 Pastaza-Ankaku
P. sp. CCS1
0.95/52
0.99/59
QCAZ45851 Pastaza-Ankaku
P. sp. UCS1
QCAZ46143 Napo-Vía Salcedo a Tena
QCAZ46140 Napo-Las Carmelas
QCAZ46144 Napo-Vía Salcedo a Tena
0.99/73
QCAZ46142 Napo-La Cueva
QCAZ46141 Napo-La Cueva
QCAZ46227 Napo-Vía Salcedo a Tena
0.99/68
QCAZ46145 Napo-Vía Salcedo a Tena
0.99/97
QCAZ46301 Pastaza-Ankaku
QCAZ45838 Pastaza-Ankaku
QCAZ45857 Pastaza-Ankaku
QCAZ45859 Pastaza-Ankaku
QCAZ45876 Pastaza-Ankaku
QCAZ45855 Pastaza-Ankaku
QCAZ45894 Pastaza-Ankaku
QCAZ45852 Pastaza-Ankaku
QCAZ45895 Pastaza-Ankaku
P. llanganati
*/94
*/95
KU202325 Napo-3Km E Santa Bárbara (GenBank)
P. chloronotus
QCAZ49670 Napo-Valle del Tambo
P. ortizi
KU202432 Napo-Santa Bárbara (GenBank)
P. supernatis
0.99/57
*/99
QCAZ53318 Napo-Vinillos
KU202623 Napo-18Km E from Santa Bárbara
QCAZ46568 Sucumbíos-Santa Bárbara
P. colonensis
0.99
88
QCAZ46218 Napo-Las Carmelas
P. sp. CCS2
/
QCAZ52275 Sucumbíos-Campamento 3
QCAZ14751 Sucumbíos-Playón San Francisco
QCAZ15392 Sucumbíos-Playón San Francisco
P. huicundo
*/92
QCAZ14755 Sucumbíos-Playón San Francisco
QCAZ52273 Sucumbíos-Cocha Seca
*/98
QCAZ39666 Carchi-Km50 Vía Tulcán
QCAZ40012 Carchi-Reserva-El Angel
QCAZ39952 Carchi-Vía Tulcán/Maldonado
QCAZ40021 Carchi-Reserva El Angel
QCAZ40010 Carchi-Reserva El Angel
QCAZ52276 Carchi-El Voladero
QCAZ12173 Carchi El Angel
QCAZ49697 Napo-Guamaní
QCAZ49709 Napo-Guamaní
QCAZ16428 Napo-Páramo de Guamaní
QCAZ15154 Pichincha-Páramo de la Virgen
QCAZ49696 Napo-Guamaní
QCAZ25182 Napo-Papallacta
P. thymelensis
0.1
♀
P. inusitatus
♂
P. ardyae
♂
P. sp. CCS1
♀
P. llanganati
♀
P. sp. CCS2
♀
P. colonensis
♂
P. thymelensis

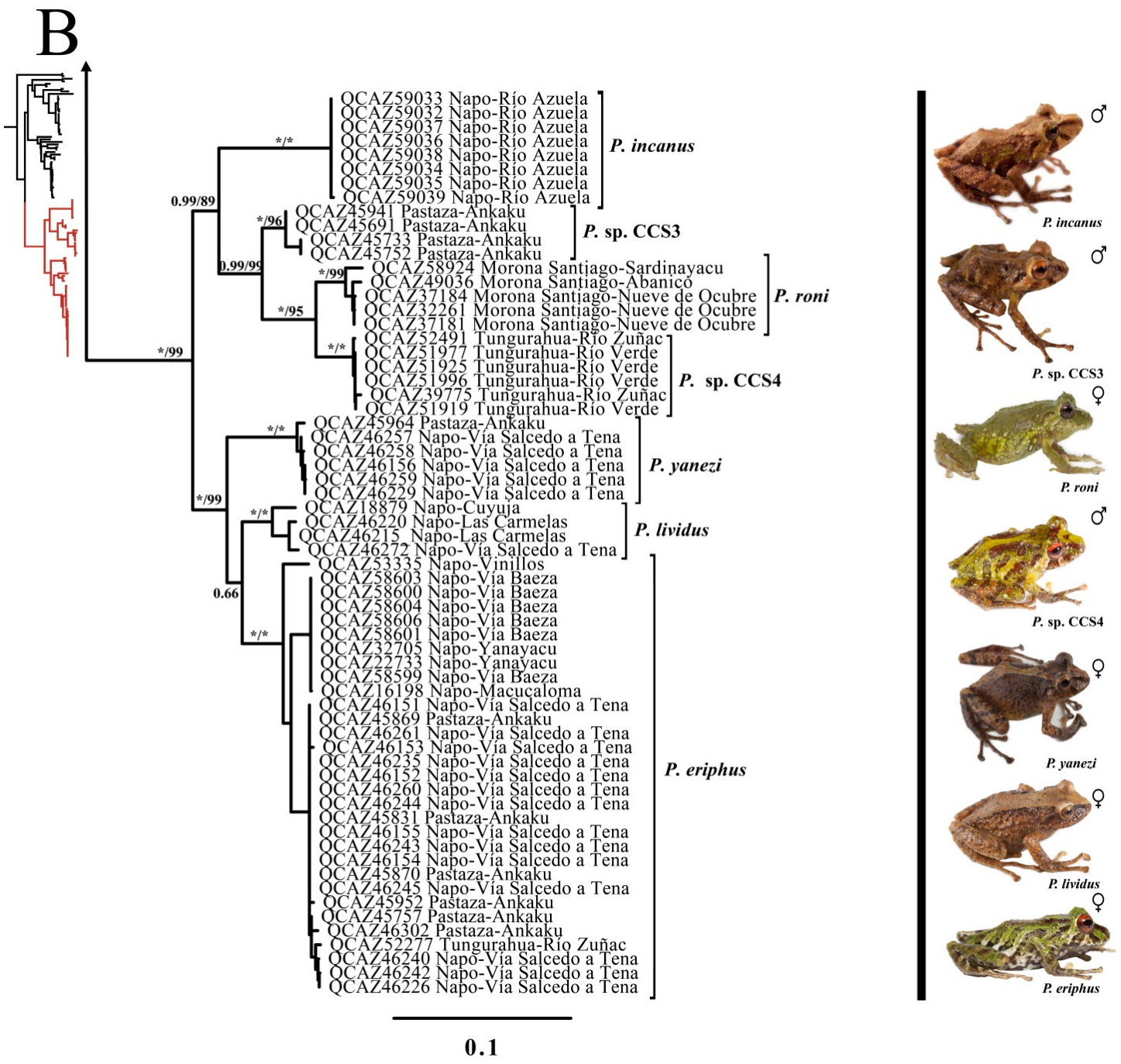
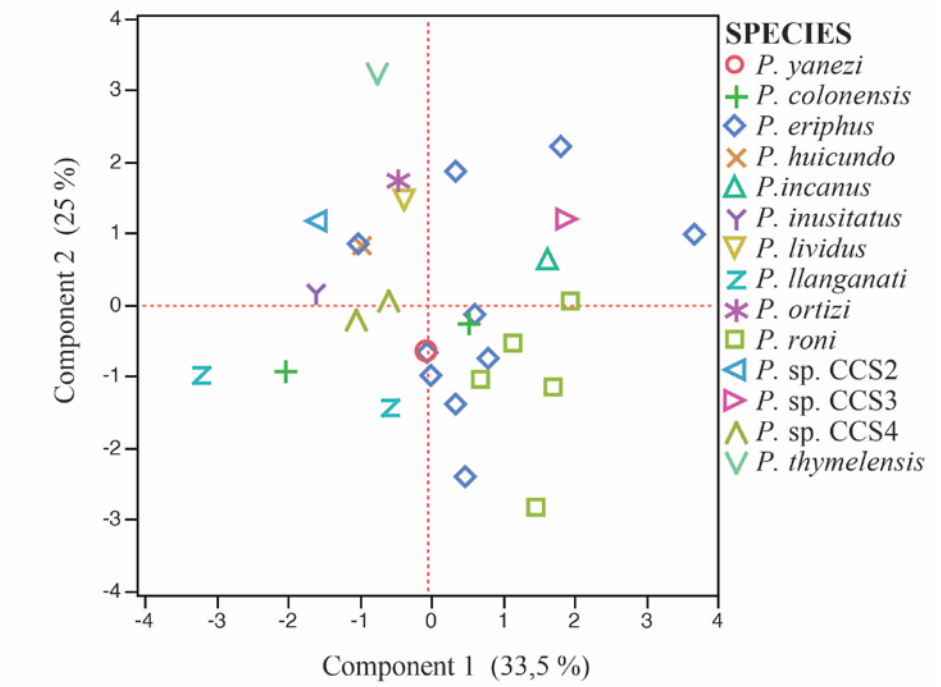
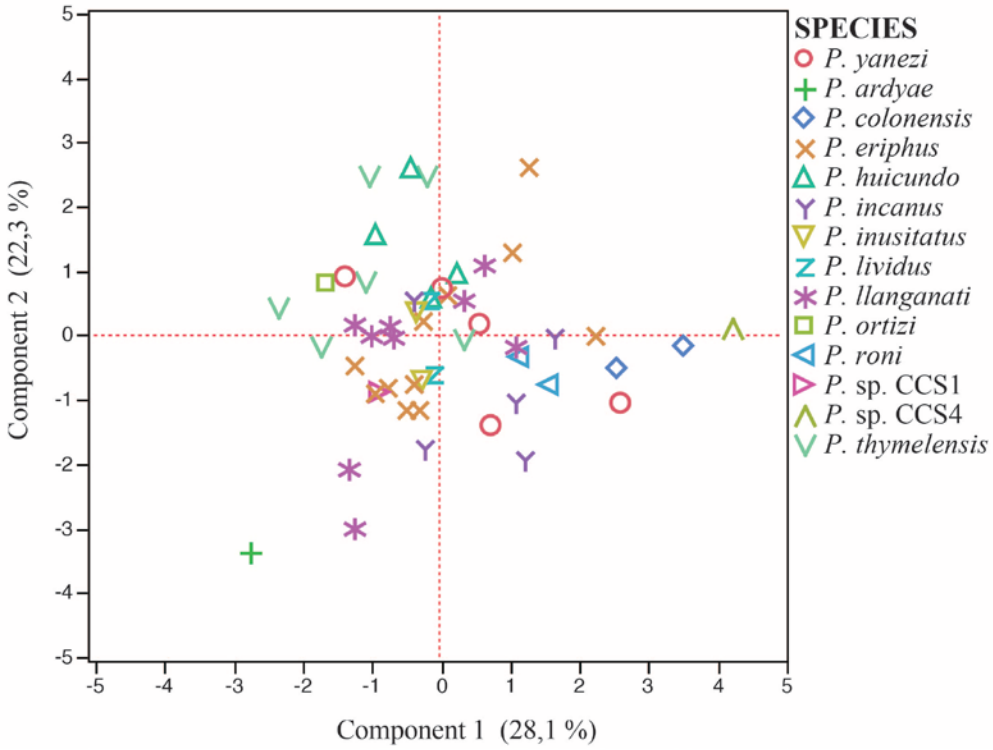

B
QCAZ59033 Napo-Río Azuela
QCAZ59032 Napo-Río Azuela
QCAZ59037 Napo-Río Azuela
QCAZ59036 Napo-Río Azuela
QCAZ59038 Napo-Río Azuela
QCAZ59034 Napo-Río Azuela
QCAZ59035 Napo-Río Azuela
QCAZ59039 Napo-Río Azuela
P. incanus
QCAZ45941 Pastaza-Ankaku
QCAZ45691 Pastaza-Ankaku
QCAZ45733 Pastaza-Ankaku
QCAZ45752 Pastaza-Ankaku
P. sp. CCS3
QCAZ58924 Morona Santiago-Sardinayacu
QCAZ49036 Morona Santiago-Abanico
QCAZ37184 Morona Santiago-Nueve de Ocubre
QCAZ32261 Morona Santiago-Nueve de Ocubre
QCAZ37181 Morona Santiago-Nueve de Ocubre
P. roni
QCAZ52491 Tungurahua-Río Zuñac
QCAZ51977 Tungurahua-Río Verde
QCAZ51925 Tungurahua-Río Verde
QCAZ51996 Tungurahua-Río Verde
QCAZ39775 Tungurahua-Río Zuñac
QCAZ51919 Tungurahua-Río Verde
P. sp. CCS4
QCAZ45964 Pastaza-Ankaku
QCAZ46257 Napo-Vía Salcedo a Tena
QCAZ46258 Napo-Vía Salcedo a Tena
QCAZ46156 Napo-Vía Salcedo a Tena
QCAZ46259 Napo-Vía Salcedo a Tena
QCAZ46229 Napo-Vía Salcedo a Tena
P. yanezi
QCAZ18879 Napo-Cuyuja
QCAZ46220 Napo-Las Carmelas
QCAZ46215 Napo-Las Carmelas
QCAZ46272 Napo-Vía Salcedo a Tena
P. lividus
QCAZ53335 Napo-Vinillos
QCAZ58603 Napo-Vía Baeza
QCAZ58600 Napo-Vía Baeza
QCAZ58604 Napo-Vía Baeza
QCAZ58606 Napo-Vía Baeza
QCAZ58601 Napo-Vía Baeza
QCAZ32705 Napo-Yanayacu
QCAZ22733 Napo-Yanayacu
QCAZ58599 Napo-Vía Baeza
QCAZ16198 Napo-Macucaloma
QCAZ46151 Napo-Vía Salcedo a Tena
QCAZ45869 Pastaza-Ankaku
QCAZ46261 Napo-Vía Salcedo a Tena
QCAZ46153 Napo-Vía Salcedo a Tena
QCAZ46235 Napo-Vía Salcedo a Tena
QCAZ46152 Napo-Vía Salcedo a Tena
QCAZ46260 Napo-Vía Salcedo a Tena
QCAZ46244 Napo-Vía Salcedo a Tena
QCAZ45831 Pastaza-Ankaku
QCAZ46155 Napo-Vía Salcedo a Tena
QCAZ46243 Napo-Vía Salcedo a Tena
QCAZ46154 Napo-Vía Salcedo a Tena
QCAZ45870 Pastaza-Ankaku
QCAZ46245 Napo-Vía Salcedo a Tena
QCAZ45952 Pastaza-Ankaku
QCAZ45757 Pastaza-Ankaku
QCAZ46302 Pastaza-Ankaku
QCAZ52277 Tungurahua-Río Zuñac
QCAZ46240 Napo-Vía Salcedo a Tena
QCAZ46242 Napo-Vía Salcedo a Tena
QCAZ46226 Napo-Vía Salcedo a Tena
P. eriphus
/
0.99/89
*/96
0.99/99
*/99
*/95
/
*/99
/
*/99
/
0.66
/
0.1
♂
P. incanus
♂
P. sp. CCS3
♀
P. roni
♂
P. sp. CCS4
♀
P. yanezi
♀
P. lividus
♀
P. eriphus

Figure 2. Axes I and II from Principal Components Analysis based on 10 morphometric variables of 15 of the 20 clades of the *Pristimantis chloronotus* species group. See Table S5 for character loadings on each component. **A.** PCA for females. **B.** PCA for males.

A


SPECIES
P. yanezi
P. colonensis
P. eriphus
P. huicundo
P.incanus
P. inusitatus
P. lividus
P. llanganati
P. ortizi
P. roni
P. sp. CCS2
P. sp. CCS3
P. sp. CCS4
P. thymelensis
Component 2 (25 %)
Component 1 (33,5 %)

B


SPECIES
P. yanezi
P. ardyae
P. colonensis
P. eriphus
P. huicundo
P. incanus
P. inusitatus
P. lividus
P. llanganati
P. ortizi
P. roni
P. sp. CCS1
P. sp. CCS4
P. thymelensis
Component 2 (22,3 %)
Component 1 (28,1 %)

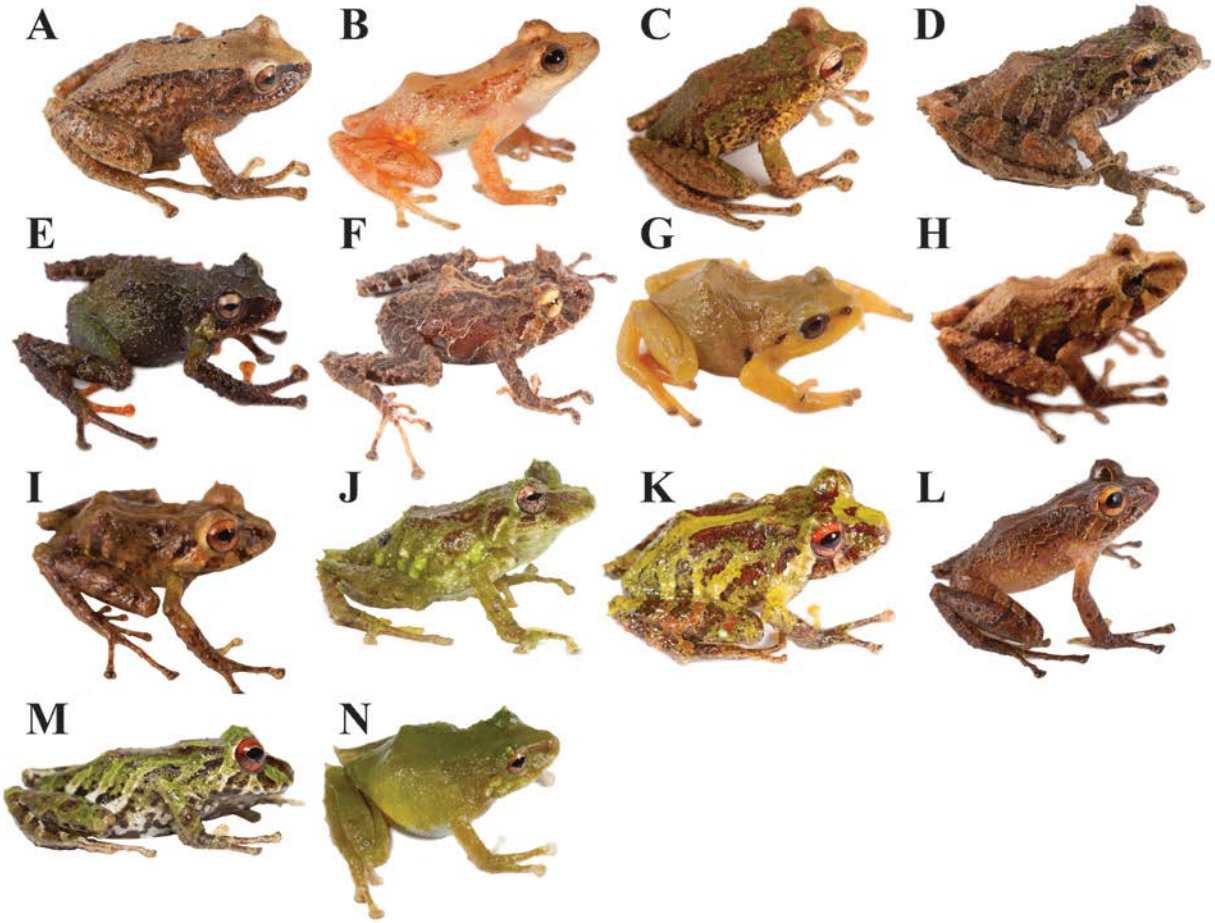


Figure 3. Dorsolateral view of live individuals of the *Pristimantis chloronotus* species group. Measurements are in mm. **A.** *Pristimantis lividus* (QCAZ 46215, ♀, SVL = 37. 77); **B.** *P. ardyae* (QCAZ 52498, ♂, SVL = 19.66); **C.** *P.* sp. CCS1 (QCAZ 45958, ♂, SVL = 27.94); **D.** *P. llanganati* (QCAZ 46227, ♂, SVL = 24.01); **E.** *P.* sp. CCS2 (QCAZ 46218, ♀, SVL = 25.89); **F.** *P. colonensis* (QCAZ 53318); **G.** *P. thymelensis* (QCAZ 39666, ♂, SVL = 21.94); **H.** *P. incanus* (QCAZ 41311); **I.** *P.* sp. CCS3 (QCAZ 45941, ♂, SVL = 17.07); **J.** *P. roni* (QCAZ 58924, ♀, SVL = 29.07); **K.** *P.* sp. CCS4 (QCAZ 51925, ♂, SVL = 19. 20); **L.** *P. yanezi* (QCAZ 46258, ♂, SVL = 23.65); **M.** *P. eriphus* (QCAZ 58603, ♂, SVL = 23.14); **N.** *P. inusitatus* (QCAZ 40149, ♀, SVL = 23.84).

Figure 4. Ventral view of live individuals of the *Pristimantis chloronotus* species group. Measurements are in mm. **A.** *Pristimantis lividus* (QCAZ 46215, ♀, SVL = 37. 77); **B.** *P. ardyae* (QCAZ 52498, ♂, SVL = 19.66); **C.** *P.* sp. CCS1 (QCAZ 45958, ♂, SVL = 27.94); **D.** *P. llanganati* (QCAZ 46227, ♂, SVL = 24.01); **E.** *P.* sp. CCS2 (QCAZ 46218, ♀, SVL = 25.89); **F.** *P. colonensis* (QCAZ 53318); **G.** *P. thymelensis* (QCAZ 39666, ♂, SVL = 21.94); **H.** *P. incanus* (QCAZ 41311); **I.** *P.* sp. CCS3 (QCAZ 45941, ♂, SVL = 17.07); **J.** *P. roni* (QCAZ 58924, ♀, SVL = 29.07); **K.** *P.* sp. CCS4 (QCAZ 51925, ♂, SVL = 19. 20); **L.** *P. yanezi* (QCAZ 46258, ♂, SVL = 23.65); **M.** *P. eriphus* (QCAZ 58603, ♂, SVL = 23.14); **N.** *P. inusitatus* (QCAZ 40149, ♀, SVL = 23.84).

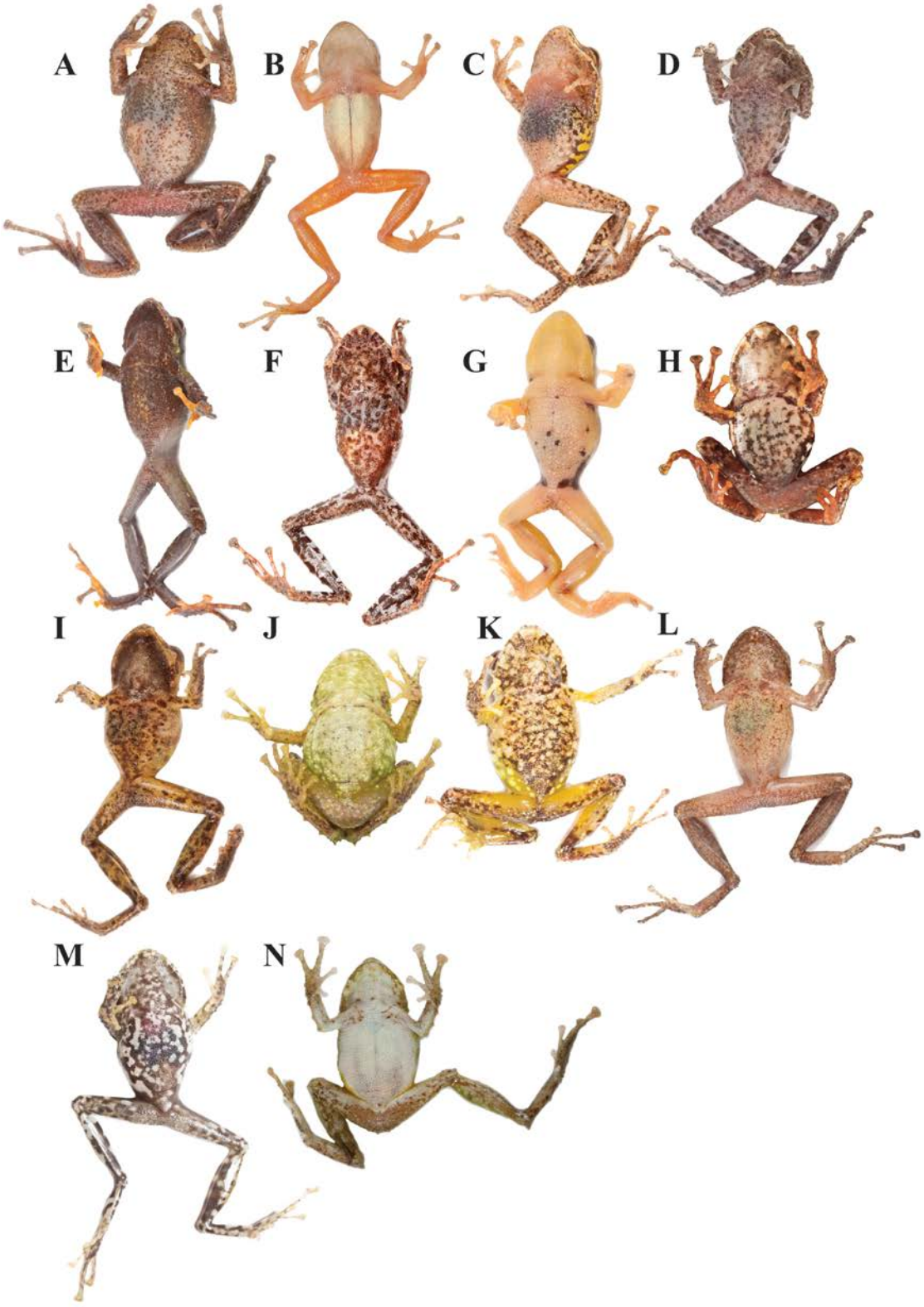
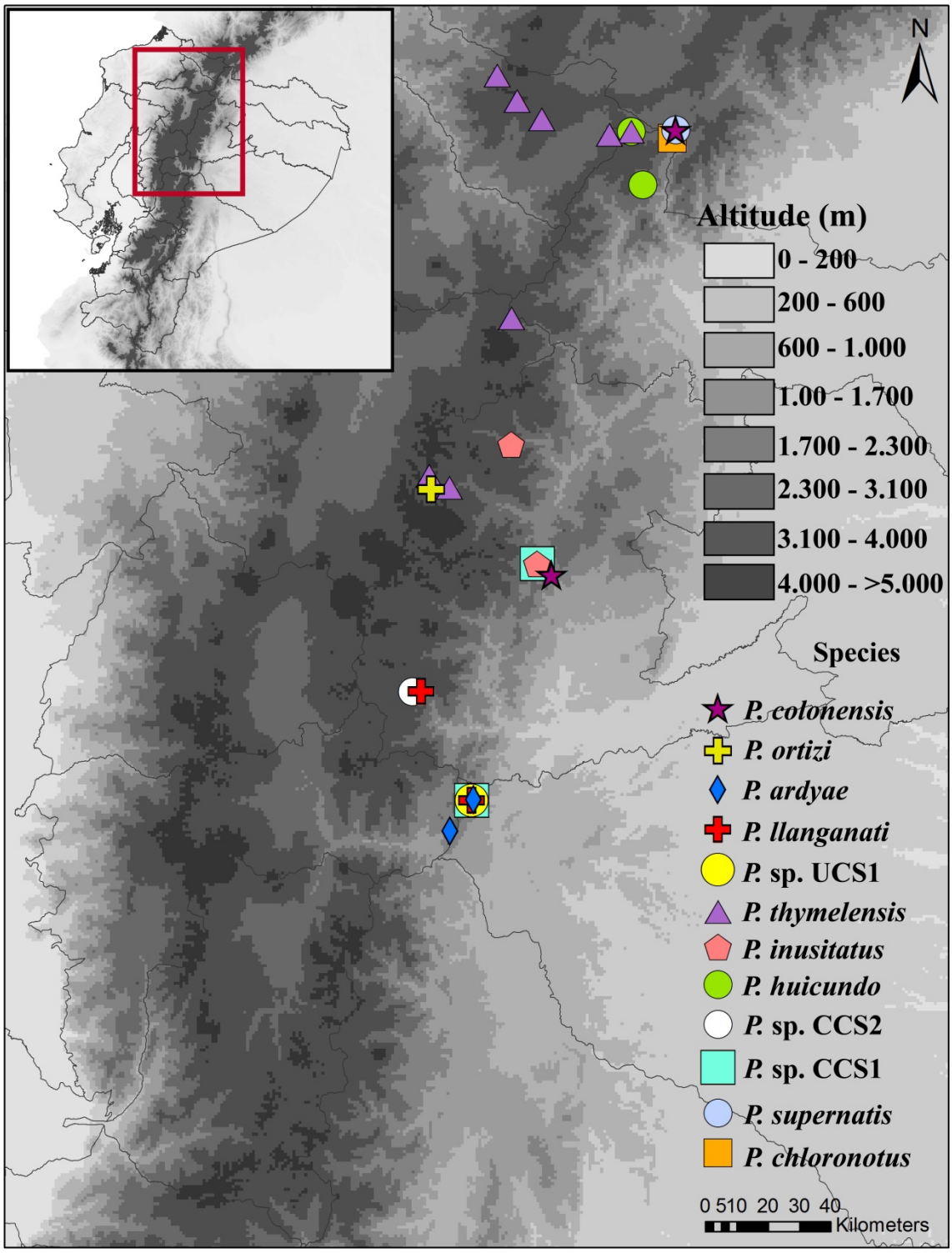
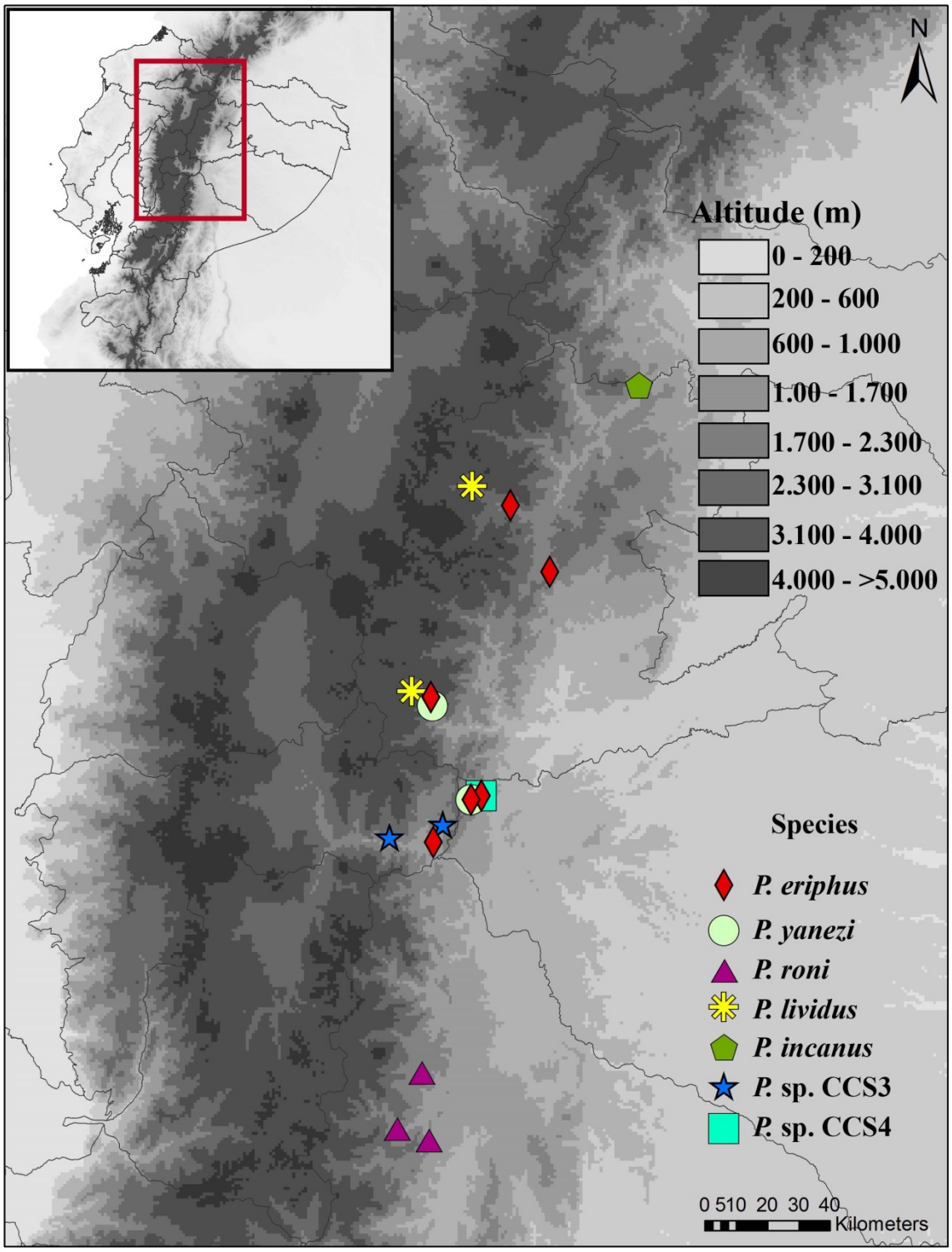

A
B
C
D
E
F
G
H
I
J
K
L
M
N

Figure 5. Map showing sampling localities for DNA sequences of *Pristiminatis chloronotus* species group and used for phylogenetic, environmental and chronobiogeographic analyses. Locality details, as well as voucher and GenBank accession numbers are listed in Appendix A.


N
Altitude (m)
0 - 200
200 - 600
600 - 1.000
1.00 - 1.700
1.700 - 2.300
2.300 - 3.100
3.100 - 4.000
4.000 - >5.000
Species
P. colonensis
P. ortizi
P. ardyae
P. llanganati
P. sp. UCS1
P. thymelensis
P. inusitatus
P. huicundo
P. sp. CCS2
P. sp. CCS1
P. supernatis
P. chloronotus
0 510 20 30 40
Kilometers


N
Altitude (m)
0 - 200
200 - 600
600 - 1.000
1.00 - 1.700
1.700 - 2.300
2.300 - 3.100
3.100 - 4.000
4.000 - >5.000
Species
P. eriphus
P. yanezi
P. roni
P. lividus
P. incanus
P. sp. CCS3
P. sp. CCS4
0 510 20 30 40
Kilometers

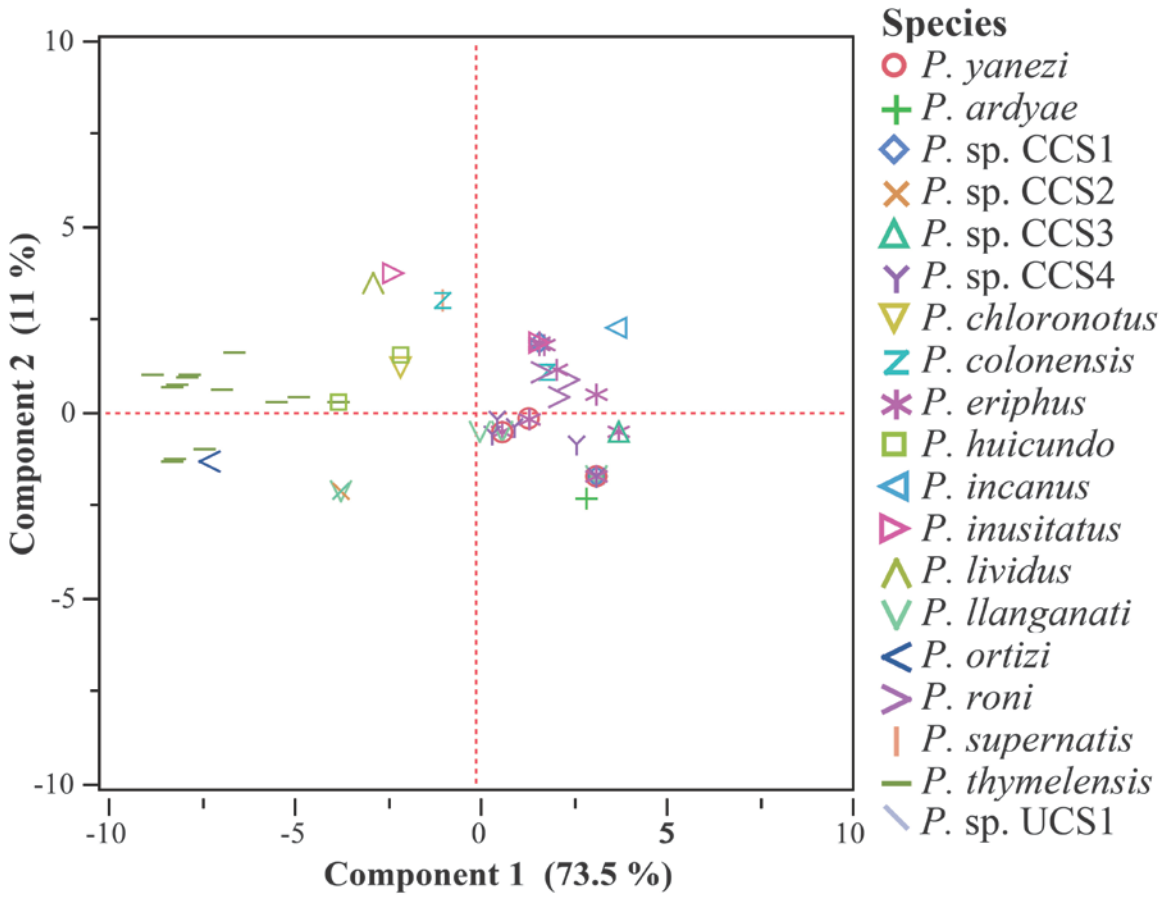


Figure 6. Axes I and II from Principal Components Analysis based on 19 bioclimatic variables taken from distribution localities of the *Pristimantis chloronotus* species group. See Table 5 for character loadings on each component.

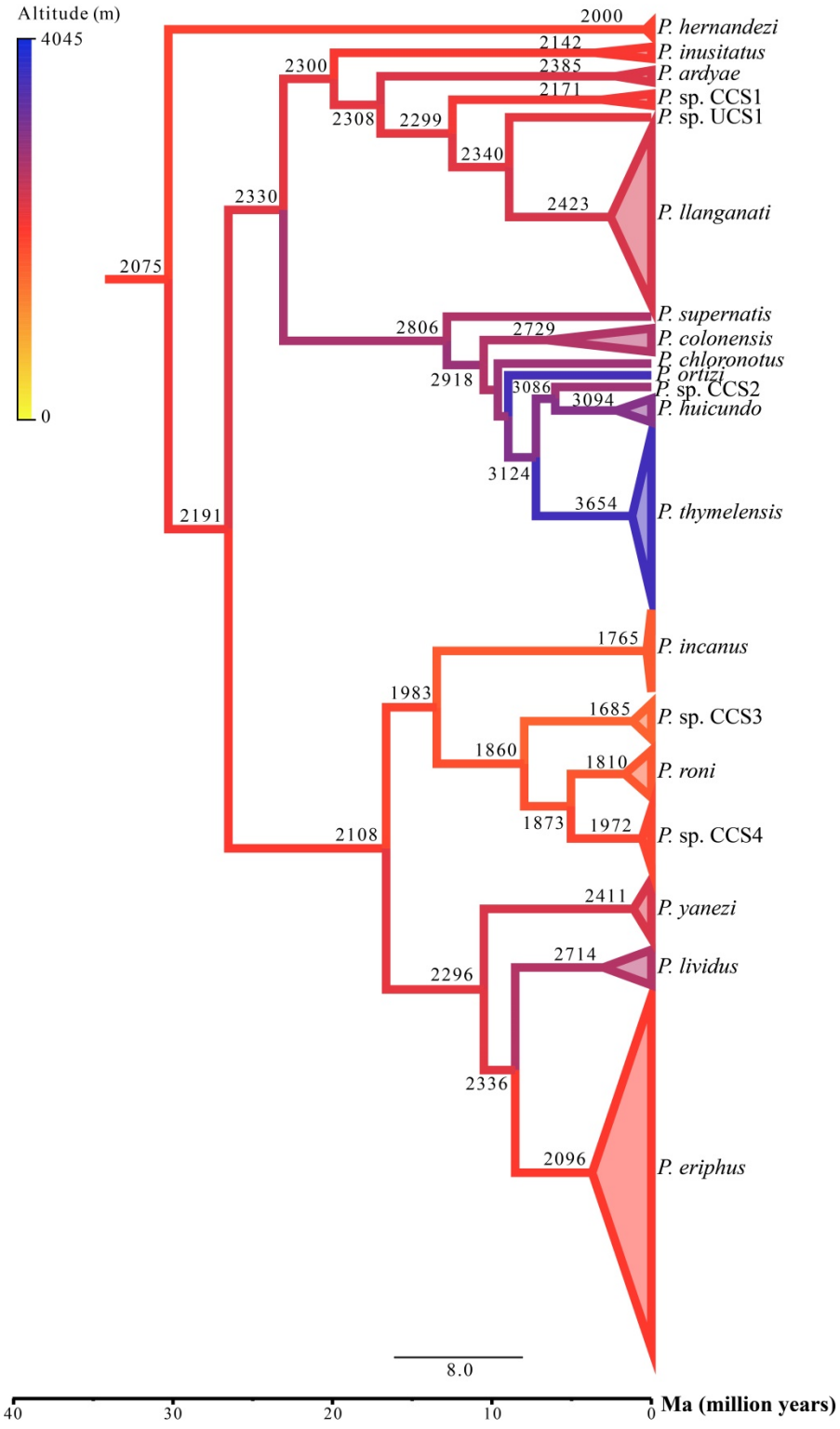


Figure 7. Phylogenetic tree of *Pristimantis chloronotus* species group, with divergence time estimates in millions of years and ancestral altitude reconstruction. Numbers above branches correspond to the altitudinal value; numbers below branches correspond to posterior probability (PP) values. Branches are colored according to the most probable altitude.

Tables

Table 1. Pairwise uncorrected genetic distances among clades of the *Pristimantis chloronotus* species group. The data shown under the diagonal correspond to the mean, standard error, and the range of the distances between clades. The number of individuals for each comparison is shown above the diagonal. Data on the diagonal in bold corresponds to intra-clade genetic distances

	Outgroup	***P. llanganati***	**P. sp. (UCS1)**	***P. inusitatus***	***P. supernatis***	***P. chloronotus***	***P. colonensis***	***P. thymelensis***	***P. huicundo***	**P. sp (CCS2)**	**P. sp (CCS1)**
Outgroup	**(0−0.283)**	*n* = 56	*n* = 41	*n* = 42	*n* = 41	*n* = 41	*n* = 43	*n* = 55	*n* = 43	*n* = 41	*n* = 41
P. llanganati	(0.173±0.010) (0.130−0.280)	**(0−0.018)**	*n* = 17	*n* = 18	*n* = 17	*n* = 17	*n* = 19	*n* = 31	*n* = 19	*n* = 17	*n* = 17
P. sp (UCS1)	(0.181±0.011) (0.135−0.268)	(0.073±0.010) (0.071−0.075)	–	*n* = 3	*n* = 2	*n* = 2	*n* = 4	*n* = 16	*n* = 4	*n* = 2	*n* = 2
P. inusitatus	(0.174±0.010) (0.135−0.261)	(0.080±0.010) (0.072−0.085)	(0.079±0.010) (0.074−0.084)	**0.010**	*n* = 3	*n* = 3	*n* = 5	*n* = 17	*n* = 5	*n* = 3	*n* = 3
P. supernatis	(0.169±0.010) (0.136−0.269)	(0.090±0.011) (0.084−0.096)	(0.108±0.012) (0.108)	(0.097±0.011) (0.095−0.099)	–	*n* = 2	*n* = 4	*n* = 16	*n* = 4	*n* = 2	*n* = 2
P. chloronotus	(0.171±0.010) (0.137−0.264)	(0.089±0.011) (0.084−0.094)	(0.095±0.012) (0.095)	(0.092±0.011) (0.091−0.094)	(0.065±0.010) (0.065)	–	*n* = 4	*n* = 16	*n* = 4	*n* = 2	*n* = 2
P. colonensis	(0.172±0.010) (0.133−0.275)	(0.082±0.010) (0.074−0.091)	(0.093±0.011) (0.093−0.111)	(0.090±0.010) (0.086−0.094)	(0.058±0.008) (0.058−0.059)	(0.058±0.008) (0.049−0.058)	**(0−0.029)**	*n* = 18	*n* = 6	*n* = 4	*n* = 4
P. thymelensis	(0.177±0.010) (0.139−0.284)	(0.090±0.010) (0.079−0.101)	(0.098±0.012) (0.096−0.100)	(0.093±0.010) (0.088−0.098)	(0.061±0.009) (0.058−0.065)	(0.050±0.008) (0.046−0.053)	(0.042±0.007) (0.035−0.053)	**(0−0.010)**	*n* = 18	*n* = 16	*n* = 16
P. huicundo	(0.183±0.010) (0.150−0.283)	(0.094±0.011) (0.087−0.099)	(0.108±0.012) (0.107−0.108)	(0.105±0.011) (0.103−0.107)	(0.066±0.009) (0.065−0.067)	(0.058±0.009) (0.057−0.060)	(0.045±0.007) (0.043−0.048)	(0.031±0.006) (0.027−0.034)	**(0−0.002)**	*n* = 4	*n* = 4
P. sp (CCS2)	(0.186±0.010) (0.153−0.282)	(0.091±0.011) (0.085−0.097)	(0.109±0.013) (0.109)	(0.105±0.011) (0.104−0.106)	(0.068±0.009) (0.068)	(0.058±0.009) (0.057)	(0.047±0.008) (0.045−0.051)	(0.033±0.007) (0.030−0.035)	(0.030±0.006) (0.029−0.035)	–	*n* = 2
P. sp (CCS1)	(0.145±0.008) (0.059−0.255)	(0.135±0.012) (0.130−0.141)	(0.140±0.013) (0.140)	(0.139±0.013) (0.136−0.141)	(0.129±0.013) (0.129)	(0.125±0.012) (0.125)	(0.138±0.012) (0.136−0.141)	(0.135±0.012) (0.131−0.135)	(0.148±0.012) (0.147−0.148)	(0.148±0.012) (0.148)	–

Table 1. Pairwise uncorrected genetic distances among clades of the *Pristimantis chloronotus* species group. The data shown under the diagonal correspond to the mean, standard error, and the range of the distances between clades. The number of individuals for each comparison is shown above the diagonal. Data on the diagonal in bold corresponds to intra-clade genetic distances

	Outgroup	***P. eriphus***	***P. roni***	**P. sp (CCS4)**	**P. sp (CCS3)**	***P. yanezi***	***P. lividus***	***P. incanus***
Outgroup	**(0−0.283)**	*n* = 70	*n* = 45	*n* = 46	*n* = 43	*n* = 46	*n* = 44	*n* = 47
P. eriphus	(0.168±0.010) (0.120−0.272)	**(0−0.018)**	*n* = 35	*n* = 36	*n* = 33	*n* = 36	*n* = 34	*n* = 37
P. roni	(0.179±0.010) (0.139−0.266)	(0.081±0.010) (0.074−0.093)	**(0.002−0.015)**	*n* = 11	*n* = 8	*n* = 11	*n* = 9	*n* = 12
P. sp (CCS4)	(0.181±0.009) (0.146−0.269)	(0.078±0.010) (0.073−0.086)	(0.036±0.007) (0.031−0.039)	**(0−0.005)**	*n* = 9	*n* = 12	*n* = 10	*n* = 13
P. sp (CCS3)	(0.180±0.011) (0.143−0.281)	(0.062±0.009) (0.056−0.072)	(0.042±0.007) (0.038−0.045)	(0.050±0.008) (0.048−0.051)	**(0−0.007)**	*n* = 9	*n* = 7	*n* = 10
P. yanezi	(0.173±0.010) (0.133−0.274)	(0.048±0.008) (0.042−0.056)	(0.089±0.010) (0.079−0.096)	(0.081±0.010) (0.077−0.086)	(0.068±0.009) (0.063−0.072)	**(0−0.011)**	*n* = 10	*n* = 13
P. lividus	(0.175±0.010) (0.133−0.271)	(0.031±0.010) (0.026−0.048)	(0.079±0.010) (0.076−0.082)	(0.075±0.010) (0.070−0.078)	(0.066±0.009) (0.064−0.068)	(0.059±0.008) (0.055−0.063)	**(0−0.015)**	*n* = 11
P. incanus	(0.172±0.010) (0.138−0.275)	(0.073±0.010) (0.068−0.079)	(0.078±0.010) (0.071−0.082)	(0.073±0.010) (0.071−0.074)	(0.066±0.010) (0.064−0.068)	(0.090±0.011) (0.086−0.095)	(0.076±0.010) (0.073−0.080)	**0.000**

Table 2. Summary of morphometric measurements for adult females of the *Pristimantis chloronotus* species group. Specimens are deposited at Museo de Zoología, Pontificia Universidad Católica del Ecuador, Quito (QCAZ) and División de Herpetología, Museo Ecuatoriano de Ciencias Naturales (DHMECN). Abbreviations used in this table are: SVL = snout-vent length; HL = head length; HW = head width; E−N = eye-nostril distance; IOD = interorbital distance; IND = internarial distance; E−Y = eye-tympanum distance; TY = tympanum diameter. All measurements are in mm. Results from Shapiro Wilk normality tests apllied to log tranfsformed data are shown at the bottom.

Species	SVL	HL	HW	E−N	IOD	IND	E−Y	TY
P. colonensis **(*n* = 2)**	28.8−34.11 (31.46)	11.21−11.3 (11.26)	11.08−11.32 (11.2)	3.08−3.68 (3.32)	3.45−3.71 (3.58)	2.27−2.36 (2.32)	1.43−2.04 (1.74)	1.05−1.14 (1.1)
P. eriphus **(*n* = 10)**	23.58−29.92 (27.17±2.13)	9.14−12.88 (10.80±1.05)	9.68−13.78 (11.18±1.16)	2.84−3.73 (3.32±0.23)	2.55−4.15 (3.15±0.50)	1.98−2.89 (2.42±0.26)	0.89−1.98 (1.39±0.36)	0.66−1.31 (1.07±0.21)
P. huicundo **(*n* = 1)**	24.5	9.27	9.72	2.57	3.25	2.46	1.2	1.01
P. incanus **(*n* = 1)**	28.02	11.18	11.61	3.57	3.65	2.58	1.9	0.99
P. inusitatus **(*n* = 1)**	23.84	8.77	9.22	2.76	3.06	2.17	1.01	0.92
P. lividus **(*n* = 1)**	37.77	12.8	13.84	3.5	4.38	3	1.48	1.25
P. llanganati **(*n* = 2)**	27.18−29.78 (28.48)	8.18−10.22 (9.20)	10.28−10.54 (10.41)	2.80−3.07 (2.94)	3.01−3.44 (3.23)	2.12−2.26 (2.19)	1.32−1.74 (1.53)	1.17−1.32 (1.23)
P. ortizi **(*n* = 1)**	29.24	11.03	11.9	3.19	2.51	3.96	2.86	1.23
P. roni **(*n* = 5)**	25.04−31.44 (28.8±2.34)	10.31−12.37 (11.54±0.8)	10.49−12.46 (11.67±0.73)	3.33−3.77 (3.56±0.18)	2.78−3.75 (3.15±0.37)	1.91−2.76 (2.42±0.32)	1.45−2.14 (1.8±0.3)	1−1.87 (1.35±0.33)
***P.* sp. CCS2** **(*n* = 1)**	25.89	9.22	10.21	2.48	3.14	2.61	1	1.01
***P.* sp. CCS3** **(*n* = 1)**	29.74	12	12.64	3.52	3.55	2.6	2.08	0.72
***P.* sp. CCS4**	27.05−27.56	8.85−10.97	10.75−11.25	3.13	3	2.20−2.34	0.71−1.25	1−1.13

(*n* = 2)		(27.31)	(9.91)	(11)			(2.27)	(0.98)	(1.07)
P. thymelensis		27.41−32.56	9.67−11.32	9.79−11.76	2.43−2.99	3.77−4.14	1.83−3.1	0−1.13	0−1.01
(*n* = 4)		(29.69±2.41)	(10.66±0.74)	(10.82±1.06)	(2.66±0.24)	(3.87±0.18)	(2.42±0.55)	(0.43±0.59)	(0.37±0.51)
P. yanezi **(*n* = 1)**		36.91	10.4	14.18	3.94	3.29	2.96	1.91	1.43
Shapiro Wilk Test	**W**	0.95	0.97	0.97	0.94	0.98	0.98	0.96	0.97
	p-value	0.12	0.43	0.47	0.05	0.75	0.88	0.25	0.48

Table 3. Summary of morphometric measurements for adult males of the *Pristimantis chloronotus* species group. Specimens are deposited at Museo de Zoología, Pontificia Universidad Católica del Ecuador, (QCAZ) and Divisón de herpetología, Museo Ecuatoriano de Ciencias Naturales (DHMECN). Abbreviations used in this table are: SVL = snout-vent length; HL = head length; HW = head width; E−N = eye-nostril distance; IOD = interorbital distance; IND = internarial distance; E−Y = eye-tympanum distance; TY = tympanum diameter. All measurements are in mm. Results from Shapiro Wilk normality tests apllied to log tranfsformed data are shown at the bottom.

Species	SVL	HL	HW	E−N	IOD	IND	E−Y	TY
P. ardyae **(*n* = 1)**	17.58	8.41	6.26	1.8	1.91	1.24	0.67	0.86
P. colonensis **(*n* = 2)**	22.23−25.84 (24.04)	8.95−10.35 (9.65)	9.21−10.59 (9.9)	2.69−3.18 (2.94)	2.57−3.55 (3.06)	2.05−2.26 (2.16)	1.5−1.79 (1.65)	0.88−1.04 (0.96)
P. eriphus **(*n* = 11)**	18.02−23.14 (19.46±1.74)	6.94−9.32 (7.6±0.71)	6.89−9.63 (7.65±0.81)	1.93−2.89 (2.32±0.31)	1.98−2.93 (2.44±0.32)	1.49−2.18 (1.79±0.23)	0.81−1.11 (0.91±0.09)	0.81−1.09 (0.91±0.07)
P. huicundo **(*n* = 4)**	19.05−21.48 (20.38±1.21)	7.56−8.16 (7.8±0.26)	7.28−8.58 (7.93±0.54)	1.8−2.17 (2.03±0.17)	2.32−2.95 (2.73±0.3)	1.86−2.35 (2.02±0.23)	0.9−1.26 (1.05±0.15)	0.65−1.06 (0.87±0.18)
P. incanus **(*n* = 5)**	14.78−18.92 (16.86±1.59)	5.86−7.94 (7.07±0.77)	5.97−7.87 (6.99±0.79)	1.81−2.21 (2.00±0.18)	1.75−2.11 (1.92±0.13)	1.22−1.57 (1.45±0.15)	0.96−1.34 (1.08±0.16)	0.40−0.85 (0.62±0.17)
P. inusitatus **(*n* = 2)**	17.82−19.37 (18.6)	7.02−7.93 (7.48)	6.79−7.59 (7.19)	2.23−2.29 (2.26)	2.35−2.44 (2.4)	1.55−1.69 (1.62)	0.81−0.98 (0.9)	0.54−0.85 (0.7)
P. lividus **(*n* = 2)**	20.36−26.6 (23.48)	8.32−9.74 (9.03)	7.8−9.85 (8.83)	2.37−2.75 (2.56)	2.53−3.50 (3.02)	1.74−2.44 (2.09)	0.99−1.13 (1.06)	0.72−0.97 (0.85)
P. llanganati **(*n* = 9)**	17.46−27.17 (24.12±3.33)	6.87−9.77 (8.33±0.99)	6.63−10.19 (9.06±1.16)	1.92−2.84 (2.45±0.28)	2.10−3.35 (2.81±0.44)	1.55−2.28 (2.08±0.24)	1.07−1.47 (1.26±0.12)	0.72−1.26 (0.99±0.19)
P. ortizi **(*n* = 1)**	21.75	8.1	8.23	2.1	2.82	2.01	0.79	0.79
P. roni **(*n* = 2)**	17.35−19.93 (18.64)	7.57−7.69 (7.63)	7.33−8.29 (7.81)	2.21−2.26 (2.24)	2.15−2.4 (2.28)	1.52−1.76 (1.64)	0.97−1.15 (1.06)	0.85−0.86 (0.86)
***P.* sp. CCS1** **(*n* = 1)**	27.94	9.92	10	2.73	2.82	2.58	1.24	1.06
***P.* sp. CCS4** **(*n* = 1)**	19.2	8.31	8.64	2.68	2.66	1.76	1.39	0.91

P. thymelensis		21.36−25.01	7.64−9.55	7.80−9.48	1.82−2.51	2.68−3.25	1.82−2.43	0−1.35	0−0.86
(*n* = 9)		(23.27±1.25)	(8.57±0.67)	(8.65±0.58)	(2.10±0.20)	(2.95±0.16)	(2.18±0.18)	(0.77±0.60)	(0.50±0.38)
P. yanezi		21.02−30.21	7.69−11.95	7.64−11.7	2.23−3.72	2.8−3.62	1.98−2.73	0.81−1.51	1.07−1.46
(*n* = 5)		(26.49±4)	(8.9±1.76)	(10.2±1.69)	(2.95±0.64)	(3.13±0.34)	(2.40±0.32)	(1.31±0.29)	(1.2±0.16)
Shapiro Wilk Test	W	0.98	0.97	0.99	0.95	0.96	0.97	0.98	0.96
	p-value	0.49	0.2	0.88	0.02	0.09	0.16	0.51	0.12

Table 4. Qualitative morphological characters for species of the *Pristimantis chloronotus* species group. Some data for *P. hernandezi* (Lynch and Ruiz-Carranza, 1983), *P. ortizi* (Guayasamín et al., 2004), *P. supernatis* (Lynch, 1979), *P. chloronotus* (Lynch, 1969) were obtained from the literature due to lack of available vouchers.

Clade	Male traits		Snout shape		Fingers
	Vocal slits	Nuptial pads	Dorsal view	Lateral view	Discs
P. hernandezi	Absent	Absent	Rounded	Rounded	Expanded, broader than long
P. inusitatus	Absent	Present	Subacuminate	Protruding, sometimes bearing a small papilla	Broadly expanded, elliptical, broad lateral fringes
P. ardyae	Present	Present	Rounded	Semitruncate	Expanded, slightly truncate
***P.* sp. CCS1**	Present	Absent	Rounded	Rounded	Broadly expanded, rounded
P. llanganati	Present	Absent	Rounded	Rounded	Broadly expanded, truncate
P. chloronotus	Present	-	Rounded	Slightly truncate	Expanded, truncate
P. ortizi	Present	Absent	Rounded	Rounded	Expanded, truncate
P. supernatis	Absent	Present	Acuminate	Rounded	Broadly expanded
P. colonensis	Present	Absent	Semirounded	Rounded	Expanded, elliptical and slighlty truncate
***P.* sp. CCS2**	-	-	Subacuminate	Rounded	Expanded, truncate
P. huicundo	Present	Absent	Rounded	Angular, usually with papilla at tip	Expanded, elliptical, broad lateral fringes
P. thymelensis	Absent	Absent	Short, rounded	Short, rounded	Barely expanded, emarginate
P. incanus	Absent	Absent	Subacuminate	Rounded	Broadly expanded, elliptical, broad lateral fringes
***P.* sp. CCS3**	Present	Absent	Rounded	Rounded	Expanded, elliptical to rounded
P. roni	Presen	Present	Rounded	Rounded	Expanded, truncate
***P.* sp. CCS4**	Absent	Absent	Rounded	Rounded	Expanded, elliptical
P. yanezi	Absent	Absent	Short, rounded	Short, rounded	Expanded, truncate
P. lividus	Absent	Present	Subacuminate to rounded	Rounded with a small papilla at tip	Broadly expanded
P. eriphus	Present	Absent	Rounded	Rounded with papilla at tip	Expanded, elliptical and slightly truncate

Table 5. Qualitative morphological characters: definition of skin structures for species of the *Pristimantis chloronotus* species group. Some data for *P. hernandezi* (Lynch and Ruiz-Carranza, 1983), *P. ortizi* (Guayasamín et al., 2004), *P. supernatis* (Lynch, 1979), *P. chloronotus* (Lynch, 1969) were obtained from the literature due to lack of available vouchers.

Clade	Texture of skin	Eyelid Tubercles	Postrictal tubercles	Heel tubercles	Dermal folds
P. hernandezi	Dorsum smooth, venter areolate	Conical	-	A prominent, conical tubercle	Dorsolateral folds absent.
P. inusitatus	Shagreen with small conical tuberlces. Venter coarsely areolate	Numerous subconical tubercles and 1 prominent conical tubercle	1 enlarged, conical tubercle	1 elongate, conical tubercle, calcar like	Dorsolateral folds absent. Discoidal fold prominent. Thick supratympanic fold
P. ardyae	Shagreen, venter areolate	2 medium, rounded, low tubercles	Indisinct, one low, rounded tubercle	1 medium, subconical tubercle surrounded by many small rounded, low tubercles	Dorsolateral folds absent. Discoidal folds weakly defined. Supratympanic fold present
***P.* sp. CCS1**	Dorsum shagreen with small conical tubercles forming ridges. Venter areolate	3 mid-elevated conical tubercles surrounded by many small, subconical tubercles	2 low, rounded tubercles	2 medium, conical tubercles	Dorsolateral and discoidal folds absent. Thick supratympanic fold
P. llanganati	Shagreen covered by minute conical tubercles. Venter areolate with scattered warts	A low conical tubercle and some low indistinct tubercles posteriorly	1-2 large conical tubercles	Heel with 2 or 3 low conical tubercles	Dorsolateral and discoidal folds absent. Thin supratympanic
P. chloronotus	Dorsum glandular with scattered small pustules. Venter areolate	1 large, subconical tubercle, surrounded or not by many small low rounded tubercles	1 large, rounded tubercle	Granular, series of many small, low tubercles	Dorsolateral folds present, indistinct. Discoidal folds present. Supratympanic fold prominent
P. ortizi	Dorsum shagreen with small flat warts on flanks. Venter areolate	1 small, conical tubercle or absent	1 large, rounded tubercle	1 small, conical tubercle or absent	Indistinct paravertebral folds, discoidal folds absent, and thick supratympanic folds

Table 5. Continued

P. supernatis	Dorsum smooth anteriorly, granular posteriorly. Venter coarsely areolate	Few, non-pungent tubercles	Present	Heel bearing small, non-conical tubercle	Dorsolateral folds absent. Discoidal folds prominent, and thick supratympanic fold
P. colonensis	Dorsum shagreen to granular. Venter areolate	A large and prominent, conical tubercle	1 large, conical tubercle	Heel with a prominent, conical tubercle	Dorsolateral folds absent. Paravertebral and discoidal folds present. Thick supratympanic fold
***P.* sp. CCS2**	Strongly tuberculate dorsal skin. Venter areolate	A prominent and large, conical tubercle	1 large, conical tubercle	1 prominent, conical tubercle	Dorsolateral folds absent. Paravertebral and discoidal folds present. Thick supratympanic fold
P. huicundo	Shagreen to warty, flanks with some flat warts Venter areolate	1 enlarged, non-conical Tubercle surrounded by some low tubercles	1-2 medium to large, rounded tubercles	1 enlarged, non-conical tubercle	Dorsolateral folds absent. Thick supratympanic folds
P. thymelensis	Dorsum granular showing fine, rounded warts. Venter coarsely areolate	1 small, conical, middle elevated tubercle	Absent	Many small, conical tubercles	Dorsolateral folds absent. Paravertebral folds present. Absence of supratympanic fold
P. incanus	Dorsum granular with scattered pustules. Venter areolate	1 large, conical tubercle surrounded by many small, subconical tubercles.	Present, large and conical tubercles	3 large, conical tubercles and 2 small, low, subconical tubercles	Absence of dorsolateral folds. Discoidal folds present. Thick supratympanic fold
***P.* sp. CCS3**	Dorsum shagreen with scattered small spicules. Venter areolate	Present, subconical, middle elevated tubercle	Present, 2 mid-elevated, conical tubercles	1 conspicuous conical tubercle surrounded by 2 lower, subconical tubercles	Dorsolateral and discoidal folds absent. **V-**shaped scapular fold. Thin supratympanic fold.
P. roni	Dorsum granular to strongly tuberculate. Venter areolate	1 large conical tubercle surrounded by many small, subconical tubercles	Present, 1middle elevated conical tubercle	3 large, conical tubercles	Dorsolateral and supratympanic folds absent. Discoidal fold present.

***P.* sp. CCS4**	Dorsum shagreen to slightly tuberculate. Venter areolate	1-2 pungent, conical tubercles surrounded by many lower, subconical tubercles	1 subconical tubercle	Three prominent, conical tubercles surrounded by 2-3 middle elevated, subconical tubercles	Dorsolateral and discoidal folds present. Narrow supratympanic fold
P. yanezi	Smooth to shagreen. Venter areolate to weakly areolate	1 distinct conical tubercle surrounded by some low indistinct rounded tubercles	1 enlarged, conical	1 low conical tubercle surrounded or not by few lower rounded tubercles	Dorsolateral and discoidal folds absent. Supratympanic fold present
P. lividus	Dorsum granular with conspicuous warts on flanks. Venter coarsely areolate	1prominent, conical tubercle	1-2 conical tubercles	2-3 large, conical tubercles	Faint dorsolateral folds. Thick and well defined supratympanic fold
P. eriphus	Dorsum shagreen to warty bearing small conical tubercles. Venter coarsely areolate	One pungent, conical tubercle and 2-4 small subconical tubercles	Present, 1-2 conical tubercles	1 prominent, conical tubercle surrounded by many small, conical tubercles	No dorsolateral folds. Prominent discoidal folds. Thick supratympanic fold

Table 6. Qualitative morphological characters: coloration patterns of species of the *Pristimantis chloronotus* species group. Some data for *P. hernandezi* (Lynch and Ruiz-Carranza, 1983), *P. ortizi* (Guayasamín et al., 2004), *P. supernatis* (Lynch, 1979), *P. chloronotus* (Lynch, 1969) were obtained from the literature due to lack of available vouchers.

Clade	Coloration					
	Dorsal	**Ventral**	**Groins**	**Flanks**	**Head Markings**	**Iris**
P. hernandezi	Gray to brown above with brown markings	Cream speckled with brown	Cream, finely reticulated with brown	-	-	-
P. inusitatus	Uniformly green to brown with reddish or brown marking,	Venter white or dirty white with brown blotches	Dirty cream to yellow	White or dirty cream	Sometimes two, reddish brown labial bars present	Variable iris coloration from green to reddish brown or grey
P. ardyae	Yellowish amber to brown with orange or brown blotches	Venter creamy yellow	Yellow amber to orange	Dirty cream	Reddish brown canthal bars and brown interorbital bar	Iris orange with black reticulations
***P.* sp. CCS1**	Green with brown marking that may form a reticulated pattern.	Cream, semi-transparent ventral skin, with dark brown and white spots	Cream with distinct yellow and brown diagonal stripes	Cream with yellow and brown diagonal stripes, and scattered brown blotches	Reddish brown canthal bars and five narrow labial bars.	Cream with black reticulations and a reddish midhorizontal band
P. llanganati	Olive green, dorsal surfaces of limbs with dark brown diagonal stripes	Dirty cream with brown mottling in the throat and chest and brown flecks in belly	White or tan with distinct black or dark brown diagonal stripes	Dirty white or white with dark brown diagonal stripes	Dark brown canthal stripe, and two broad dark brown labial bars	Iris coppery with a reddish horizontal stripe
P. chloronotus	Pale orange-brown to brown with brown spots	Cream to creamy yellow or white with faint or distinct brown and black spots and reticulations	White to cream with brown to nearly black bars	Cream to white with pale brown bars	Brown canthal stripe and supratympanic streak	Iris bright brownish red with a few black reticulations and a dark brown horizontal streak
P. ortizi	Yellow or greenish, sometimes with gold specks	White with dark brown specks	Dark brown with bright green patches	Variable, from gray to yellow or brow with white	-	-

Table 6. Continued

				or greenish yellow spots		
P. supernatis	Tan, brown, or nearly black bearing a pattern of brown to black reticulation	Cream, rarely bearing faint brown spots	Dull cream, yellow-cream, or pink, reticulated	Yellowish cream to brown with scattered dark brown flecks arranged in diagonal stripes	Lips bearing a cream stripe. Dark brown, nearly black, interorbital stripe, and supratympanic streak	Iris bright golden-yellow heavily reticulated with black, bearing a horizontal reddish brown streak
P. colonensis	Yellowish brown to dark brown, bearing scattered dark brown flecks	Dirty cream to reddish brown with cream mottling in the throat, chest and belly	Reddish brown or dark brown with narrow white diagonal stripes	Flanks having narrow white diagonal stripes	Dark brown, interorbital stripe, 3-4 labial bars and canthal streak	Variable, iris green to yellow always with black reticulations
***P.* sp. CCS2**	Olive green, darker coloration on the anterior half of the body	Uniformly dark brown with faint dirty cream, small blotches. Inner two fingers and inner two toes bright orange	Uniformly grayish cream	Uniformly dark brown coloration	Distinct dark brown facemask extending onto the snout below the canthus rostralis	Golden brown without reticulations
P. huicundo	Greenish brown to orange brown with or without darker brown markings. A green middorsal blotch	Cream gray to greenish yellow with small dark brown spots, marks or warts	Yellow to gray	Flanks light green-gray to brown, sometimes bearing small cream spots	White stripe in outer edge of upper eyelid; interorbital, canthal, and supratympanic stripes dark brown	Golden brown with fine black reticulation and dark brown horizontal streak
P. thymelensis	Dorsum greenish grey to brown, speckled lightly to heavily with silvery grey or creamy grey	White or creamy grey to dirty yellow heavily reticulated with dark brown or black	Same hue as the dorsum, but paler. Sometimes speckled heavily with grey or creamy grey	Sometimes same color as the dorsum or reddish brown to dark brown, but usually with grey or creamy grey marbling	Faint brown canthal stripe and dark brown to black supratympanic stripes, labial stripe cream to light brown	Coppery-bronze to brown with dark brown or black reticulations
P. incanus	Green or olive brown with dark brown or reddish brown mottling. Dorsal	Cream with dark brown and reddish brown reticulations	Uniformly dark red or reddish brown with glossy white spots	Dark red or reddish brown with glossy white spots. Sometimes	Interorbital stripe, canthus streak and two labial bars dark brown or reddish	Iris bronze with black reticulations

Table 6. Continued

	surfaces of limbs with reddish brown diagonal stripes			with green blotches	brown	
***P.* sp. CCS3**	Olive green with dark brown blotches and faint brown mottling. Dorsal surfaces of limbs with dark brown diagonal bars	Yellowish cream heavily reticulated with dark brown flecks	Uniformly greenish cream with faint and small brown blotches, semi-transparent skin	Cream with scattered and faint small specks	Interorbital stripe, canthal strikes, dark brown. Irregular brown blotch in the middle of the snout	Iris reddish coppery
P. roni	Uniformly green to greenish brown, scattered areas of dorsum with brown or reddishh marks.	Greenish cream to dirty cream with or without dark brown mottling	Greenish yellow to reddish yellow bearing white or cream blotches arranged in diagonal stripes	Variable, green to brown, also bearing white or cream scattered blotches or distributed along the diagonal stripes	Canthal streaks, interorbital bar, supratympanic stripes and two labial bars brown	In females iris bronze heavily reticulated with black, in males uniformly bronze or cupper
***P.* sp. CCS4**	Olive green to greenish brown with reddish brown chevrons. Males usually with X-shaped reddish brown mark on scapular region	Dirty cream to brown heavily reticulated with dark brown or black and bearing small cream or white blotches	In females, greenish yellow with white or cream blotches, sometimes those blotches arranged in diagonal stripes. In males, brightly yellow sometimes bordered by red lines	Flanks barred cream or green and brown or reddish brown, sometimes bearing white or cream blotches	Broad interorbital bar, canthal streak, supratympanic brown or reddish brown	Iris red or reddish coppery
P. yanezi	Yellowish brown to dark brown with scattered pale brown or orange blotches and black flecks, bearing a faint middorsal hourglass-shaped band	Light cream to dirty cream with dark brown flecks and with or without dark brown mottling on the throat	Cream or brownish cream	Dark brown or olive brown with distinct dark brown to black flecks and diffuse dark brown diagonal stripes	Dark brown interorbital bar and sides of head brown with darker vertical labial bars	Iris reddish coppery
P. lividus	Pale brown to dark brown, sometimes with a grayish green hue. Dorsum bearing scattered black flecks	Cream with scattered brown or black flecks	Dark brown or blue to grayish blue	Dark brown, cream or white, with or without black reticulations	Dark brown facemask extending onto the snout below the canthus rostralis	Iris bronze
P. eriphus	Green, mossy,	Cream or dirty	Cream with oblique	Barred with black	Interorbital bar,	Variable, reddish

Table 6. Continued

	greenish brown or completely brown with dark brown chevrons. Dorsal surfaces of limbs with dark brown diagonal bars	cream, in males heavily suffused with dark brown or black. In females, conspicuous black mottling on cream background	white and black bars, sometimes faint barred or bearing yellowish cream to brightly yellow blotches	and white, sometimes yellowish cream to brigthly yellow with scattered brown flecks	supratympanic streak, canthal stripe and two labial bars below the orbital are dark brown	coppery to gray with green or red blotches or bars

Table 7. Sympatric species of the *Pristimantis chloronotus* species group. Localities, number of sampled specimens per species, identification, and altitudinal range are provided.

Locality	Taxa	Sampling	Altitude
Ankaku Reserve, San Rafael community, Santa Clara, Pastaza province, Ecuador	*P. ardyae*	1	2320
	P. llanganati	9	2300−2350
	P. yanezi	1	2280
	P. eriphus	6	2000−2300
	P. sp. CCS1	1	2300
	P. sp. CCS3	4	1668
	P. sp. UCS1	1	2300
Yanayacu Biological Station, Napo province, Ecuador	*P. inusitatus*	1	2453
	P. eriphus	8	1800−2000
	P. sp. CCS1	1	2000
Las Carmelas, Napo province, Ecuador	*P. lividus*	2	2883
	P. sp. CCS2	1	2883
	P. llanganati	1	2483
Salcedo-Tena road, Napo province, Ecuador	*P. llanganati*	4	2853−2883
	P. lividus	1	2883
	P. eriphus	14	2095−2253
	P. yanezi	5	2095−2253
Río Zuñac, Tungurahua province, Ecuador	*P. ardyae*	1	2464
	P. eriphus	1	1269
	P. sp. CCS4	2	2067−2359
Playón San Francisco, Sucumbíos province, Ecuador	*P. huicundo*	2	3500−3600
	P. thymelensis	1	3700
Santa Bárbara, Sucumbíos province, Ecuador	*P. chloronotus*	1	-
	P. supernatis	1	-
	P. colonensis	1	2800

Table 8. Node ages in millions of years and altitudinal reconstruction in meters of representative lineages of *Pristimantis chloronotus* species group. For each node estimated age with the 95% high posterior density interval (95% HPD, the shortes interval that contains 95% of the sampled values) are presented. HPD values correspond to the tree presented in Fig. S4. Node ages correspond to the calibrated tree presented in Fig. 9.

Clade/taxon	Node age		Altitude (m)
	Age	95% HPD	
P. hernandezi	0.371	0.002−1.235	2000
P. inusitatus	3.519	2.566−4.568	2142
P. ardyae	2.236	1.4−3.237	2385
P. sp. CCS1	3.117	1.997−4.332	2171
P. llanganati, *P.* sp. UCS1	8.918	6.863−11.218	2340
P. llanganati	2.559	1.548−3.765	2423
P. chloronotus, *P. supernatis*, *P. colonensis*, *P. ortizi*, *P.* sp. CCS2, *P. huicundo*, *P. thymelensis*	12.826	11.301−14.341	2806
P. chloronotus, *P. ortizi*, *P.* sp. CCS2, *P. huicundo*, *P. thymelensis*	9.627	–	–
P. colonensis	6.538	5.352−7.75	2729
P. ortizi, *P.* sp. CCS2, *P. huicundo*, *P. thymelensis*	8.975	–	–
P. sp. CCS2, *P. huicundo*	6.027	5.017−7.092	3086
P. huicundo	2.176	1.424−3.011	3094
P. thymelensis	1.208	0.9−1.551	3654
P. incanus	0.295	0.065−0.68	1765
P. sp. CCS3	1.169	0.309−2.329	1685
P. roni	1.666	0.907−2.649	1810
P. sp. CCS4	0.589	0.288−1.128	1972
P. yanezi	1.118	0.759−1.534	2411
P. lividus	3.008	1.937−4.19	2714
P. eriphus	3.716	2.662−5.075	2096
Split into two major subclades: 1) *P. inusitatus* to *P. thymelensis*; 2) *P. incanus* to *P. eriphus*	26.53	24.428−28.818	2191
Split of the first major subclade into two lower subclades: 1) *P. inusitatus* to *P. llanganati*; 2) *P. supernatis* to *P. thymelensis*	23.078	21.519−24.641	2330
Split of the second major subclade into two lower subclades: 1) *P. incanus* to *P.* sp. CCS4; 2) *P. yanezi* to *P. eriphus*	16.6343	14.895−18.444	2108

Table 9. Number of species discovered on taxonomic reviews of frogs of the genus *Pristimantis* based on genetic evidence. Threshold values of genetic distances to identify candidate species are in parentheses next to the genetic marker (*16S*). The "Percentage Increase" column shows the number of described (D) species (above bar) and the number of new described (ND) or undescribed (U) species (below bar).

Taxa	Percentage increase	Genetic Marker	Region	Reference
P. bipunctatus, *P. stictogaster*, *P. bromeliaceus*	100% (3D/3ND)	12S	Montane forests of the Cordillera Yanachaga in Central Peru	Duellman and Hedges (2007)
P. ockendeni complex	300% (1D/3ND)	*Cytb*, 16S (4.5%)	Upper Amazon rainforest of Ecuador	Elmer and Cannatella (2008)
P. ridens species complex	200% (1D/2U)	ND2, COI, "WANCY" region, $tRNA^{Met}$	Lowland wet forests of isthmian Central America	Wang et al. (2008)
P. peruvianus, *P. danae*	50% (2D/2ND)	16S (2.9%)	Amazonian versant of the Andes and adjacent low-lands of Central Bolivia and southern Peru.	Padial and De la Riva (2009)
P. calcarulatus complex	200% (1D/2ND)	16S (7.1%)	Montane cloud forest of northwestern Ecuadorian Andes	Hutter and Guayasamín (2015)
P. acuminatus complex	300% (1D/3ND)	COI, 12S, 16S (1.6%)	Upper Amazon Basin of Ecuador and Peru	Ortega-Andrade et al. (2015)
P. walkeri complex	200% (1D/2ND)	12S, 16S (5.2%)	Choco and Andes in northwestern Ecuador	Arteaga et al. (2016)
P. lacrimosus complex	4% (20D/1ND	12S, 16S (4.3%), COI, *Cytb*, CXCR4, NCX1, POMC, Rag-1, SLC8A3 Tyr	Amazon Basin and adjacent slopes of the Andes from Colombia to Bolivia. Humid forests on the Pacific versant of Ecuador and Colombia	Rivera-Correa and Daza (2016)
P. chloronotus Species group	46% (15D/5U/2ND)	16S (3%), ND1, RAG1	Eastern Andean slopes of Colombia and Ecuador	This study

Supplementary material

Figure S1. Putative species delimitation of members of the *Pristimantis chloronotus* species group. Maximum likelihood phylogeny with Bayesian support for the 28 lineages recognized by the PTP analysis. Monophyletic groups in red indicate a single putative species as well as terminal branches in blue.

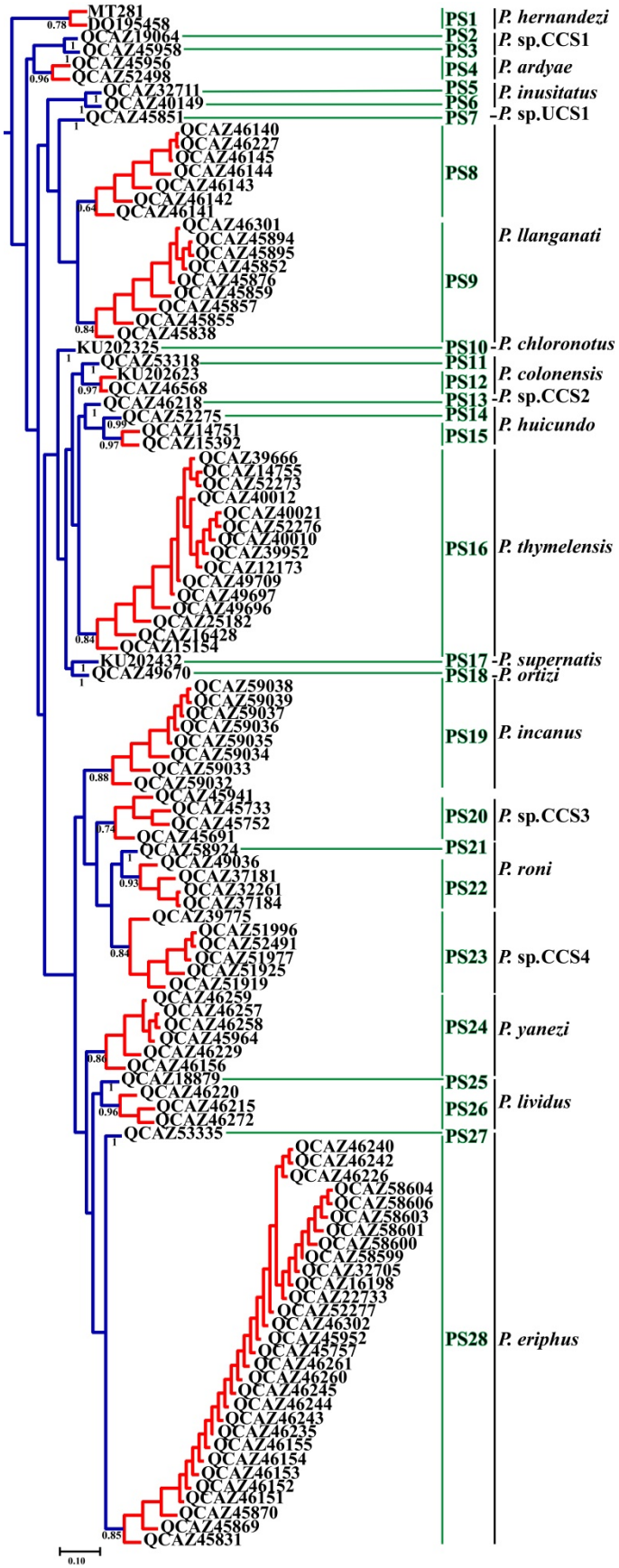
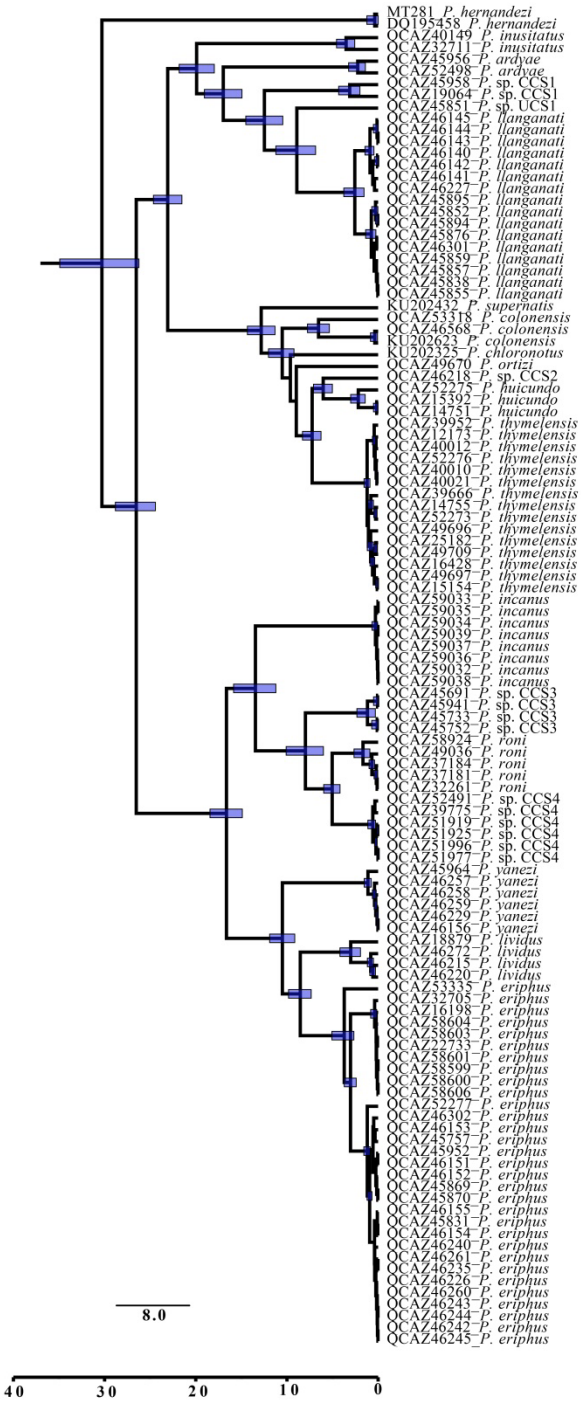

MT281
DQ195458
QCAZ19064
QCAZ45958
QCAZ45956
QCAZ52498
QCAZ32711
QCAZ40149
QCAZ45851
QCAZ46140
QCAZ46227
QCAZ46145
QCAZ46144
QCAZ46143
QCAZ46142
QCAZ46141
QCAZ46301
QCAZ45894
QCAZ45895
QCAZ45852
QCAZ45876
QCAZ45859
QCAZ45857
QCAZ45855
QCAZ45838
KU202325
QCAZ53318
KU202623
QCAZ46568
QCAZ46218
QCAZ52275
QCAZ14751
QCAZ15392
QCAZ39666
QCAZ14755
QCAZ52273
QCAZ40012
QCAZ40021
QCAZ52276
QCAZ40010
QCAZ39952
QCAZ12173
QCAZ49709
QCAZ49697
QCAZ49696
QCAZ25182
QCAZ16428
QCAZ15154
KU202432
QCAZ49670
QCAZ59038
QCAZ59039
QCAZ59037
QCAZ59036
QCAZ59035
QCAZ59034
QCAZ59033
QCAZ59032
QCAZ45941
QCAZ45733
QCAZ45752
QCAZ45691
QCAZ58924
QCAZ49036
QCAZ37181
QCAZ32261
QCAZ37184
QCAZ39775
QCAZ51996
QCAZ52491
QCAZ51977
QCAZ51925
QCAZ51919
QCAZ46259
QCAZ46257
QCAZ46258
QCAZ45964
QCAZ46229
QCAZ46156
QCAZ18879
QCAZ46220
QCAZ46215
QCAZ46272
QCAZ53335
QCAZ46240
QCAZ46242
QCAZ46226
QCAZ58604
QCAZ58606
QCAZ58603
QCAZ58601
QCAZ58600
QCAZ58599
QCAZ32705
QCAZ16198
QCAZ22733
QCAZ52277
QCAZ46302
QCAZ45952
QCAZ45757
QCAZ46261
QCAZ46260
QCAZ46245
QCAZ46244
QCAZ46243
QCAZ46235
QCAZ46155
QCAZ46154
QCAZ46153
QCAZ46152
QCAZ46151
QCAZ45870
QCAZ45869
QCAZ45831
0.10
PS1
PS2
PS3
PS4
PS5
PS6
PS7
PS8
PS9
PS10
PS11
PS12
PS13
PS14
PS15
PS16
PS17
PS18
PS19
PS20
PS21
PS22
PS23
PS24
PS25
PS26
PS27
PS28
P. hernandezi
P. sp.CCS1
P. ardyae
P. inusitatus
P. sp.UCS1
P. llanganati
P. chloronotus
P. colonensis
P. sp.CCS2
P. huicundo
P. thymelensis
P. supernatis
P. ortizi
P. incanus
P. sp.CCS3
P. roni
P. sp.CCS4
P. yanezi
P. lividus
P. eriphus

Figure S2. Bayesian chronogram with 95% highest posterior density (HPD) for *Pristimantis chloronotus* species group. ranges of the divergence times estimated by BEAST v.1.8.0 . The analysis is based on 16S, ND1, and RAG1. All the sequences used are shown. The bars are the height of the 95% highest posterior density. The posterior probabilities of the relationship are specified in Table 5. The analysis was performed in BEAST v.1.8.0 by calibrating the tree with the inferred ages by Pyron (2004).


MT281_P. hernandezi
DQ195458_P. hernandezi
QCAZ40149_P. inusitatus
QCAZ32711_P. inusitatus
QCAZ45956_P. ardyae
QCAZ52498_P. ardyae
QCAZ45958_P. sp. CCS1
QCAZ19064_P. sp. CCS1
QCAZ45851_P. sp. UCS1
QCAZ46145_P. llanganati
QCAZ46144_P. llanganati
QCAZ46143_P. llanganati
QCAZ46140_P. llanganati
QCAZ46142_P. llanganati
QCAZ46141_P. llanganati
QCAZ46227_P. llanganati
QCAZ45895_P. llanganati
QCAZ45852_P. llanganati
QCAZ45894_P. llanganati
QCAZ45876_P. llanganati
QCAZ46301_P. llanganati
QCAZ45859_P. llanganati
QCAZ45857_P. llanganati
QCAZ45838_P. llanganati
QCAZ45855_P. llanganati
KU202432_P. supernatis
QCAZ53318_P. colonensis
QCAZ46568_P. colonensis
KU202623_P. colonensis
KU202325_P. chloronotus
QCAZ49670_P. ortizi
QCAZ46218_P. sp. CCS2
QCAZ52275_P. huicundo
QCAZ15392_P. huicundo
QCAZ14751_P. huicundo
QCAZ39957_P. thymelensis
QCAZ12175_P. thymelensis
QCAZ40012_P. thymelensis
QCAZ52276_P. thymelensis
QCAZ40010_P. thymelensis
QCAZ40021_P. thymelensis
QCAZ39666_P. thymelensis
QCAZ14755_P. thymelensis
QCAZ52273_P. thymelensis
QCAZ49696_P. thymelensis
QCAZ25182_P. thymelensis
QCAZ49700_P. thymelensis
QCAZ16428_P. thymelensis
QCAZ49697_P. thymelensis
QCAZ15154_P. thymelensis
QCAZ59033_P. incanus
QCAZ59035_P. incanus
QCAZ59034_P. incanus
QCAZ59039_P. incanus
QCAZ59037_P. incanus
QCAZ59036_P. incanus
QCAZ59032_P. incanus
QCAZ59038_P. incanus
QCAZ45691_P. sp. CCS3
QCAZ45941_P. sp. CCS3
QCAZ45733_P. sp. CCS3
QCAZ45752_P. sp. CCS3
QCAZ58924_P. roni
QCAZ49036_P. roni
QCAZ37184_P. roni
QCAZ37181_P. roni
QCAZ52261_P. roni
QCAZ52491_P. sp. CCS4
QCAZ39775_P. sp. CCS4
QCAZ51919_P. sp. CCS4
QCAZ51925_P. sp. CCS4
QCAZ51996_P. sp. CCS4
QCAZ51977_P. sp. CCS4
QCAZ45964_P. yanezi
QCAZ46257_P. yanezi
QCAZ46258_P. yanezi
QCAZ46259_P. yanezi
QCAZ46229_P. yanezi
QCAZ46156_P. yanezi
QCAZ18879_P. lividus
QCAZ46273_P. lividus
QCAZ46215_P. lividus
QCAZ46220_P. lividus
QCAZ53335_P. eriphus
QCAZ32705_P. eriphus
QCAZ16198_P. eriphus
QCAZ58604_P. eriphus
QCAZ58603_P. eriphus
QCAZ22733_P. eriphus
QCAZ58601_P. eriphus
QCAZ58599_P. eriphus
QCAZ58600_P. eriphus
QCAZ58606_P. eriphus
QCAZ52277_P. eriphus
QCAZ46302_P. eriphus
QCAZ46153_P. eriphus
QCAZ45757_P. eriphus
QCAZ45952_P. eriphus
QCAZ46151_P. eriphus
QCAZ46152_P. eriphus
QCAZ45869_P. eriphus
QCAZ45870_P. eriphus
QCAZ46155_P. eriphus
QCAZ45831_P. eriphus
QCAZ46154_P. eriphus
QCAZ46240_P. eriphus
QCAZ46261_P. eriphus
QCAZ46235_P. eriphus
QCAZ46226_P. eriphus
QCAZ46260_P. eriphus
QCAZ46243_P. eriphus
QCAZ46244_P. eriphus
QCAZ46242_P. eriphus
QCAZ46245_P. eriphus
8.0
40
30
20
10
0

Gen	Primer name	Sequence (5'–3')	Direction	Source
16S Mitochondrial	16L19	AATACCTAACGAACTTAGCGATAGCTGGTT	F	Heinicke et al. (2007)
	16L34	TTTAACGGCCGCGGTATCCTAACCG	F	Heinicke et al. (2007)
	16H36E	AAGCTCCAWAGGGTCTTCTCGTC	R	Heinicke et al. (2007)
	16H47	AAAGRGCTTAGRTCTTTYGCA	R	Heinicke et al. (2007)
ND1 Mitochondrial	WL384	GAGATWGTTTGWGCAACTGCTCG	F	Moen and Wiens (2008)
	WL379	GCAATAATYATYTGAACMCC	R	Moen and Wiens (2008)
	16S_Frog	TTACCCTRGGGATAACAGCGCAA	F	Wiens et al. (2005)
	tMet_frog	TTGGGGTATGGGCCCAAAAGCT	R	Wiens et al. (2005)
RAG1 Nuclear	RAG1FF2	ATGCATCRAAAATTCARCAAT	F	Heinicke et al. (2007)
	RAG1FR2	CCYCCTTTRTTGATAKGGWCATA	R	Heinicke et al. (2007)

Table S1. List of primers used in the present study for amplification and sequencing of two mitochondrial genes (16s and ND1) and one nuclear gene (RAG1).

Gen	PCR protocol
16S Mitochondrial	1 Cycle: 2 min 94°C, 30s 42°C, 1 min 72°C 5 Cycles: 30s 94°C, 30s 42°C, 1 min 72°C 22 Cycles: 30s 94°C, 30s 50°C, 1 min 72°C 1 Cycle: ∞ 4°C
ND1 Mitochondrial	1 Cycle: 2 min 94°C, 30s 50°C, 1 min 72°C 10 Cycles: 30s 94°C, 30s 50°C, 1 min 72°C 29 Cycles: 30s 94°C, 30s 58°C, 1 min 72°C 1 Cycle: 5 min 72°C
RAG1 Nuclear	1 Cycle: 5 min 94°C 32 Cycles: 30s 94°C, 30s 60°C, 30s 72°C 1 Cycle: 7 min 72°C 1 Cycle: ∞ 4°C

Table S2. PCR protocols: thermal conditions and cycles for each gene (Mitochondrial: 16S, ND1; Nuclear: RAG1). Temperatures are expressed in degrees Centigrade.

Abbreviation	Environmental variable	PC1	PC2	PC3
BIO1	Annual mean temperature	0.259	0.11	-0.001
BIO2	Mean diurnal temperature range (mean of monthly [maximum temperature – minimum temperature])	0.203	0.214	**-0.428**
BIO3	Isothermality (BIO2/BIO7 x 100)	-0.032	**0.646**	0.11
BIO4	Temperature seasonality (standard deviation of monthly temperature)	0.068	**-0.571**	**-0.377**
BIO5	Minimum temperature of coldest month	0.26	0.084	-0.082
BIO6	Maximum temperature of warmest month	0.256	0.092	0.077
BIO7	Temperature range (maximum temperature of the warmest month – minimum temperature of the coldest month)	0.214	0.046	**-0.461**
BIO8	Mean temperature of wettest quarter (i.e., mean temperature of the four consecutive wettest months)	0.256	0.148	0.013
BIO9	Mean temperature of driest quarter	0.26	0.09	-0.031
BIO10	Mean temperature of warmest quarter	0.259	0.098	-0.016
BIO11	Mean temperature of coldest quarter	0.257	0.135	0.007
BIO12	Annual precipitation	0.252	-0.128	0.189
BIO13	Precipitation of wettest month	0.247	-0.12	0.251
BIO14	Precipitation of the driest month	0.251	0.01	0.074
BIO15	Precipitation seasonality (standard deviation of monthly precipitation)	-0.137	-0.038	**0.407**
BIO16	Precipitation of driest quarter	0.253	-0.17	0.173

BIO17	Precipitation of wettest quarter	0.253	-0.044	0.067
BIO18	Precipitation of warmest quarter	0.209	-0.153	0.356
BIO19	Precipitation of coldest quarter	0.252	-0.194	0.075
	Eingenvalue	13.963	2.09	1.387
	% of variance explained	73.487	11.002	7.300
	Cumulative % explained	73.487	84.489	91.789

Table S3. Principal component analysis on environmental data for *Pristimantis chloronotus* species group. Loadings and percentage of explained variance for principal components I−III based on environmental data. Bold numbers indicate highest loadings.

Morphometric variable	Females				Males			
	PC1	**PC2**	**PC3**	**PC4**	**PC1**	**PC2**	**PC3**	**PC4**
Head length (HL)	0.513	0.02	0.358	0.055	0.3	-0.227	-0.254	**0.817**
Head width (HW)	**0.579**	0.199	-0.104	0.069	**0.638**	0.033	0.007	-0.09
Eye-nostril distance (E−N)	**0.482**	-0.16	**-0.41**	-0.273	**0.517**	-0.234	0.326	-0.004
Interorbital distance (IOD)	-0.053	**0.566**	**0.486**	0.28	0.128	**0.623**	0.213	0.275
Internarial distance (IND)	0.221	**0.559**	-0.356	0.24	0.127	**0.7**	-0.022	0.026
Tympanum-eye distance (E−Y)	0.337	-0.331	**0.559**	-0.106	**0.441**	0.022	**-0.431**	**-0.491**
Tympanum diameter (TY)	0.069	**-0.439**	-0.131	**0.878**	0.089	-0.117	**0.773**	-0.078
Eingenvalue	2.342	1.747	0.949	0.817	1.966	1.564	1.336	0.913
% of variance explained	33.462	24.959	13.555	11.667	28.089	22.336	19.083	13.041
Cumulative % explained	33.462	58.421	71.976	83.643	28.089	50.425	69.508	82.549

Table S4. Principal component analysis on morphometric data for *Pristimantis chloronotus* species group. Loadings and percentage of explained variance for principal components I−IV based on environmental data. Bold numbers indicate highest loadings.

	P. sp. CCS2	*P.* sp. CCS3	*P.* sp. CCS4	*P. colonensis*	*P. eriphus*	*P. huicundo*	*P. incanus*	*P. inusitatus*	*P. lividus*	*P. llanganati*	*P. ortizi*	*P. roni*	*P. thymelensis*	*P. yanezi*
P. sp. CCS2	1	0	0	0	0	0	0	0	0	0	0	0	0	0
P. sp. CCS3	0	1	0	0	0	0	0	0	0	0	0	0	0	0
P. sp. CCS4	0	0	2	0	0	0	0	0	0	0	0	0	0	0
P. colonensis	0	0	0	2	0	0	0	0	0	0	0	0	0	0
P. eriphus	0	0	0	0	9	0	0	0	0	0	0	1	0	0
P. huicundo	0	0	0	0	0	1	0	0	0	0	0	0	0	0
P. incanus	0	0	0	0	0	0	1	0	0	0	0	0	0	0
P. inusitatus	0	0	0	0	0	0	0	1	0	0	0	0	0	0
P. lividus	0	0	0	0	0	0	0	0	1	0	0	0	0	0
P. llanganati	0	0	0	0	0	0	0	0	0	2	0	0	0	0
P. ortizi	0	0	0	0	0	0	0	0	0	0	1	0	0	0
P. roni	0	0	0	0	0	0	0	0	0	0	0	5	0	0
P. thymelensis	0	0	0	0	0	0	0	0	0	0	0	0	1	0
P. yanezi	0	0	0	0	0	0	0	0	0	0	0	0	0	1

Table S5. Results of the discriminant function analysis of females specimens based on eight morphometric variables. Rows represent true identities of individuals based on their genetic clades, whereas rows indicate which group individuals were assigned to by analysis

	P. ardyae	*P.* sp. CCS1	*P.* sp. CCS4	*P. colonensis*	*P. eriphus*	*P. huicundo*	*P. incanus*	*P. inusitatus*	*P. llanganati*	*P. ortizi*	*P. roni*	*P. thymelensis*	*P. lividus*	*P. yanezi*
P. ardyae	1	0	0	0	0	0	0	0	0	0	0	0	0	0
P. sp. CCS1	0	1	0	0	0	0	0	0	0	0	0	0	0	0
P. sp. CCS4	0	0	1	0	0	0	0	0	0	0	0	0	0	0
P. colonensis	0	0	0	2	0	0	0	0	0	0	0	0	0	0
P. eriphus	0	0	0	0	10	0	0	0	0	0	0	0	1	0
P. huicundo	0	0	0	0	0	3	0	0	0	0	0	0	1	0
P. incanus	0	0	0	0	0	0	4	1	0	0	1	0	0	0
P. inusitatus	0	0	0	0	1	0	0	1	0	0	0	0	0	0
P. llanganati	0	0	0	0	0	1	0	0	6	0	0	0	0	2
P. ortizi	0	0	0	0	0	0	0	0	0	1	0	0	0	0
P. roni	0	0	0	0	0	0	0	0	0	0	2	0	0	0
P. thymelensis	0	0	0	0	0	1	0	0	0	1	0	3	1	0
P. lividus	0	0	0	0	0	0	0	0	0	0	0	0	1	0
P. yanezi	0	0	0	0	0	0	0	0	1	0	0	0	1	3

Table S6. Results of the discriminant function analysis of males specimens based on eight morphometric variables. Rows represent true identities of individuals based on their genetic clades, whereas rows indicate which group individuals were assigned to by analysis

Appendix A

All samples belong to genus *Pristimantis*, except for *Craugastor longirostris*, *Oreobates quixensis*, and *Hypodactylus sp.* which are part of the outgroup. An asterisk * in the species column indicates that this individual was included in morphometric analyses and a number sign # in the same column indicates that there is available photographs in live for that specimen. An asterisk * in the gene column indicates that there is available only a partial sequence of that gene. For each individual, museum voucher, source, locality and GenBank accession number are detailed. Acronyms for museums are: QCAZ = Museo de Zoología de la Pontificia Universidad Católica del Ecuador, Ecuador; MECN = Museo Ecuatoriano de Ciencias Naturales, Ecuador; KU = The University of Kansas, USA; MT = Mariane Targino, Brazil; JJM = Jonh Jairo Mueses-Cisneros, Colombia. The collection locality abbreviations are: BI = Bosque integral; BP = Bosque protector; EC = Estación Científica; PN = Parque Nacional; RE = Reserva Ecológica; ZA = Zona de amoritguamiento. Sequences in bold were obtained from de GenBank.

Species	Institutional voucher number	Field collection number	Country	Department /Province	Locality	Latitude	Longitude	Mitochondrial genes		Nuclear genes
								16S	ND1	RAG1
hernandezi[#]		JJM210	Colombia	Putumayo	Valle de Sibundoy, Carretera Pasto-Mocoa, 2750 msnm			**DQ195458**[*]		
hernandezi		MT281	Colombia	Caquetá	Florencia			X[*]		

inusitatus	QCAZ32711		Ecuador	Napo	Cosanga, EC Yanayacu, 1800 msnm	-0.599	-77,89	X	X	X
inusitatus[*#]	QCAZ40149	SC25519	Ecuador	Napo	Oyacachi, Puente del Chaupi, 2453 msnm	-0,257	-77,97	X	X	X
ardyae[*#]	QCAZ45956	SC29492	Ecuador	Pastaza	Mera, San Rafael, ZA PN Llanganates, 2320 msnm	-1,276	-78,07	X	X	X
ardyae[#]	QCAZ52498	SC35233	Ecuador	Tungurahua	Baños, RB Río Zuñac, 2464 msnm	-1,367	-78,14	X	X	X
P. sp. (CCS1)	QCAZ19064	SC1072	Ecuador	Napo	Cosanga, EC Yanayacu, 2000 msnm	-0,599	-77,89	X	X	X
P. sp. (CCS1)[*#]	QCAZ45958	SC29511	Ecuador	Pastaza	Mera, San Rafael, ZA PN Llanganates, 2300 msnm	-1,28	-78,08	X	X	X
P. sp. (UCS1)	QCAZ45851	SC29507	Ecuador	Pastaza	Mera, San Rafael, ZA PN Llanganates, 2300 msnm	-1,28	-78,08	X[*]		
llanganati[*]	QCAZ45838	SC29490	Ecuador	Pastaza	Mera, San Rafael, ZA PN Llanganates, 2300 msnm	-1,28	-78,08	X[*]		
llanganati[*]	QCAZ45852	SC29508	Ecuador	Pastaza	Mera, San	-1,28	-78,08	X[*]		

					Rafael, ZA PN Llanganates, 2300 msnm			
llanganati[*]	QCAZ45855	SC29512	Ecuador	Pastaza	Mera, San Rafael, ZA PN Llanganates, 2300 msnm	-1,28	-78,08	X[*]
llanganati[*]	QCAZ45858	SC29515	Ecuador	Pastaza	Mera, San Rafael, ZA PN Llanganates, 2300 msnm	-1,28	-78,08	
llanganati[*]	QCAZ45876	SC29535	Ecuador	Pastaza	Mera, San Rafael, ZA PN Llanganates, 2300 msnm	-1,28	-78,08	X[*]
llanganati[*]	QCAZ45894	SC29558	Ecuador	Pastaza	Mera, San Rafael, ZA PN Llanganates, 2300 msnm	-1,28	-78,08	X[*]
llanganati[*]	QCAZ46140	SC29720	Ecuador	Napo	Sector La Cueva, union ríos Mulatos y Langoa, 2483 msnm	-0,96	-78,22	X[*]
llanganati[*#]	QCAZ46221	SC29721	Ecuador	Napo	Sector La Cueva, union ríos Mulatos y Langoa,	-0,96	-78,22	

llanganati[*#]	QCAZ46227	SC29759	Ecuador	Napo	2483 msnm Carretera Salcedo-Tena, 2253msnm	-0,985	-78,19	X[*]	X
llanganati[*]	QCAZ45895	SC29559	Ecuador	Pastaza	Mera, San Rafael, ZA PN Llanganates, 2300 msnm	-1,28	-78,08	X[*]	
llanganati[*]	QCAZ46301	SC29493	Ecuador	Pastaza	Mera, San Rafael, ZA PN Llanganates, 2320 msnm	-1,28	-78, 073	X[*]	
llanganati	QCAZ45857	SC29514	Ecuador	Pastaza	Mera, San Rafael, ZA PN Llanganates, 2300 msnm	-1,28	-78,08	X[*]	
llanganati	QCAZ45859	SC29516	Ecuador	Pastaza	Mera, San Rafael, ZA PN Llanganates, 2300 msnm	-1,28	-78,08	X[*]	
llanganati	QCAZ46141	SC29722	Ecuador	Napo	Sector La Cueva, union ríos Mulatos y Langoa, 2483 msnm	-0,96	-78,22	X[*]	
llanganati	QCAZ46142	SC29723	Ecuador	Napo	Sector La Cueva, union ríos Mulatos y Langoa,	-0,96	-78,22	X[*]	

llanganati	QCAZ46143	SC29724	Ecuador	Napo	2483 msnm Sector Las Carmelas, vía Salcedo-Tena, 2883 msnm	-0,97	-78,25	X*		
llanganati	QCAZ46144	SC29725	Ecuador	Napo	Sector Las Carmelas, vía Salcedo-Tena, 2883 msnm	-0,97	-78,25	X*		
llanganati	QCAZ46145	SC29726	Ecuador	Napo	Sector Las Carmelas, vía Salcedo-Tena, 2883 msnm	-0,97	-78,25	X*		
chloronotus	KU202325	WED 52959	Ecuador	Napo	3.5km E Santa Barbara			**AY326007***		
supernatis	KU202432	WED 52961	Ecuador	Napo	3.5km E Santa Barbara			**AY326005***		
*ortizi**	QCAZ49670	SC31526	Ecuador	Napo	Papallacta, Valle del Tambo, 3631 msnm	-0,39	-78,20	X	X	X
colonensis#*	QCAZ46568	SC32547	Ecuador	Sucumbíos	Santa Bárbara, vía La Bonita 2600msnm	0,65	-77,49	X	X	X
colonensis	KU202623	WED 52979	Ecuador	Napo	18km E Santa Barbara			**AY326002***		
colonensis	QCAZ53318	SC36556	Ecuador	Napo	Cosanga, Vinillos, 2425 msnm	-0,63	-77,85	X	X	X
*colonensis**	QCAZ46696	SC32684	Ecuador	Sucumbíos	1 km vía Santa Bárbara, Playón de	0.63	-77,52			

supernatis[*]	QCAZ46569	SC32548	Ecuador	Sucumbíos	San Francisco, 2826 msnm Santa Bárbara, carretera vieja a La Bonita, 2600 msnm	0,65	-77,49			
P. sp. (CCS2)[*#]	QCAZ46218	SC29696	Ecuador	Napo	Las Carmelas, vía Salcedo-Tena, 2883 msnm	-0.97	-78,25	X	X	X
P. sp. (CCS2)[*]	QCAZ52275 DHMECN 6390		Ecuador	Sucumbíos	Campamento 3, 2614 msnm	0,49	-77,59	X	X	X
huicundo	QCAZ14749	SC310	Ecuador	Sucumbíos	Playón de San Francisco, 3230 msnm	0,64	-77,62			
huicundo	QCAZ14750	SC311	Ecuador	Sucumbíos	Playón de San Francisco, 3229 msnm	0,64	-77,62			
huicundo[*]	QCAZ14751	SC317	Ecuador	Sucumbíos	Playón de San Francisco, 3600 msnm	0,64	-77,62	X		
huicundo[*]	QCAZ15391	SC98	Ecuador	Sucumbíos	Playón de San Francisco, 3500 msnm	0,64	-77,62			
huicundo[*]	QCAZ15392	SC39	Ecuador	Sucumbíos	Playón de San Francisco, 3500 msnm	0,64	-77,62	X	X	X
huicundo[*]	QCAZ15394	SC112	Ecuador	Sucumbíos	Playón de San	0,64	-77,62			

					Francisco, 3500 msnm					
thymelensis[*]	QCAZ12173	AGG593	Ecuador	Carchi	RE Páramo de El Ángel	0,73	-77,95	X		
thymelensis[*]	QCAZ14755	SC303	Ecuador	Sucumbíos	El Playón, 3700 msnm	0,64	-77,62	X		X
thymelensis[*]	QCAZ15154		Ecuador	Pichincha	Páramo de La Virgen	-0,33	-78,21	X	X	X
thymelensis[*]	QCAZ16428	CP4003	Ecuador	Napo	Páramo de Guamaní, 4000 msnm	-0,36	-78,19	**EF493516**		X
thymelensis[*]	QCAZ25182	SC5041	Ecuador	Napo	Papallacta	-0,38	-78,14	X		X
thymelensis[*] [#]	QCAZ39666	SC25089	Ecuador	Pichincha	RE Cayambe-Coca, Laguna de San Marcos, 3438 msnm	0,11	-77,96	X	X	X
thymelensis[*]	QCAZ40010	SC27430	Ecuador	Carchi	RE El Ángel, Laguna El Voladero, 3730 msnm	0,68	-77,88	X		X
thymelensis[*]	QCAZ40011	SC27431	Ecuador	Carchi	RE El Ángel, Laguna El Voladero, 3730 msnm	0,68	-77,88			
thymelensis[*]	QCAZ40012	SC27432	Ecuador	Carchi	RE El Ángel, Laguna El Voladero, 3730 msnm	0,68	-77,88	X		X
thymelensis[*]	QCAZ40020	SC27442	Ecuador	Carchi	RE El Ángel, Laguna El Voladero, 3730 msnm	0,68	-77,88			
thymelensis[*]	QCAZ40021	SC27460	Ecuador	Carchi	Laguna El Voladero,	0,68	-77,88	X		X

thymelensis[*]	QCAZ40022	SC27461	Ecuador	Carchi	3730 msnm RE El Ángel, 3617 msnm	0,66	-77,89			
thymelensis[*]	QCAZ49696	SC31552	Ecuador	Napo	Guamaní, 3950 msnm	-0,35	-78,20	X		
thymelensis[*]	QCAZ49697	SC31553	Ecuador	Napo	Guamaní, 3950 msnm	-0,35	-78,20	X		X
thymelensis	QCAZ49709	SC31565	Ecuador	Napo	Guamaní, 3640 msnm	-0,33	-78,20	X		X
incanus[*]	QCAZ59032 DHMECN 11587	PBM444	Ecuador	Napo	Gonzalo Pizarro, El Reventador	-0,09	-77,60	X[*]		
incanus[*]	QCAZ59033 DHMECN 11588	PBM447	Ecuador	Napo	Gonzalo Pizarro, El Reventador	-0,09	-77,60	X[*]		
incanus[*]	QCAZ59034 DHMECN 11589	PBM448	Ecuador	Napo	Gonzalo Pizarro, El Reventador	-0,09	-77,60	X[*]		
incanus[*]	QCAZ59035 DHMECN 11590	PBM449	Ecuador	Napo	Gonzalo Pizarro, El Reventador	-0,09	-77,60	X[*]		
incanus[*]	QCAZ59036 DHMECN 11592	PBM454	Ecuador	Napo	Gonzalo Pizarro, El Reventador	-0,09	-77,60	X[*]		
incanus[*]	QCAZ59037 DHMECN 11595	PBM469	Ecuador	Napo	Gonzalo Pizarro, El Reventador	-0,09	-77,60	X[*]		
incanus[*]	QCAZ59038 DHMECN 11596	PBM470	Ecuador	Napo	Gonzalo Pizarro, El Reventador	-0,09	-77,60	X[*]		
incanus[*]	QCAZ59039 DHMECN 11597	PBM472	Ecuador	Napo	Gonzalo Pizarro, El Reventador	-0,09	-77,60	X[*]		
P. sp. (CCS3)	QCAZ45691	SC29281	Ecuador	Pastaza	Mera, San Rafael, ZA PN Llanganates, 1668 msnm	-1,27	-78,05	X[*]		

P. sp. (CCS3)*	QCAZ45733	SC29360	Ecuador	Pastaza	Mera, San Rafael, ZA PN Llanganates, 1668 msnm	-1,27	-78,05	X*		
P. sp. (CCS3)	QCAZ45752	SC29381	Ecuador	Pastaza	Mera, San Rafael, ZA PN Llanganates, 1668 msnm	-1,27	-78,05	X*		
P. sp. (CCS3)*#	QCAZ45941	SC29279	Ecuador	Pastaza	Mera, San Rafael, ZA PN Llanganates, 1668 msnm	-1,27	-78,05	X*		
P. sp. (CCS3)	QCAZ45948	SC29292	Ecuador	Pastaza	Mera, San Rafael, ZA PN Llanganates, 1668 msnm	-1,27	-78,05	X*		
*roni**	QCAZ32261	SC16773	Ecuador	Morona Santiago	7, 6 km W de 9 de Octubre, vía Guamote-Macas, 1715 msnm	-2,23	-78,29	X	X	X
roni	QCAZ37181	SC19675	Ecuador	Morona Santiago	9 de Octubre, 1729 msnm	-2,22	-78,29	X*		
*roni**	QCAZ37184	SC19683	Ecuador	Morona Santiago	9 de Octubre, 1729 msnm	-2,22	-78,29	X	X	X
*roni***	QCAZ49036	YSNA136	Ecuador	Morona Santiago	BP Abanico, 1646 msnm	-2,26	-78,20	X	X	X
*roni***	QCAZ58924	SC49113	Ecuador	Morona	PN Sangay,	-2,06	-78,22	X*		X

				Santiago	Sardinayacu, 1943 msnm					
P. sp. (CCS4)[*]	QCAZ39775	SC25613	Ecuador	Tungurahua	RE Minga, Río Zuñac, 2127 msnm	-1,35	-78,16	X[*]		
P. sp. (CCS4)[#]	QCAZ51919	SC38641	Ecuador	Tungurahua	Río Verde, 1600 msnm	-1,40	-78,30	X	X	X
P. sp. (CCS4)[*#]	QCAZ51925	SC38647	Ecuador	Tungurahua	Río Verde, 1600 msnm	-1,40	-78,30	X	X	X
P. sp. (CCS4)[#]	QCAZ51977	SC38680	Ecuador	Tungurahua	Río Verde, 2000 msnm	-1,37	-78,32	X	X	X
P. sp. (CCS4)[*#]	QCAZ51996	SC33705	Ecuador	Tungurahua	Río Verde, 2000 msnm	-1,39	-78,31	X	X	X
P. sp. (CCS4)[#]	QCAZ51997	SC33706	Ecuador	Tungurahua	Río Verde, 2000 msnm	-1,39	-78,31			
P. sp. (CCS4)	QCAZ52491	SC35360	Ecuador	Tungurahua	RB Río Zuñac, 2067 msnm	-1,37	-78,15	X	X	X
lividus	QCAZ18879	SC1228	Ecuador	Napo	Guango Lodge, 2717 msnm	-0,38	-78,07	X		
lividus[*#]	QCAZ46215	SC29681	Ecuador	Napo	Sector Las Carmelas, 2883 msnm	-0,97	-78,25	X	X	X
lividus[*#]	QCAZ46220	SC29716	Ecuador	Napo	Sector Las Carmelas, 2883 msnm	-0,97	-78,25	X	X	X
lividus[*#]	QCAZ46272	SC29839	Ecuador	Napo	Sector Las Carmelas, 2883 msnm	-0,97	-78,25	X	X	X
lividus[#]	QCAZ46279	SC29849	Ecuador	Napo	Sector Las Carmelas 2883 msnm	-0,97	-78,25			
yanezi[*#]	QCAZ45964	SC29566	Ecuador	Pastaza	Comunidad San Rafael, 2280 msnm	-1,28	-78,08	X	X	X
yanezi	QCAZ46156	SC29766	Ecuador	Napo	Carretera Salcedo-Tena, 2253	-0,99	-78,19	X[*]		

					msnm					
yanezi[*#]	QCAZ46229	SC29757	Ecuador	Napo	Carretera Salcedo-Tena, 2253 msnm	-0,99	-78,19	X[*]		
yanezi[*]	QCAZ46240	SC29798	Ecuador	Napo	Vía Salcedo-Tena km60, 2095 msnm	-1,01	-78,19	X	X	X
yanezi[*#]	QCAZ46257	SC29817	Ecuador	Napo	Vía Salcedo-Tena, 2095 msnm	-1,01	-78,19	X	X	X
yanezi[*#]	QCAZ46258	SC29818	Ecuador	Napo	Vía Salcedo-Tena, 2095 msnm	-1,01	-78,19	X	X	X
yanezi[*#]	QCAZ46259	SC29819	Ecuador	Napo	Vía Salcedo-Tena, 2095 msnm	-1,01	-78,19	X	X	X
*eriphus**	QCAZ16193	SC550	Ecuador	Napo	Macucaloma	-0,60	-77,89			
eriphus	QCAZ16194	SC538	Ecuador	Napo	Macucaloma	-0,60	-77,89			
*eriphus**	QCAZ16198	SC539	Ecuador	Napo	Macucaloma	-0,60	-77,89	X	X	X
*eriphus**	QCAZ22729	SC1251	Ecuador	Napo	Cosanga, EC Yanayacu, 2000 msnm	-0,60	-77,89			
*eriphus**	QCAZ22733	SC2634	Ecuador	Napo	Cosanga, EC Yanayacu, 2000 msnm	-0,60	-77,89	X[*]		
*eriphus**	QCAZ32705		Ecuador	Napo	Cosanga, EC Yanayacu, 1800 msnm	-0,60	-77,89	X	X	X

*eriphus**	QCAZ37181	SC19675	Ecuador	Morona Santiago	Nueve de octubre, 1729 msnm	-2,22	-78,29	X*		
eriphus	QCAZ45757	SC29391	Ecuador	Pastaza	Reserva Ankaku ZA PN Llanganates, 2000 msnm	-1,27	-78,05	X	X	X
eriphus	QCAZ45831	SC29482	Ecuador	Pastaza	Reserva Ankaku ZA PN Llanganates, 2266 msnm	-1,27	-78,07	X*		
*eriphus**	QCAZ45869	SC29526	Ecuador	Pastaza	Reserva Ankaku ZA PN Llanganates, 2350 msnm	-1,28	-78,08	X*		
eriphus	QCAZ45870	SC29527	Ecuador	Pastaza	Reserva Ankaku ZA PN Llanganates, 2350 msnm	-1,28	-78,08	X*		
eriphus#*	QCAZ45952	SC29427	Ecuador	Pastaza	Reserva Ankaku ZA PN Llanganates, 2266 msnm	-1,27	-78,07	X	X	X
eriphus	QCAZ46151	SC29760	Ecuador	Napo	Carretera Salcedo-Tena, 2253 msnm	-0,99	-78,19	X*		
eriphus	QCAZ46152	SC29761	Ecuador	Napo	Carretera Salcedo-Tena, 2253	-0,99	-78,19	X*		

					msnm Carretera Salcedo-					
eriphus	QCAZ46153	SC29762	Ecuador	Napo	Tena, 2253 msnm Carretera Salcedo-	-0,99	-78,19	X*		
eriphus	QCAZ46154	SC29763	Ecuador	Napo	Tena, 2253 msnm Carretera Salcedo-	-0,99	-78,19	X*		
eriphus	QCAZ46155	SC29764	Ecuador	Napo	Tena, 2253 msnm Carretera Salcedo-	-0,99	-78,19	X*		
*eriphus**#	QCAZ46226	SC29758	Ecuador	Napo	Tena, 2253 msnm Carretera Salcedo-	-0,99	-78,19	X	X	X
*eriphus**	QCAZ46235	SC29784	Ecuador	Napo	Tena, 2095 msnm Carretera Salcedo-	-1,01	-78,19	X*		
eriphus	QCAZ46239	SC29796	Ecuador	Napo	Tena, 2095 msnm Carretera Salcedo-	-1,01	-78,19			
*eriphus**	QCAZ46240	SC29798	Ecuador	Napo	Tena, 2095 msnm Carretera Salcedo-	-1,01	-78,19	X	X	X
eriphus#	QCAZ46241	SC29800	Ecuador	Napo	Tena, 2095 msnm Carretera Salcedo-	-1,01	-78,19			
*eriphus**#	QCAZ46242	SC29801	Ecuador	Napo	Tena, 2095 msnm Carretera Salcedo-	-1,01	-78,19	X	X	X
eriphus	QCAZ46243	SC29802	Ecuador	Napo	Tena,	-1,01	-78,19			

eriphus	QCAZ46244	SC29803	Ecuador	Napo	Tena, 2095 msnm Carretera Salcedo-Tena, 2095 msnm	-1,01	-78,19			
*eriphus**	QCAZ46245	SC29804	Ecuador	Napo	Carretera Salcedo-Tena, 2095 msnm	-1,01	-78,19			
eriphus#*	QCAZ46260	SC29820	Ecuador	Napo	Carretera Salcedo-Tena, 2095 msnm	-1,01	-78,19	X*		
*eriphus**	QCAZ46261	SC29821	Ecuador	Napo	Carretera Salcedo-Tena, 2095 msnm	-1,01	-78,19	X*		
eriphus#*	QCAZ46262	SC29822	Ecuador	Napo	Carretera Salcedo-Tena, 2095 msnm	-1,01	-78,19			
eriphus#*	QCAZ46302	SC29557	Ecuador	Pastaza	Reserva Ankaku, ZA PN Llanganates 2300 msnm	-1,28	-78,08	X	X	X
eriphus	QCAZ52277	DHMECN 5209	Ecuador	Tungurahua	RE Río Zuñac, 1269 msnm	-1,40	-78,19	X	X	X
eriphus	QCAZ53335	SC36573	Ecuador	Napo	Vinillos, 2171 msnm	-0,62	-77,85	X*		
eriphus	QCAZ58599	SC36044	Ecuador	Napo	EC Yanayacu	-0,59	-77,88	X*		
*eriphus**	QCAZ58600	SC36045	Ecuador	Napo	EC Yanayacu	-0,59	-77,88	X*		
eriphus	QCAZ58601	SC36051	Ecuador	Napo	EC Yanayacu	-0,59	-77,88	X*		
*eriphus**	QCAZ58603	SC36054	Ecuador	Napo	EC Yanayacu	-0,59	-77,88	X*		

*eriphus**	QCAZ58604	SC36061	Ecuador	Napo	EC Yanayacu	-0,59	-77,88	X*		
*eriphus**	QCAZ58606	SC36069	Ecuador	Napo	EC Yanayacu	-0,59	-77,88	X*		
quaquaversus	QCAZ25676	SC11567	Ecuador	Pastaza	Pomona, 846 msnm	-1,63	-77,91	**JN991463***		**JQ025201**
sp.	QCAZ45775	SC29411	Ecuador	Pastaza	Comunidad San Rafael ZA PN Llanganates, 2000 msnm	-1,27	-78,05	X*		
ockendeni	QCAZ25428	SC11383	Ecuador	Sucumbíos	La Selva Lodge, 245 msnm	0,50	-76,37	**JN991457***		**JQ025195**
librarius	QCAZ25852	SC11229	Ecuador	Napo	Serena, 561 msnm	-1,10	-77,93	**JN991451***		**JQ025188**
inusitatus	KU218015							**EF493677***		
sp	QCAZ58609	SC36072	Ecuador	Napo	EC Yanayacu	-0,59	-77,88			
sp	QCAZ58608	SC36034	Ecuador	Napo	San Isidro, Cuyuja, 1994 msnm	-0,45	-77,95	X*		
sp	QCAZ58607	SC36022	Ecuador	Napo	San Isidro, Cuyuja, 1994 msnm	-0,45	-77,95	X*		
buckleyi	QCAZ39975	SC27344	Ecuador	Carchi	Chilmá Bajo, 2076 msnm	0,87	-78,05	X*		X
galdi	QCAZ32368	SC3876	Ecuador	Zamora Chinchipe	El Pangui, Valle de Río Blanco	-3,63	-78,59	**EU186670***		**EU186746**
colomai	QCAZ17101		Ecuador	Esmeraldas	Alto Tambo, 253 msnm	0,92	-78,57	**EF493354**		**EF493440**
appendiculatus	QCAZ16365	SC3030	Ecuador	Pichincha	Quebrada Zapadores, 1900 msnm	-0,24	-78,74	X*		X
phyrromerus	QCAZ13769	CP2090	Ecuador	Bolívar	BP Cashca Totoras,	-1,72	-78,98	X	X	X

verecundus	QCAZ12410		Ecuador	Cotopaxi	2900 msnm BI Otonga, 1500 msnm	-0,42	-79,00	X		
cf. *laticlavis*	QCAZ49655		Ecuador	Pichincha	Reserva Las Gralarias, 2024 msnm	-0,008	-78,73	X		X
crenunguis	QCAZ15319		Ecuador	Santo Domingo de los Tsáchilas	Vía Toachi-Chiriboga	-0,30	-78,87	X		X
rubicundus	QCAZ26551	SC10570	Ecuador	Morona Santiago	Gral Leonidas Plaza Gutiérrez, 1013 msnm	-2,93	-78,41	X	X	X
thymelensis		TNHC-GDC 14370						**JX564889**		
thymelensis	WED 53004		Ecuador	Carchi	12km W Tufino, 3520m			**AY326009***		
w-nigrum	QCAZ46256	SC29816	Ecuador	Napo	Vía Salcedo-Tena, 2095 msnm	-1,009	-78,19	X	X	X
O. quixensis	QCAZ25520	SC11493	Ecuador	Pastaza	Kapawi Lodge, 239 msnm	-2,54	-76,86	X	X	X
C. longirostris	QCAZ19764		Ecuador	Esmeraldas	Durango, Río San José	-1,05	-78,63	X		X
H. sp.	QCAZ45959	SC29531	Ecuador	Pastaza	Comunidad San Rafael ZA PN LLanganates, 2300 msnm	-1,28	-78,08	X	X	X
roni	QCAZ58897	SC48042	Ecuador	Morona Santiago	PN Sangay, Sardinayacu	-2,10	-78,16	X*		
roni	QCAZ58896	SC48028	Ecuador	Morona	PN Sangay,	-2,10	-78,16	X*		X

roni	QCAZ58879	SC49131	Ecuador	Santiago Morona Santiago	Sardinayacu PN Sangay, Sardinayacu	-2,10	-78,16	X*	X
sp.	QCAZ45953	SC29437	Ecuador	Pasataza	Comunidad San Rafael ZA PN LLanganates,, 2266	-1,28	-78,07	X*	
sp.	QCAZ45940	SC29278	Ecuador	Pastaza	Comunidad San Rafael ZA PN Llanganates, 1668 msnm	-1,27	-78,05	X*	
sp.	QCAZ45948	SC29292	Ecuador	Pastaza	Comunidad San Rafael ZA PN Llanganates, 1668 msnm	-1,27	-78,05	X*	
sp.	QCAZ45832	SC29483	Ecuador	Pastaza	Comunidad San Rafael ZA PN Llanganates, 2266 msnm	-1,28	-78,07	X*	
sp.	QCAZ45780	SC29419	Ecuador	Pastaza	Comunidad San Rafael ZA PN Llanganates, 1668 msnm	-1,27	-78,05	X*	
sp.	QCAZ45784	SC29428	Ecuador	Pastaza	Comunidad San Rafael ZA PN Llanganates, 2266 msnm	-1,28	-78,07	X*	
sp.	QCAZ45770	SC29405	Ecuador	Pastaza	Comunidad	-1,27	-78,05	X*	

					San Rafael ZA PN Llanganates, 2000 msnm			
sp.	QCAZ45767	SC29401	Ecuador	Pastaza	Comunidad San Rafael ZA PN Llanganates, 2000 msnm	-1,27	-78,05	X*
sp.	QCAZ45748	SC29377	Ecuador	Pastaza	Comunidad San Rafael ZA PN Llanganates, 1668 msnm	-1,27	-78,05	X*
sp.	QCAZ45745	SC29373	Ecuador	Pastaza	Comunidad San Rafael ZA PN Llanganates, 1668 msnm	-1,27	-78,05	X*
cremnobates	QCAZ45744	SC29372	Ecuador	Pastaza	Comunidad San Rafael ZA PN Llanganates, 1668 msnm	-1,27	-78,05	X*
sp.	QCAZ45743	SC29371	Ecuador	Pastaza	Comunidad San Rafael ZA PN Llanganates, 1668 msnm	-1,27	-78,05	X*
sp.	QCAZ45720	SC29346	Ecuador	Pastaza	Comunidad San Rafael ZA PN Llanganates	-1,27	-78,05	X*

altamazonicus	QCAZ18243	SC7850	Ecuador	Zamora Chinchipe	, 1668 msnm Shaime, Nangaritza, 908 msnm	-4,32	-78,66	X*	X
sp.	QCAZ16101	CP4028	Ecuador	Napo	Río Salado	-0,20	-77,70	X*	X
quaquaversus	QCAZ16150								**JQ025200**
thymlenesis	QCAZ16428								

DECLARACIÓN Y AUTORIZACIÓN

Yo, María José Navarrete, CI. 1003514690 autora del trabajo de graduación titulado: "Systematics of the *Pristimantis chloronotus* species group (Anura, Craugastoridae) with insights into their historic biogeography", previa a la obtención del grado académico de **LICENCIADA EN CIENCIAS BIOLÓGICAS** en la **Facultad de Ciencias Exactas y Naturales:**

1.- Declaro tener pleno conocimiento de la obligación que tiene la Pontificia Universidad Católica del Ecuador, de conformidad con el artículo 144 de la Ley Orgánica de Educación Superior, de entregar a la SENESCYT en formato digital una copia del referido trabajo de graduación para que sea entregado al Sistema Nacional de Información de La Educación Superior del Ecuador para su difusión pública respetando los derechos de autor.

2.- Autorizo a la Pontifica Universidad Católica del Ecuador a difundir a través del sitio web de la Biblioteca de la PUCE el referido trabajo de titulación, respetando las políticas de propiedad intelectual de la Universidad.

Quito, 07 de febrero del 2017

María José Navarrete

1003514690